EMPTY FRUIT BUNCHES AS SUSTAINABLE SOURCE FOR CELLULOSE NANOCRYSTAL EXTRACTION

WONG TING JUN

A project report submitted in partial fulfilment of the requirements for the award of Bachelor of Engineering (Honours) Chemical Engineering

Lee Kong Chian Faculty of Engineering and Science
Universiti Tunku Abdul Rahman

April 2019

DECLARATION

I hereby declare that this project report is based on my original work except for citations and quotations which have been duly acknowledged. I also declare that it has not been previously and concurrently submitted for any other degree or award at UTAR or other institutions.

Signature   :   _____

Name   :   Wong Ting Jun

ID No.   :   14UEB03119

Date   :   _____

APPROVAL FOR SUBMISSION

I certify that this project report entitled **"EMPTY FRUIT BUNCHES AS SUSTAINABLE SOURCE FOR CELLULOSE NANOCRYSTAL EXTRACTION"** was prepared by **WONG TING JUN** has met the required standard for submission in partial fulfilment of the requirements for the award of Bachelor of Engineering (Honours) Chemical Engineering at Universiti Tunku Abdul Rahman.

Approved by,

Signature   :   _____

Supervisor   :   Dr. Ng Law Yong

Date   :   _____

The copyright of this report belongs to the author under the terms of the copyright Act 1987 as qualified by Intellectual Property Policy of Universiti Tunku Abdul Rahman. Due acknowledgement shall always be made of the use of any material contained in, or derived from, this report.

ACKNOWLEDGEMENTS

ABSTRACT

Nowadays, enormous interest has been manifested in utilizing biomass wastes as a renewable resource for energy and advanced material production besides promoting waste reduction. The aim of this study is to elucidate the potential applicability of empty fruit bunches (EFB) as native botanic material for the extraction of cellulose nanocrystals (CNC). Raw empty fruit bunches were subjected to two different pre-treatment steps, namely alkali-treatment and bleaching to extract cellulose. Acid hydrolysis was then implemented to extract cellulose nanocrystals in aqueous suspension. In order to extract high purity cellulose nanocrystals, it is crucial to remove natural recalcitrance such as hemicellulose and lignin resides in the empty fruit bunch fibres. Chemical composition analysis using Designer Energy Ltd. Method proved that cellulose nanocrystals produced have high cellulose content up to 73.74 %. Besides, the effects of pre-treatment and acid hydrolysis toward the quality of cellulose samples produced were investigated by various characterisation methods. Scanning electron microscopy equipped with energy dispersive X-ray (SEM-EDX) showed that the cellulose nanocrystals exhibit spherical-like shape with an average diameter of around 56.1 to 105 nm. The size of cellulose nanocrystals was further confirmed by dynamic light scattering (DLS) technique, which showed that the major size distribution of the cellulose nanocrystal samples was in the range from 80.59 to 456.8 nm. X-ray diffraction analysis (XRD) exhibited that cellulose nanocrystals extracted has a relatively high crystallinity index of 83.4862 %. Hemicellulose and lignin compounds were successfully removed in the absence of peaks at 1593.97 and 1237.91 cm^{-1} in Fourier-transform infrared spectroscopy (FTIR) spectrum. Thermogravimetric analysis (TGA) was used to identify the thermal stability of cellulose nanocrystals, which demonstrated the decomposition of cellulose nanocrystals between 60 to 800 °C. In this study, cellulose nanocrystals with high purity and crystallinity have been successfully derived from empty fruit bunch biomass wastes and through an environmentally benign approach.

TABLE OF CONTENTS

CHAPTER

LIST OF TABLES

LIST OF FIGURES

LIST OF SYMBOLS / ABBREVIATIONS

at%	atomic percent, %
C_{SA}	concentration of sulphuric acid available in laboratory, wt%
C	cellulose content, %
CrI	crystalline index, %
d	lattice planar distance, nm
d_H	hydrodynamic diameter of particles, m
D	translational diffusion coefficient, m^2/s
HC	holocellulose content, %
I_{am}	intensity of diffraction attributed to amorphous cellulose, count
I_{002}	maximum intensity of the diffraction peak, count
k_B	Boltzmann's constant, J/K
m	mass of sulphuric acid in 100 g of 64 wt% sulphuric acid solution, g
T	temperature, °C
V	volume of sulphuric acid required, ml
wt%	weight percent, %
W_{CP}	weight of dry cellulose and petri dish, g
W_f	weight of sample after treatment, g
W_i	weight of sample before treatment, g
W_H	weight of dried holocellulose samples, g
W_{HP}	weight of dry holocellulose and petri dish, g
W_P	weight of petri dish, g
W_S	weight of dried biomass samples, g
Y_{ATEFB}	yield of alkali-treated empty fruit bunch sample, %
Y_{CMF}	yield of bleached cellulose microfibre sample, %
Y_{CNC}	yield of cellulose nanocrystal sample, %
λ	wavelength, nm
θ	diffraction angle, °
η_o	viscosity of the solvent, kg/(m·s)
ρ	density of sulphuric acid, g/ml
ATEFB	alkali-treated empty fruit bunches

CMF	cellulose microfibrils
CNC	cellulose nanocrystals
CNF	cellulose microfibrils
DLS	Dynamic Light Scattering
EDX	Energy Dispersive X-ray
EFB	empty fruit bunches
FESEM	Field Emission Scanning Electron Microscopy
FTIR	Fourier Transform Infrared Spectroscopy
LCA	Life-Cycle Assessment
SEM	Scanning Electron Microscopy
TEM	Transmission Electron Microscopy
TGA	thermogravimetric analysis
TEMPO	(2,2,6,6-Tetramethylpiperidin-1-yl)oxyl
XRD	X-Ray Diffraction

LIST OF APPENDICES

CHAPTER 1

INTRODUCTION

1.1   General Introduction

Cellulose is a complex polysaccharide or carbohydrate that composed of up to 3000 glucose repeating units in a linear chain. It is a tough, water-insoluble and fibrous substance (Mariano et al., 2014). Cellulose is commonly discovered in the protective plant cell walls, specifically in woody portions of plant tissues such as stems, trunks and stalks. Typically, cellulose is made up of 90 % and 33 % basic structural components in cotton and vegetable, respectively (Bittar, 2012). Cellulose consists of D-glucose units connected by β-1,4 glycoside bonds as displayed in Figure 1.1.
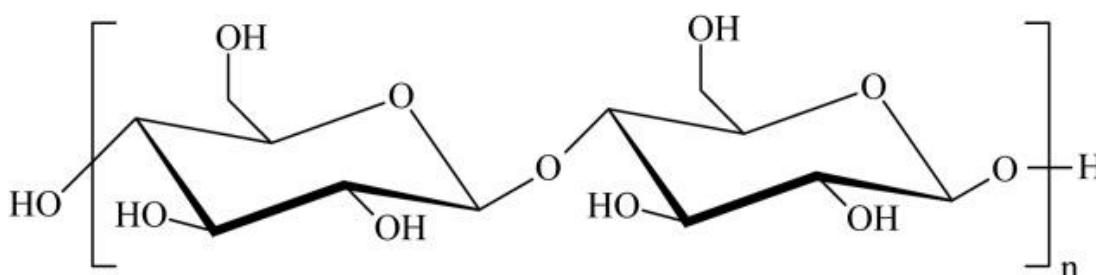
Figure 1.1: Chemical Structure of Cellulose (Adapted from Mariano, El Kissi and Dufresne, 2014)

As cellulose is a natural polymer, cellulose is renowned for its excellent biodegradability, biocompatibility and low cytotoxicity (Athinarayanan et al., 2018). These benefits have encouraged cellulose to have close relations with some manufacturing industries. For instance, textiles, clothes, cellophane and even medicines are relying strongly on cellulose. Production of cellulose is approximated to be $10^{11} - 10^{12}$ tons annually (Kukrety et al., 2018). This indicates the tremendous market demand for cellulose. Surprisingly, sources of cellulose production are not only obtainable from plants. Animals such as tunicates, algae and even bacteria could also contribute as sources of cellulose (Trache et al., 2017). Plant sources, however, is dominating the cellulose raw material extraction because it is rather economically feasible and has high accessibility compared to other sources. Among the plant sources, lignocellulosic agro-industrial by-products are preferable.

There are several examples of lignocellulosic agro-industrial by-products. In this study, oil palm biomass by-products such as empty fruit bunches (EFB) is emphasised. Malaysia as one of the largest manufacturers of oil palm has contributed to mass production of oil palm biomass. In specific, oil palm biomass constitutes 85.5 % wastes produced in Malaysia. For empty fruit bunches solely, there are about 19.8 million tonnes of biomass being produced per year on wet basis (Abdullah et al., 2016). Other major oil palm biomass wastes are oil palm trunk and frond. This fact is greatly astonishing and researchers have been brainstormed to dispose or utilise this great amount of empty fruit bunch biomass produced. One of the current targets is the extraction of cellulose nanocrystals from empty fruit bunches to convert it into value-added biopolymer which can be used in various industries such as paperboard manufacturing, green fertilizer development and bioethanol production. This can reduce the impact to the environment as the wastes are converted into useful substances.

Cellulose can be classified based on different particle sizes and structures for distinct applications. Figure 1.2 exhibits the general classification of cellulose.
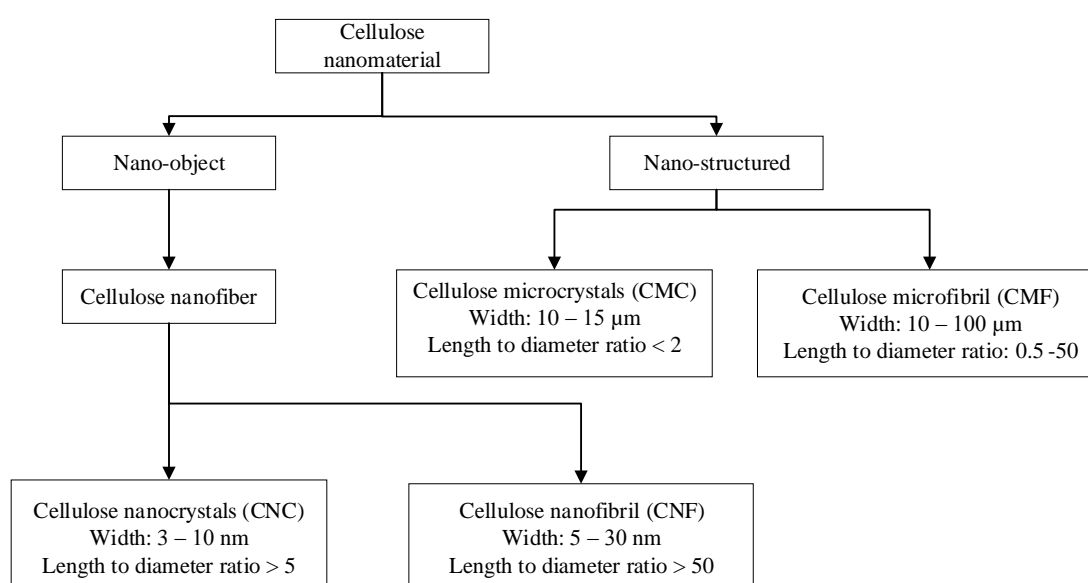
Figure 1.2: Classification of Cellulose (Adapted from Kargarzadeh et al., 2017)

As raw empty fruit bunch is an irregular heavy deposition of hemicellulose, lignin, inorganic components, wax and also composite with compact fibrillar packing, separation of cellulose requires the breaking and opening of chemical aromatic bonds including C–C, R–O–R, hydroxide bond of the lignin, R–O–R and RCOOR of the

hemicelluloses or celluloses (Abdullah et al., 2016). Extraction of cellulose can be accomplished by dislocating the packed composite structure of hydrogen bonding. This can be prepared by using mechanical, chemical and physical routes (Abdullah et al., 2016). In this circumstance, the interest is to remove hemicellulose and lignin and focus on obtaining a maximum yield of pure cellulose, which is hierarchically structured material that composed of both amorphous domains and crystalline domains.

After cellulose fibres are obtained, it can be mechanically or chemically broken down to produce nanosized cellulose, namely cellulose nanocrystals or cellulose nanowhiskers (CNC) and nanocelluloses (NC). These cellulose nanomaterials have some superior characteristics such as large specific surface area that ranges from 250 to $500\,\text{m}^2/\text{g}$, low density of about $1.6\,\text{g/cm}^3$, high crystallinity up to 90 % and high tensile strength at around of $7.5\,\text{GPa}$, extremely high elastic modulus of approximately $100–140\,\text{GPa}$ and high aspect ratio ranges from a factor of 10 to 100 (Bandera et al., 2014).

Several steps of pre-treatment are necessary in order to extract cellulose nanocrystals from empty fruit bunches. For examples, physical, chemical and thermal pre-treatments can be conducted on empty fruit bunches. Physical pre-treatment of empty fruit bunches was ground by a grinder for size reduction. The ground empty fruit bunch fibres would have an average size of 1 to 2 cm (Ariffin et al., 2008). Chemical pre-treatment was done by soaking the hammer-milled empty fruit bunch fibres in sodium hydroxide solution and soaked in tap water overnight. On the other hand, in thermal pre-treatment, empty fruit bunch fibres were treated by soaking the fibres in distilled water and then autoclaved at 121 ºC (Ariffin et al., 2008). These pre-treatments have one common objective, which is to increase the purity of the cellulose nanocrystals that can be extracted from empty fruit bunches.

1.2   Importance of the Study

Palm oil industry yields a tremendous amount of lignocellulosic residues that exist in the form of solid wastes. In Malaysia, one of the major lignocellulosic residues is empty fruit bunches. From the previous study, approximately 23 % of empty fruit bunches are generated per tonnes of processed fresh fruit bunches in the palm oil mill (Derman et al., 2018). The yield of fresh fruit bunches was 15.91 tonnes per hectare in 2016 (Derman et al., 2018). As 23 % of overall fresh fruit bunches processed will be converted into empty fruit bunches, the total production of empty fruit bunches

annually was approximately 3.66 tonnes per hectare in 2016 (Derman et al., 2018). Obviously, empty fruit bunches emerged as a potential source for the extraction of cellulose and further downstream fabrication of liquid biofuel (such as biodiesel and bioethanol) via fermentation methods.

Additionally, the motivation to convert oil palm biomass into useful substances is supported by the fact that oil palm biomass comprises about 90 % of the production of palm oil, while the remaining 10 % constitute of oil produced from the extraction of palm oil from fresh fruit bunches (Derman et al., 2018). Figure 1.3 displays the yield of crude palm oil and fresh fruit bunches in Malaysia from 2007 to 2016. According to Figure 1.3, after fresh fruit bunches are subjected to several processing steps, approximately 80 % of empty fruit bunches will be produced from the overall fresh fruit bunches processed. Thus, approximately 80 % of oil palm biomass will be disposed as waste materials after the extraction of palm oil (Derman et al., 2018). The biomass wastes are usually buried or combusted with no further investigation to increase their values. This study emphasises on the complete valorisation of the empty fruit bunches and also to carry out sustainable practices which bring benefits to the environment.
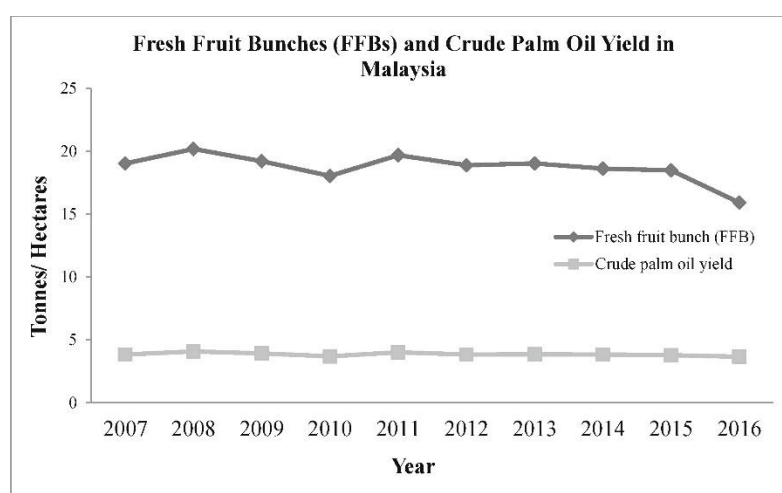
Figure 1.3: Fresh Fruit Bunches and Crude Palm Oil Production in Malaysia
(Adapted from Derman et al., 2018)

Of late, an increasing effort has been made to reduce the waste of oil palm resources to mitigate the environmental pollution that arises from improper biomass disposal. As other option such as recycling of empty fruit bunches is not possible, incineration and landfill are the remaining options to cater with a large amount of side

products generated from the processing of edible oil. This undoubtedly increases the cost to process and dispose the oil palm biomass residue. Due to its high cellulosic content, empty fruit bunches possess a great potential for cellulose nanocrystal extraction (Fatah, 2015). Thus, conversion of empty fruit bunches into useful cellulose nanocrystals can save the environment besides using it as composite material. Also, empty fruit bunch fibres can be considered as a green material that has the possibility to replace certain synthetic materials. Utilization of the green material, aligns well with the global trends of sustainable development and design, water preservation and energy efficiency (Fatah, 2015). The processing of natural fibres will not emit large amount of greenhouse gases, which are the main culprit for global warming. In comparison, the production of synthetic fibres (such as polyethylene fibres) escalates the carbon dioxide emission, which is not so environmental friendly.

Cellulose nanocrystals exhibit outstanding characteristics such as high aspect ratio, large surface area, high modulus and high mechanical strength (Mishra et al., 2018). These impressive properties of cellulose nanocrystals have been proved as a superior reinforced component for the synthesis of polymer composites. However, there are still few drawbacks utilising cellulose nanocrystals to fabricate polymer composite. Cellulose nanocrystals are generally reckoned of its high hydrophilicity, which makes them incompatible with hydrophobic polymers. To mitigate this drawback, more intense studies are required. Besides, the yield of extractable cellulose nanocrystals from empty fruit bunches is not well-investigated. Therefore, it is noteworthy to carry out study on the extractable yield of cellulose nanocrystals.

1.3   Problem Statement

Malaysia is blessed with pleasant weather and endowed with vast areas of land that promote the cultivation of oil palm plantation. Availability of the oil palm biomass, particularly oil palm trunk and the continuous supply of the waste materials, have gained the attention of researchers. Researchers continue to work on full valorisation of oil palm tree, which is desired to develop energy-efficient means to reduce environmental pollution by waste reduction. Hence, extraction of cellulose nanocrystals from oil palm fruit bunches has been suggested to further utilise the oil palm wastes.

Numerous researches were made to investigate the yield of cellulose nanocrystals from other sources such as kenaf, white cotton and hemp (Jonoobi et al.,

2015). However, little researches have attempted to evaluate the extraction of cellulose nanocrystals from empty fruit bunches. Therefore, the information regarding the extraction methods used and their respective effects toward cellulose nanocrystal extraction are insufficient. It is thus noteworthy to determine whether chemomechanical treatment and sulphuric acid hydrolysis are effective for the extraction of cellulose nanocrystals.

In addition, it is vital to assess whether the samples produced using chemomechanical treatment and sulphuric acid hydrolysis in this study is in good agreement with samples fabricated from other reported works using other sources of raw materials. Thus, several characterisation methods need to be implemented to evaluate the physical and chemical properties of samples thoroughly. Based on previous work, agglomeration of cellulose nanocrystals can easily occur during a cellulose nanocrystals drying process or during the mixing process with hydrophobic matrices (Fatah, 2015). Therefore, the roles of characterisation methods, such as scanning electron microscopy (SEM) and dynamic light scattering (DLS), become crucial to evaluate the outcomes of chemo-mechanical treatment and sulphuric acid hydrolysis in this study.

1.4   Aims and Objectives

The general aim of this research project is to justify the potential utilisation of empty fruit bunch biomass wastes in cellulose nanocrystal extraction. Cellulose nanocrystal extraction will allow full valorisation of empty fruit bunches besides promoting waste reduction.

The main objectives of the project are listed as follows:

(i)   To study the effects of chemo-mechanical treatment and sulphuric acid hydrolysis towards the extraction of cellulose nanocrystals from empty fruit bunches.

(ii)   To determine the morphology, chemical compositions, topography and crystallographic information of the cellulose nanocrystal samples.

1.5   Scope and Limitation of the Study

As the objectives are addressed, it is essential to establish the scope that specifies the range of study conducted. The first priority is to emphasise on the extraction of cellulose nanocrystals from empty fruit bunches. The cellulose extraction will be

indicated by the removal of hemicelluloses, resin and lignin. This activity is segregated into few stages, in which cellulose will be extracted in the form of microfibres from empty fruit bunches by alkali and bleaching treatment, followed by isolation of cellulose nanocrystals from the cellulose microfibres by acid hydrolysis method (Jonoobi et al., 2015). There might be a slight variance of the necessary conditions implemented in this research based on the results obtained. Cellulose nanocrystals that are successfully fabricated will be characterised by various techniques such as X-ray diffraction (XRD), scanning electron microscopy (SEM) and Fourier transform infrared spectroscopy (FTIR).

There are some limitations in this study. First, the most desired conditions to convert empty fruit bunches into cellulose nanocrystals will not be analysed. The empty fruit bunch samples will be treated based on a few different parameters instead of trying all possible approaches due to time constraint. In such, analysis of variance (ANOVA) analysis of the response surface model (RSM) to interpret the interaction among all input parameters will be excluded. Next, the characterisation of cellulose samples will focus on a few techniques that are important to this study only. For instance, particle size analysis using field emission scanning electron microscopy (FESEM) will not be carried out and will be replaced by other relevant technique such as Malvern Zetasizer or dynamic light scattering (DLS). Furthermore, the applications of cellulose nanocrystals to produce reinforced composite will not be studied and investigated.

1.6   Contribution of the Study

Throughout this research, numerous sources that are available for cellulose nanocrystal extraction are found in journals. Significance of empty fruit bunches as a viable source of cellulose nanocrystals will be stated and assessed by comparing it to other sources in terms of sustainability, availability and cellulose content.

Other than that, different methods that are utilised to fabricate cellulose nanocrystals will be evaluated in terms of its mechanisms, processing conditions and cellulose yield. Therefore, the method that will be used to produce cellulose nanocrystals in this study can be concluded based on the information obtained from various studies. In addition, the characterisation methods can be used to evaluate the efficiency of methods selected based on the physical and chemical properties of cellulose produced. Hence, the results of this project can be used to suggest a more

effective production mechanism for cellulose with the utilisation of lignocellulose biomass waste from palm oil industry.

1.7 Outline of the Report

The arrangement of the thesis is summarised as follows:

Chapter 1 comprises of the introduction and background of the project. Problem statement, aims and objectives, importance of study, limitations and contribution of the report are included. Chapter 2 is literature review. It focuses on the viable sources suitable for extraction of cellulose nanocrystals studied by researchers and highlighted the significance of empty fruit bunches as cellulose source in Malaysia. Besides, various methods utilised to extract cellulose nanocrystals are evaluated and studied to determine the most suitable approach to synthesize cellulose nanocrystals from empty fruit bunches. Chapter 3 is methodology and work plan, which covers the steps to extract or isolate cellulose nanocrystals in details. This includes three main treatments, which are alkaline treatment, bleaching process and acid hydrolysis. Characterisation methods and their details are also described in this section to assist in the analysis and observation of the changes after chemical treatments are carried out. Subsequently, Chapter 4 encompasses results and discussion. It elaborates the results obtained and interpretation of the corresponding results to evaluate the effectiveness of the approach utilised in addition to the yield of cellulose nanocrystal extraction from empty fruit bunches. Lastly, Chapter 5 is the conclusion of the study. The findings are summarised in this section and any recommendations for future works will be proposed.

CHAPTER 2

LITERATURE REVIEW

2.1   Introduction

The development in nanotechnology has greatly contributed to major advances in society (Dowling, 2004). This newly-developed technology possesses tremendous potential in revolutionise many industrial sectors. Production of cellulose nanocrystals is not an exception. This product has made good use of natural raw materials besides its broad applications. The conversion of natural raw materials to cellulose nanocrystals is considered as an environmental-friendly approach due to minimal emission of greenhouse gases and fully valorisation of useful materials (Loh, 2017). Several choices of sustainable raw materials are suitable to extract cellulose nanocrystals. In this study, empty fruit bunches will be chosen as a viable and sustainable source for cellulose nanocrystal extraction.

In order to isolate cellulose nanocrystals from the source selected, pre-treatment and hydrolysis steps are compulsory (Taflick et al., 2017). This review has listed a few approaches that are currently available and feasible for cellulose nanocrystal isolation. Hence, comparisons are made between a few methods that are commonly used. Conversion yield, ease of processing, availability of raw materials required and quality of cellulose nanocrystals produced will be predominantly emphasised. Furthermore, characterisation techniques are determined to analyse the cellulose nanocrystals yielded from a particular method. This is important to identify and evaluate cellulose nanocrystals based on its structural properties, morphologies, functional groups, crystallinity and lastly, shape and size distribution (Skoog, D. A., Holler, F. J., and Nieman, 1998).

2.2   Sustainable Sources for Cellulose and Cellulose Nanocrystal Extraction

Sustainable means capability to be supported as the basic necessities to maintain an action or a process, which satisfy continuity of the operation (Opon and Henry, 2019). However, the term "sustainable" can be defined quite differently. Sustainable can be classified under three major pillars of sustainability, namely social sustainability, environmental sustainability and economic sustainability (Opon and Henry, 2019).

These three pillars describe sustainable in different aspect, which lay a foundation of sustainability.

In this study, the sustainable source of cellulose nanocrystal production is majorly classified under environmental sustainability. However, interrelation exists among the three pillars of sustainability (Opon and Henry, 2019). For instance, economic sustainability through the utilisation of empty fruit bunch will result in higher profit for the industry as well.

Cellulose can be obtained from a wide range of animals, bacteria and plants (George and Sabapathi, 2015). Different sources of cellulose will yield distinct structures, properties and sizes of cellulose (George and Sabapathi, 2015). In other words, cellulose nanocrystal production could be varied depending on the sources from which it is extracted. This provides researchers a broad range of choices to study such as types of cellulose sources, reaction parameters and processing methods. In the following subsection, brief overview of the cellulose and cellulose nanocrystals sources are introduced.

2.2.1 Plants

Plants are the main potential sources of cellulose as plants are relatively cheap and abundant (George and Sabapathi, 2015). Plants are also known as lignocellulosic sources, including both woody and non-woody plants. Plant fibers or lignocellulosic natural fibers are normally characterised based on the origin of the plant. Leaf, seed, fruit, grass, straw and stem fibers are potential sites for cellulose extraction (Trache et al., 2017). This indicates that more than half portion of the plants are valuable resources for cellulose nanocrystal production. In term of plants, the sustainable sources are rice husk, sisal, wood, kenaf, coconut husk and hemp (Trache et al., 2017). To date, the main origins of the cellulose are cotton fibers and wood pulp. Chemical compositions of nanofibres from various lignocellulosic sources are listed in Table 2.1.

Table 2.1: Chemical Composition of Nanofibres from Various Lignocellulosic Sources

Materials	Cellulose (%)	Hemicellulose (%)	Lignin (%)	Extractive (%)	References
Kenaf (stem)	63.5 ± 0.5	17.6 ± 1.4	12.7 ± 1.5	4 ± 1	(Jonoobi et al., 2015)
Wheat straw	43.2 ± 0.15	34.1 ± 1.2	22.0 ± .1	–	(Alemdar and Sain, 2008)
Soy hulls	56.4 ± 0.92	12.5 ± 0.72	18.0 ± 2.5	–	(Alemdar and Sain, 2008)
Hemp	75.56	10.66	6.61	–	(Wang et al., 2007)
Flax	73.0 ± 7.0	13.0 ± 2.0	5.0 ± 1.0	–	(Bhatnagar and Sain, 2005)
Empty fruit bunch	40.0 ± 2.0	23.0 ± 2.0	21.0 ± 1.0	–	(Jonoobi et al., 2015)
Pineapple leaf	81.3 ± 2.4	12.3 ± 1.3	3.5 ± 0.6	–	(Cherian et al., 2010)
Bagasse	70.6	26.8	–	Ash 16.8 %	(Hassan et al., 2012)
Rice straw	61.9	22.5	–	Ash 16.8 %	(Hassan et al., 2012)
Bamboo	41.8 ± 1.9	27.2 ± 4.3	81.3 ± 2.4	23.2 ± 2.7	(Xie et al., 2016)
Jute (stem)	68.3	15.4	10.7	–	(Jonoobi et al., 2015)
Sugar beet pulp	22	32	2	–	(Jonoobi et al., 2015)
White cotton	97.7 ± 2.2	0.5 ± 0.4	0.4 ± 0.1	–	(Jonoobi et al., 2015)
Banana (pseudo stem)	69.9	19.6	5.7	–	(Abraham et al., 2011)

Cotton fibers have a slightly greater advantage due to its relatively low non-cellulosic component content in comparison to woody materials. On the other hand, wood is abundant in nature, which makes it an attractive starting material for cellulose and its downstream derivative extraction. Wood comprises of the hierarchical structure of natural composite, which are hemicellulose, lignin and cellulose. Effective elimination of the lignin, hemicellulose and other impurities will ultimately result in the production of high purity celluloses. Recently, top-down techniques are the common approach to fabricate cellulose nanocrystals from various plant resources (Trache et al., 2017). These techniques work on the basis of the wood materials as the main sources for cellulose nanocrystal production. Interestingly, competition for woody materials arose from numerous sectors such as pulp and paper industries, building construction and manufacture of furniture, which have induced difficulties to obtain woody materials due to its scarcity. Not to mention that some of the regions have limited access to woody materials. Thus, non-woody lignocellulosic fiber such as aquatic plants, grasses and even agricultural wastes (such as empty fruit bunch) has become the target sources for cellulose extraction and led to more intense research and study in recent year (Trache et al., 2017).

Of late, potential sources of cellulose nanocrystal production have been discovered, which including miscanthus giganteus, mango seeds, tea leaves, oil palm, risk husk and sugarcane bagasse (Cudjoe et al., 2017). Exploration of these valuable resources is defined as a green approach that utilises agricultural wastes to reduce the burden of environmental impact to the earth. As a result, different extraction processes and conditions have been successfully devised to isolate cellulose, which differs in morphology, crystallinity, geometrical structure, mechanical properties and porosity (Trache et al., 2017).

2.2.2   Tunicates

Apart from lignocellulosic sources, other living organisms including animals, can also be employed to produce cellulose microfibrils and nanocrystals. Parts of tunicates comprise of cellulose that is extractable and it is also the only animal source of cellulose (Kargarzadeh et al., 2017). Tunicates are marine invertebrate animals, which are classified under members of sub-phylum Tunicata (George and Sabapathi, 2015). The name "Tunicata" has been derived from its unique integumentary tissue the "tunic", which covers the entire epidermis of the animal (Trache et al., 2017). The

cellulose microfibrils act as a skeletal structure in the tunic tissue. In the plasma membrane of tunicates epidermal cells, it comprises of cellulose-synthesizing enzyme complexes, which are responsible for cellulose production (Trache et al., 2017).

Two classes of tunicates, *Ascidiacea* and *Thaliacea,* contain tunics (Trache et al., 2017). More than 2300 of *Ascidiacea* species are discovered over the globe. Among those species, sea squirt becomes the focus of research in cellulose extraction (Kargarzadeh et al., 2017). Other precious sources of cellulose are *Halocynthia papillosa*, *Metandroxarpa uedai* and *Halocynthia roretzi* (Kargarzadeh et al., 2017). Almost all tunicates share the same properties in which the purified cellulose fraction termed tunicin can be extracted in the tunic tissue. It is composed of about 27 % of nitrogen-containing compounds and 60 % of celluloses by dry weight (Trache et al., 2017). Due to the vast number of tunicate species available for cellulose production, the properties of cellulose yield might be very different. Tunicate cellulose consists of almost pure cellulose of CIβ allomorph type with high crystallinity (Kargarzadeh et al., 2017).

Several approaches are available to extract cellulose nanocrystals from tunicates. TEMPO-mediated oxidation, acid hydrolysis and enzymatic hydrolysis are the possible methods for cellulose nanocrystals preparation (Zhao et al., 2015). The recovery yield, molecular mass and size of the tunicate cellulose yield compared with the initial tunicate cellulose are summarised in Table 2.2:

Table 2.2: Recovery Yield, Molecular Mass and Size of the Tunicate Cellulose
Nanocrystals Compared to Tunicate Cellulose (Zhao et al., 2015)

	Tunicates cellulose	Enzymatic hydrolysis	TEMPO-mediated oxidation	Acid hydrolysis
Recovery yield (%)	100	73.4	62.8	30.0
Mass-average molar mass, M_w	731000	46300	30900	5720
Number-average molar mass, M_n	66000	29200	21800	2170
Polydispersity index, PDI	11.1	1.58	1.42	2.65
Size (nm)				
Width	16.04 ± 0.64	17.1 ± 2.7	15.9 ± 2.0	20.0 ± 2.8
Length	> 1000	> 1000	1590 ± 759	694 ± 312

2.2.3   Algae

There are various types of algae utilisable for cellulose nanocrystal extraction. For examples, grey, red, brown and green algae are the commonly used algae for cellulose nanocrystal extraction (George and Sabapathi, 2015). The fabrication of cellulose nanocrystals from red algae has hiked up tremendously from 5.3 million tons to 10.8 million tons in 2006 to 2011 (Trache et al., 2017). Hence, the Gelidium red algae seem to be a new promising choice for cellulose nanocrystal production other than woody biomass because of red algae availability (Trache et al., 2017). However, green algae are the most preferred species for cellulose extraction. Common cellulose-producing algae belong to the order Siphonocladales (such as *Boergesenia, Dictyosphaeria, Valonia* and *Siphonocladus*) and order Cladophorales (such as *Microdyction, Chaetomorpha, Cladophora* and *Rhizoclonium*) (George and Sabapathi, 2015).

Among the green algae, *Cladophora* or *Valonia* produces cellulose that exhibits a high degree of crystallinity. In this case, the degree of crystallinity can even exceed 95 % (Trache et al., 2017). Variety of the cellulose microfibril structures, however, depend on the origins of algae species due to the biosynthesis process.

Cellulose nanocrystals with a large aspect ratio can be extracted from the cell walls of algae. The processing method is quite similar to the cellulose nanocrystal extraction from plants. Generally, three processing steps are arranged chronologically, which are alkaline treatment, bleaching and acid hydrolysis (Chen et al., 2016). These treatments are compulsory in order to isolate highly-crystalline structure of cellulose nanocrystals from other contents. The studies of cellulose composition contained in the algae before and after the treatments are summarised in Table 2.3.

Table 2.3: Chemical Composition Analysis of Untreated Fibres, Alkali-treated Cellulose, Extracted Cellulose and Acid-treated Nanocellulose of Red Algae (Chen et al., 2016)

Material	α-cellulose (wt%)	Hemicellulose (wt%)	Lignin (wt%)	Ash (wt%)	Extractives (wt%)
Untreated fibres	17.2 ± 2.3	29.5 ± 1.4	4.5 ± 0.3	30.4 ± 0.5	17.6 ± 0.9
Alkali-treated cellulose	55.7 ± 1.1	8.2 ± 0.6	3.4 ± 0.6	27.4 ± 0.9	–
Bleached cellulose	88.6 ± 0.6	2.0 ± 0.2	0.7 ± 0.3	8.3 ± 0.2	–
Acid hydrolysed nanocellulose	90.8 ± 0.8	1.3 ± 0.1	<0.5	8.2 ± 0.1	–

2.2.4 Bacteria

Cellulose-producing bacteria have been deeply studied during the past decades, especially in term of their biosyntheses and applications (Machado et al., 2016). Bacterial celluloses are often the products of primary metabolic processes of cellulose-producing bacteria. The concoction of bacterial cellulose can be quite unique (such as *Gluconacetobacter xylinus*) (Kargarzadeh et al., 2017). With appropriate conditions to culture the medium, these bacteria are capable of synthesizing cellulose microfibrils in the form of a thick gel that constitute up to 99 % water (Kargarzadeh et al., 2017). Similar to other cellulose-synthesising sources, the cellulose resulted has a highly

crystalline network structure, enhanced biodegradability, superior chemical stability, high mechanical properties, high chemical purity, non-toxicity and lightweight (Trache et al., 2017). Due to its excellent properties, bacterial cellulose stands on par with celluloses produced from woody resources and is acknowledged as one of the sustainable sources for cellulose nanocrystal production to be applied in the reinforced polymer composite (Vasconcelos et al., 2017).

The culturing conditions for bacterial cellulose production rested upon a few criteria, which are carbon sources, incubation period, temperature, concentration of inoculum and rotational speed of impeller (Zeng et al., 2011). There are still many criteria that can affect the quality of cellulose produced. The parameters were previously optimised using an experimental design (Zeng et al., 2011).

Currently, the most efficient cellulose producers are gram-negative acetic acid bacteria or as known as *Acetobacter xylinum. Acetobacter xylinum* can transform organic substrates and glucose into cellulose within few days (Trache et al., 2017). This sole reason has made *Acetobacter xylinum* the highest producer of bacterial cellulose.

2.3 Oil Palm

Oil palm is a species of *Elaeis guineensis* that belongs to the Palmacea family. This species was originated from tropical forest of West Africa (Okahisa et al., 2018a). Nowadays, it becomes one of the most valuable plants in Indonesia, Thailand and Malaysia. Each of these countries has cultivated up to millions acre of oil palm. Typically, a normal oil palm has an average lifespan of approximately 25 years. A mature oil palm has 7 to 13 m in height and about 45 to 65 cm in diameter, which is measured 1.5 m from the ground level (Abdul et al., 2012). More than hundred years ago, oil palm plantation was introduced into Malaysia and subsequently, the very first cultivation of oil palm was carried out in Selangor in 1917 (Malaysian Palm Oil Council, 2012). Not long after that, large-scale plantation of oil palm scheme commenced and developed at a fast pace. Malaysia was acknowledged as the first country for large-scale planting and processing of oil palm (Fatah, 2015).

Malaysia is accounted for approximately 60 % of the oil and fat production of the world. It is also renowned as the world's second largest producer and exporter of the palm oil (Abdul et al., 2012). However, the production of palm oil in Indonesia has surpassed Malaysia and Malaysia is now the second largest palm oil producing country

with only a slight disadvantage compared to Indonesia (Malaysian Palm Oil Council, 2012). The processing of palm oil is mainly for the production of edible cooking oil. Palm oil yield is one of the largest oil production among other types of plant-based oils. For instance, the palm oil yield is approximately 8 times higher than sunflower oil, 6.5 times greater than rapeseed oil and almost 13 times more than soybean oil (Chang, 2014). This sole reason has made palm oil popular among the oil processors. In other words, oil palm plantation and palm oil production are still operating in enormous scale despite not being the largest producer of the world. Therefore, the amount of biomass generated from oil palm plantation and palm oil production will be tremendous, including fronds, empty fruit bunches, trunks and residue biomass fraction (Derman et al., 2018). Implicitly, if this large amount of oil palm biomass is not handled appropriately, it will definitely induce a severe environmental menace.

2.3.1   Oil Palm Biomass

Biomass is the general term for all organic derivatives that originate from living organisms and plants. In oil palm biomass case, it is a by-product of oil palm agricultural wastes that occasionally left in the plantation estate during pruning, milling and replanting of the oil palm tree (Wu et al., 2017). Generally, oil palm biomass is characterised as a lignocellulosic substance that comprises of 50 % of cellulose, 25 % of lignin and 25 % of hemicellulose in its cell walls (Abdul et al., 2012).

As mentioned above, oil palm biomass consists of few fragments such as oil palm fronds, oil palm empty fruit bunches, pressed fruit fibers, palm oil mill effluents and oil palm fronds (Chang, 2014). Among those oil palm biomasses produced, oil palm frond has the largest constituent, which is up to 70 % of total biomass, whereas empty fruit bunch and oil palm trunk comprise of 10 % and 5 % of the total biomass generated, respectively (Fatah, 2015). Based on the facts, it was specified that approximately 89 % of the oil palm biomass contributed to the fertilizer and biofuel production annually. About 70 million tonnes of oil palm biomass, including fronds, empty fruit bunches and trunks, were generated in Malaysia during 2006 (Abdul et al., 2012). Obviously, this indicates that Malaysia is deluged by oil palm biomass. Not to mention that the growth of palm oil industry activities such as improvement of oil extraction rate, expansion of mill capacity and acceleration of oil palm replanting are forecasted to escalate the total oil palm biomass availability in Malaysia (Loh, 2017).

Due to this large amount of oil palm biomass accessible in Malaysia, it can be classified as sustainable and renewable sources that can be replenished from time to time. Thus, multiple applications of oil palm biomass have started to bloom and develop as researches discovered more and more functional status of oil palm biomass, suggesting that full valorisation of oil palm biomass is possible. Simultaneously, the studies on applications of oil palm biomass can help to relieve the disposal problems (Loh, 2017).

Intensive research and development (R&D) endeavour in the palm oil sector have created few applications in bio-based products via abundant oil palm biomass available in Malaysia (Palamae et al., 2017). The possible applications that can be implemented commercially are the extraction of cellulose nanocrystals, cellulose microfibrils and cellulose nanofibrils as reinforcing medium to be embedded in the matrices as an alternative material for hybrid composites, bio-composite industries and pulp and paper industries (Abdul et al., 2012).

2.3.2   Oil Palm Empty Fruit Bunch (EFB)

Empty fruit bunch is the remaining portion of fresh fruit bunch after the fruits are extracted or removed prior to oil pressing. Empty fruit bunches are solid residues that are estimated to account for one-fifth of the fresh fruit weight (Chang, 2014). Before the exploration of empty fruit bunches as sustainable feedstocks for cellulose nanocrystal extraction, empty fruit bunches were converted into fuel to produce steam by incineration (Chang, 2014). The resulting ashes will be applied as soil conditioner and fertilizer as the ashes contain some precious nutrients and trace elements that are beneficial to the plants (Zhengqing Zhang et al., 2018). Incineration of empty fruit bunches, however, is not encouraged due to the large amount of greenhouse gases emitted to the environment, especially carbon dioxide gas (Hwang et al., 2017). Carbon dioxide gas is well-known in trapping radiation and heat in the atmosphere that could lead to global warming. The emission of carbon dioxide gas is expected to raise several global issues. Naturally, empty fruit bunches disposal will rest upon the decomposition method or to be used as organic mulch in the plantation (Anyaoha et al., 2018). Therefore, development to valorise empty fruit bunches should be encouraged and implemented.

Empty fruit bunch is a bulky brown bunch that is irregular in shape. It is approximately 3.5 kg in mass, has a thickness up to 130 mm, 300 mm width and 300

mm in length (Chang, 2014). Due to the steam sterilisation process in palm oil processing and natural way of maturation, empty fruit bunches usually encompasses a considerable amount of moisture (Loh, 2017). Table 2.4 summarises some materials and chemical compositions in dried empty fruit bunches. Table 2.5 discloses the composition of various types of celluloses in untreated and pre-treated empty fruit bunches. From Table 2.5, it shows that α-cellulose is dominant in empty fruit bunches, which is responsible for higher cellulose yield in cellulose nanocrystal extraction. Thus, empty fruit bunch is indeed a viable source available for the manufacturing of cellulose nanocrystals and its derivatives.

Table 2.4: Chemical Composition of Empty Fruit Bunch (Chang, 2014)

Properties	Values
Moisture (%)	2.40 – 14.28
Proximate analysis based on dry basis (wt%)	
Volatile matter	70.03 – 83.86
Fixed carbon	8.97 – 18.30
Ash	1.30 – 13.65
Ultimate analysis based on dry and ash-free basis (wt%)	
Carbon (C)	43.80 – 54.76
Hydrogen (H)	4.37 – 7.42
Oxygen (O)	38.29 – 47.76
Nitrogen (N)	0.25 – 1.21
Sulphur (S)	0.035 – 1.10
Chemical composition based on dry basis (wt%)	
Cellulose	23.7 – 65.0
Hemicellulose	20.58 – 33.52
Lignin	14.1 – 30.45
Extractive	3.21 – 3.70

Table 2.5: Chemical Composition of Different Types of Cellulose in Untreated and Pre-treated Empty Fruit Bunch Fibres (Ying et al., 2014)

	Untreated EFB fibres	Water pre-treated EFB fibres	Acid pre-treated EFB fibres	Alkaline pre-treated EFB fibres
Solid yield (wt%)	100	51.1	53.0	53.8
Holocellulose (wt%)	88.1 ± 1.0	67.8 ± 2.4	69.7 ± 0.3	87.9 ± 1.0
α-cellulose (wt%)	56.0 ± 0.5	72.6 ± 0.4	69.3 ± 0.6	57.1 ± 0.1
β-cellulose (wt%)	<0.1 ± 0.6	20.4 ± 0.3	25.7 ± 1.0	3.9 ± 0.2
γ-cellulose (wt%)	44.0 ± 0.2	7.0 ± 0.1	5.0 ± 0.4	39.0 ± 1.0

Apart from that, the employment of empty fruit bunches in cellulose nanocrystal production meets the requirements and principles of life-cycle assessment (LCA). Life-cycle assessment is the investigation of the input, output, products and the possible environmental consequences arouse from products (Montafia and Gnansounou, 2017). The methodology involves the study of the entire life cycle of the products from raw materials, production processes, transportation and distribution of products and lastly the utilisation of the products to the end of life stage (Vaskan et al., 2018). This assessment evaluates the environmental impacts of the employment of empty fruit bunches as the sustainable source of cellulose nanocrystal extraction. In this case, expansion of empty fruit bunch applications can reduce oil palm biomass wastes, suggesting that it is beneficial to both environment and economy (Abdulrazik et al., 2017).

2.4   Cellulose Nanocrystal Production Methods

Cellulose nanocrystal isolation from lignocellulosic arrays of empty fruit bunches necessitates a series of processes. This series of processes is generally divided into two stages in which the first stage is the pre-treatment and the second stage is the cellulose nanocrystal isolation. Pre-treatment or solvent extraction is significant to eliminate extractives, lignin and hemicellulose content from the empty fruit bunch fibres. There are various types of extractives exist in empty fruit bunch fibres, such as lignans, flavonoids, waxes and complex phenolics (Taflick et al., 2017). However, after this step, pre-treatment is only half-completed. Bleaching process is necessary to achieve

the desired degree of whiteness. The main shortcoming of bleaching is the formation of dioxins, which is a toxic organic compound (Taflick et al., 2017).

Subsequently, cellulose nanocrystals can be extracted by hydrolysis under controlled conditions. Most commonly used hydrolysis agent is acid. As the amorphous region subsides in the remaining cellulose is rather weak, it is susceptible to acid attack and destroyed, leaving only cellulose with strong crystalline segments (Achaby et al., 2018). At this stage, cellulose nanocrystals extracted are needle-shaped nanoparticles with high surface area, aspect ratio and crystallinity (Taflick et al., 2017). Homogenisation will be required in the next step to uniformly disperse the cellulose nanocrystals contained in suspension as tiny particles have a high tendency to agglomerate. Finally, the cellulose nanocrystal suspension will be freeze-dried to obtain a bright-white solid sample.

2.4.1   Pre-treatment of Empty Fruit Bunches

Pre-treatment process is suggested as the first stage of the cellulose nanocrystal extraction from various biomass sources. The functions of pre-treatment are to effectively dissociate the natural recalcitrance besides altering the macroscopic and microscopic size, biomass chemical composition and structure from fibers (Harmsen et al., 2010). This operation can significantly improve downstream processes efficiency for cellulose extraction. In this case, cellulose, hemicellulose and lignin are contained in the bulk empty fruit bunch fibers. Thus, the main pre-treatment is to segregate desired cellulose from lignin and hemicellulose as depicted in Figure 2.1. Generally, pre-treatment can be classified into few categories, which are physical, biological, chemical and multiple or combined pre-treatment such as ammonia fiber freeze explosion (AFEX), CO_2 explosion pre-treatment, sulphite pre-treatment and steam explosion to overcome the recalcitrance of lignocellulose (Harmsen et al., 2010).

Effect of Pretreatment

Cellulose

Lignin

Amorphous Region

Crystalline Region

Pretreatment
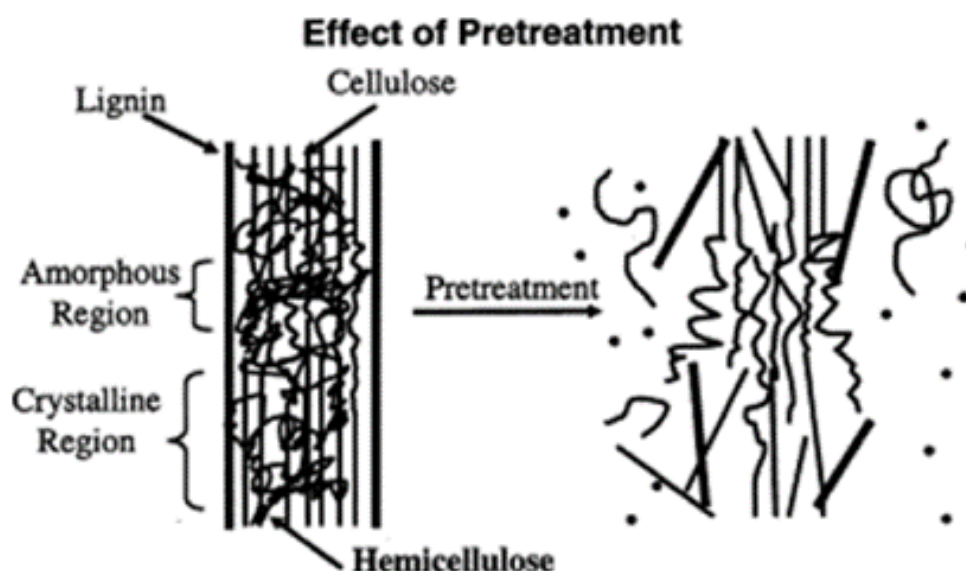
Hemicellulose

Figure 2.1: Illustration of Pre-treatment Process in Empty Fruit Bunch Fibres (Adapted from Harmsen et al., 2010)

2.4.1.1 Alkali Pre-treatment

The liquid agent of pre-treatment, NaOH, should be transported uniformly into the pores of lignocellulose. The transportation mechanisms of the pre-treatment agent can be classified into two. First, it involves liquid agent penetration into the capillaries. Second, it involves diffusion of the liquid agent via cell walls, pit membranes and interfaces (Harmsen et al., 2010). Penetration refers to the flow of liquid agent into the air-filled pores of the lignocellulose, which is assisted by hydrostatic pressure, whereas diffusion can be defined as the diffusion of soluble substances and ions via the layer of water located in the cell wall, pit membrane structure and interfaces that are affected by variation in concentration gradient (Sun and Cheng, 2002). In comparison, diffusion is a slow process. Initially, the sodium hydroxide solution must penetrate into lignocellulose. At this stage, penetration is the main mechanism. New channels or pores will be created along with the initial reactions such as lignin removal on the surface of lignocelluloses. This occurrence will further enhance the penetration of sodium hydroxide solution into the lignocellulose. Besides, the penetration of sodium hydroxide solution into the matrices of lignocellulose during the pre-treatment can be amplified by the swelling of lignocellulose (Xu et al., 2016). After complete penetration of sodium hydroxide solution into the pores of lignocellulose biomass, diffusion process will take place. In this process, molecular diffusion replaces the reactants after they are consumed in chemical reactions with lignocelluloses. The

transfer of sodium hydroxide solution and dissolved substances from lignocelluloses will occur via diffusion. Therefore, the degradation reactions of lignocellulose can be considered as a diffusion-controlled mechanism.

The chemical reactions between the alkaline solution and lignocelluloses mainly involve cellulose, hemicellulose and lignin. Lignin reactions lead to the dissolution and degradation of lignin, which can enhance the enzymatic hydrolysis in the following steps (Sun and Cheng, 2002). Alkali pre-treatment can efficiently break the ester bonds cross-linking xylan and lignin via solvation and saponification (Liu et al., 2018). Typical lignocellulose degradation of lignin is the fracture of the phenol-type α-aryl ethers, the cleavage of the phenol-type β-aryl ethers and the fracture of the non-phenol-type β-aryl ethers, whereas the decomposition of amorphous cellulose and hemicellulose are represented by cellulose peeling reaction, alkaline hydrolysis of cellulose and the sulphide fracture of the phenol-type β-aryl ethers (Xu et al., 2016). The lignin, hemicellulose and amorphous cellulose degradation mechanisms are illustrated in Figure 2.2, 2.3, 2.4 and 2.5 (Xu et al., 2016).
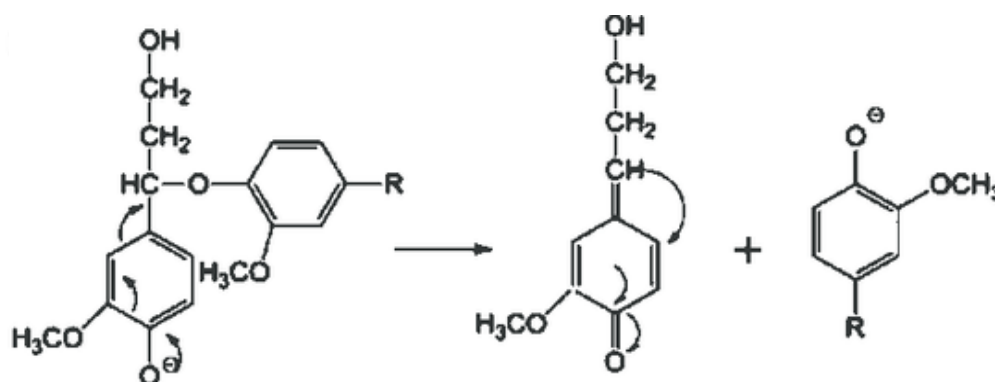
Figure 2.2: Reaction of Lignin under Alkali Pre-treatment: Fragmentation of the Phenol Type α-aryl Ethers (Adapted from Xu, Li and Mu, 2016)
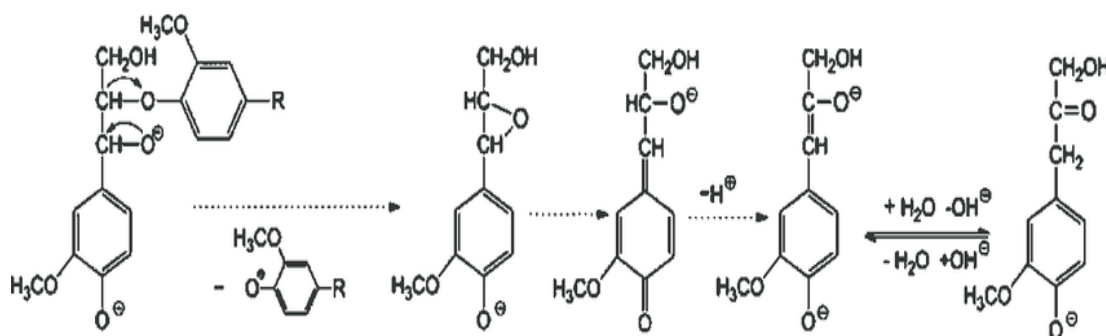
Figure 2.3: Reaction of Lignin under Alkali Pre-treatment: The Cleavage of the Phenol Type β-aryl Ethers (Adapted from Xu, Li and Mu, 2016)
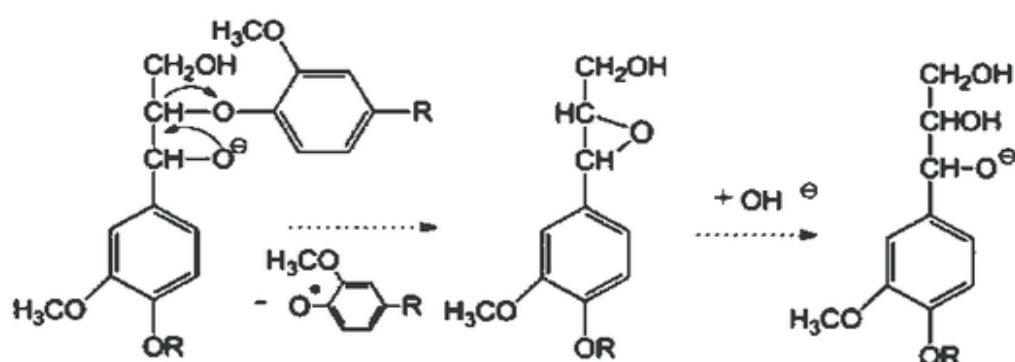
Figure 2.4: Reaction of Lignin under Alkali Pre-treatment: The Fracture of the Non-phenol Type β-aryl Ethers (Adapted from Xu, Li and Mu, 2016)
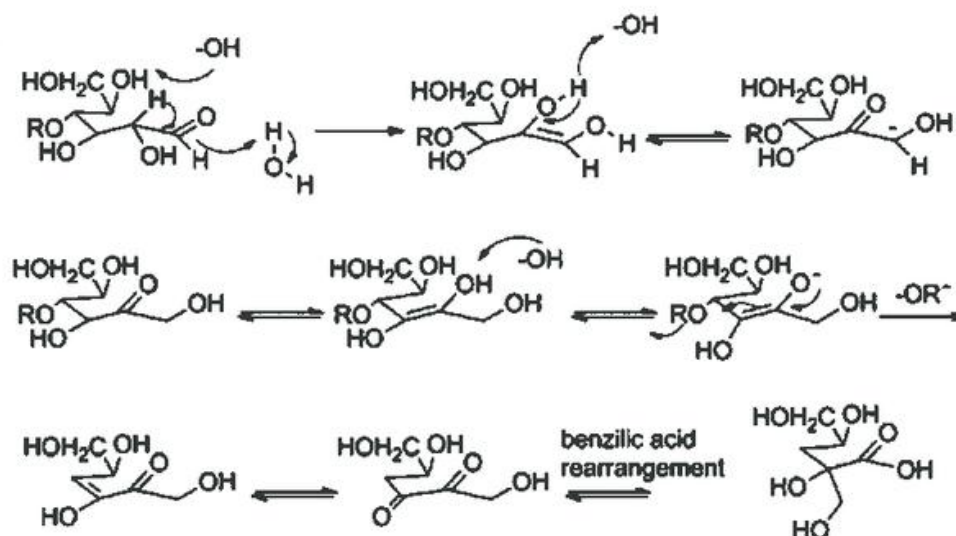
Figure 2.5: Reaction of Lignin under Alkali Pre-treatment: Peeling Reaction of Cellulose (Adapted from Xu, Li and Mu, 2016)

2.4.1.2   Hydrothermal Pre-treatment

Hydrothermal pre-treatment is the refinement of lignocellulosic biomass with the aids of hot water under high pressure such as steam explosion. Hydrothermal water and hot compressed water are equivalent terms that can be defined as water under elevated pressure and temperature. At this state, hydrogen bonds in water are weakened and dissociate to form aggregates of concentrated molecules. This can induce changes in physiochemical characteristics of water and subsequently lead to decomposition of lignocellulosic biomass structures, causing cellulose to be separated.

Hydrothermal pre-treatment is working based on short-term heating in a hot high-pressure saturated steam at a temperature of 180 to 210 °C (Kargarzadeh et al., 2017). This condition is maintained for a few minutes. It induces partial hydrolysis and expansion of the fiber cell walls. This pre-treatment step, in the presence of compressed water, is completed with a sudden decompression. This is when the flash evaporation of water induces a great force and lead to the rupture of material (Gao et al., 2016). This effect results in a considerable breakdown of the plant material structure. In other words, this will lead to the degradation of lignin, fibrillation of fibres and hydrolysis of hemicellulose. The dominant factors that can affect the reaction are the temperature of medium and reaction time. The addition of certain chemicals, for instance, sodium hydroxide or sulphuric acid, can promote hydrothermal efficiency (Kargarzadeh et al., 2017).

The purpose of hydrothermal pre-treatment to alter the structure of lignocellulosic biomass, especially on lignin and hemicellulose. Different from cellulose, hemicellulose is heterogeneous, branched and amorphous polysaccharides, which is less stable than the cellulose (Yu et al., 2013). During the hydrothermal pre-treatment, the organic acid and water released from hemicellulose side chain will catalyse the dissociation of long hemicellulose chains to become a shorter chain of oligomers (Patel et al., 2016). The disintegration of bonding between hemicellulose and lignin leads to the distortion of the hydrogen bond between the cellulose. Examples of well-known reactions for degradation of hemicellulose are hydrolysis of hemicelluloses to sugars, followed by dehydration of hexoses and pentoses. On the other hand, lignin appears as a complex amorphous structure (Gao et al., 2016). Simultaneously, the cellulose and hemicellulose are tightly connected to the lignin by covalent and hydrogen bonds. During the hydrothermal pre-treatment, the depolymerization is signaled by cleavage of ester bonds and β-O-4 linkages whereas

repolymerization is represented by acid-catalysed condensation. This can produce aromatic compounds with less side-chain (Gao et al., 2016). The fragmentation of lignin is shown in Figure 2.6. However, it is virtually impossible to eliminate all the lignin during a hydrothermal pre-treatment because of the re-deposition of lignin on biomass surface.

Figure 2.6: Fragmentation of Lignin Structure During a Hydrothermal Pre-treatment (Adapted from Gao et al., 2016)

2.4.1.3 Organosolv and H_2O_2 Pre-treatment

Organosolv pre-treatment is a process to extract lignin from lignocellulosic feedstocks with organic solvents or their aqueous solutions (Zhao et al., 2009). Organosolve pre-treatment has several advantages. First, recovery of organic solvents is relatively easy by using distillation and it is readily recycled for another cycle of pre-treatment. The chemical recovery in organosolv pre-treatment can isolate carbohydrates such as hemicellulose (as syrup) and lignin (as a solid material). Second, organosolv pre-treatment makes use of all the biomass components. Organosolv pre-treatment can proceed in a large number of aqueous organic solvent systems with or without added catalysts in the temperature range of 100 to 250°C with moderately high efficiency (Zhao et al., 2009).

Organic solvents that are commonly used varies from low boiling point solvent such as methanol to high boiling point solvent such as glycerol. In most cases, alcohols are often the main choice for organic solvents. Recent studies discovered that normal primary alcohols will be a better agent compared to secondary or tertiary alcohols in delignification processes (Zhao et al., 2009). Thus, methanol and ethanol are undoubtedly preferred for alcohol-based organosolv pre-treatment. Besides, ethanol and methanol have the advantage in ease of recovery by simple distillation with low

energy requirement due to its low boiling point. In this pre-treatment, hydrolysis of the internal bonds between lignin-hemicellulose and lignin bonds are the dominant reaction. For instance, the 4-O-methylglucuronic acid ester bond is hydrolysed from the α-carbons between the lignin units (Zhao et al., 2009). The mechanism of organosolv pre-treatment using ethanol as organic solvent is illustrated in Figure 2.7.
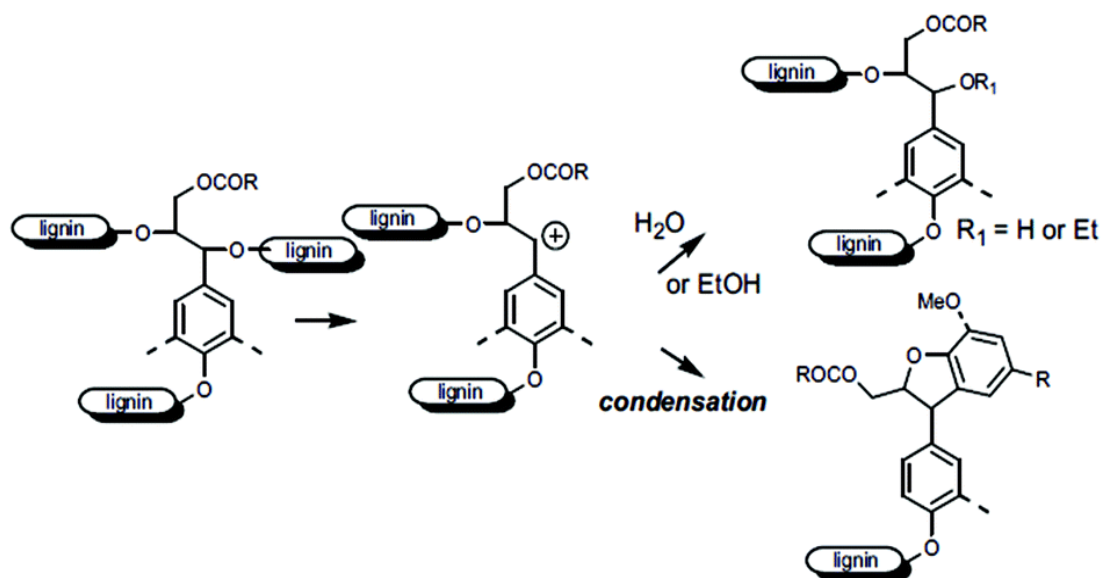
Figure 2.7: Mechanism of Organosolv Pre-treatment of Cellulose Using Ethanol (Adapted from Zhang et al., 2016)

Other reactions occurred during organosolv pre-treatment are acid-catalysed degradation of the monosaccharides into furfural and 5-hydroxymethyl furfural in addition to the hydrolysis of glycosidic bonds in hemicelluloses to a smaller extent (Zhang et al., 2016). Not to mention that condensation reactions also exist between lignin and these reactive aldehydes.

When acid catalysts are incorporated, the rate of delignification will increase and higher yields of xylose can be obtained. Catalysts that can be used including magnesium, calcium or barium chloride or nitrate and mineral acids (Zhao et al., 2009). After this stage, aqueous hydrogen peroxide will further delignify pre-treated empty fruit bunches. This step is often addressed as bleaching. Most of the lignin and hemicellulose will be solubilised, but the cellulose will remain in solid form. In short, organosolv pre-treatment yields three distinct fractions, which are aqueous hemicellulose stream, a relatively pure cellulose fraction and dry lignin. Another common suggestion to improve the selectivity of cellulose during pre-treatment is to

combine organosolv pre-treatment with ultrasound technology. Ultrasound provides physical augmentation via mass transfer, surface erosion and shear forces as well as producing oxidizing radical chemical effects (Ofori-Boateng and Lee, 2014). Thus, it encourages the cleavage of linkages between the hemicellulose and lignin by degrading lignin compounds via hydroxyl attack of the phenolic ring (Ofori-Boateng and Lee, 2014).

2.4.2   Cellulose Nanocrystal Extraction after Pre-treatment

Isolation of cellulose nanocrystals is the second stage in the production of cellulose nanocrystals from the source fibers. Isolation of cellulose nanocrystals usually involves acid hydrolysis. Other methods that can be used including enzymatic hydrolysis, TEMPO oxidation and the use of ionic liquid for the isolation of cellulose nanocrystals. Subsequently, the post-treatment of hydrolysed celluloses, including sonication and purification, can ensure that the cellulose nanocrystals extracted are well-dispersed without agglomeration (Chieng et al., 2017).

2.4.2.1   Acid Hydrolysis

Cellulose nanocrystals are commonly prepared by acid hydrolysis of a purified cellulose starting material such as cellulose microfibres (CMF). The acid is used to hydrolyse the amorphous region of the cellulose in which the disordered regions of cellulose can be disintegrated by hydrolytic cleavage of the glycosidic bond, whereas the highly ordered cellulose fractions will remain unconverted as it is less susceptible to acid attack (Cheng et al., 2017). This can produce a suspension of rod-like whiskers whose dimensions rely on cellulose origin and pre-treatment method (Dong et al., 2016). Normally, the length and diameter of nanocellulose are less than 1 μm and 100 nm, respectively, without agglomeration (Cheng et al., 2017).

Acid hydrolysis of purified cellulosic material is carried out using strong mineral acids under controlled acid concentration, temperature and reaction time to produce a high yield of cellulose nanocrystals. Various mineral acids can be used for this purpose (such as sulphuric acid, phosphoric acid, hydrochloric acid, nitric acid, formic acid and hydrobromic acid) (Kargarzadeh et al., 2017). In this aspect, the effect of mixture consists of hydrochloric and organic acids (such as butyric acid) as the hydrolysing agent has also been studied. When sulphuric is used as a hydrolysing agent, it reacts with the hydroxyl groups on the surface of nano-crystallites, which leads to

the formation of sulphonic groups that are negatively charged (Kargarzadeh et al., 2017). The acid hydrolysis of amorphous regions of cellulose chains encompasses rapid protonation of glucosidic oxygen or cyclic oxygen. Subsequently, the addition of water will cause a slow splitting of the glucosidic bonds as shown in Figure 2.8 (Kargarzadeh et al., 2017).
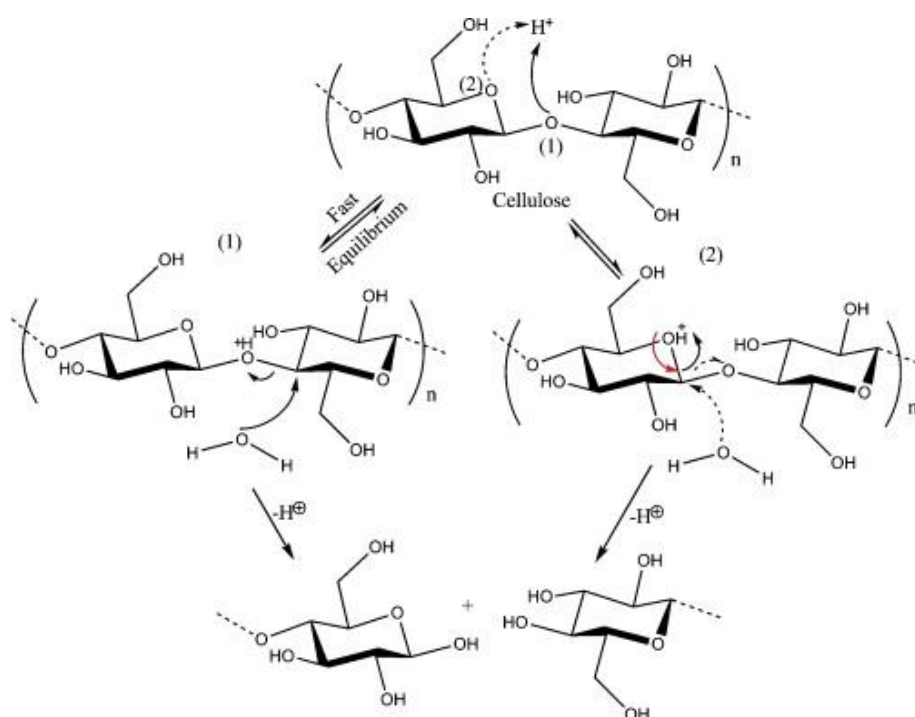
Figure 2.8: Mechanism of Cellulose Chain Acid Hydrolysis (Adapted from Kargarzadeh et al., 2017)

This can result in short chain fragments while preserving the basic backbone structure. The hydrolysis of cellulose by sulphuric acid also involves partial esterification of the hydroxyl groups as shown in Figure 2.9. Esterification causes the attachment of negatively charged sulphate groups on the cellulose nanocrystal structure (Dong et al., 2016). This induces the repulsion forces between cellulose layers that can prevent cellulose nanocrystals from forming aggregates. This phenomenon is also known as anionic stabilisation (Cheng et al., 2017).
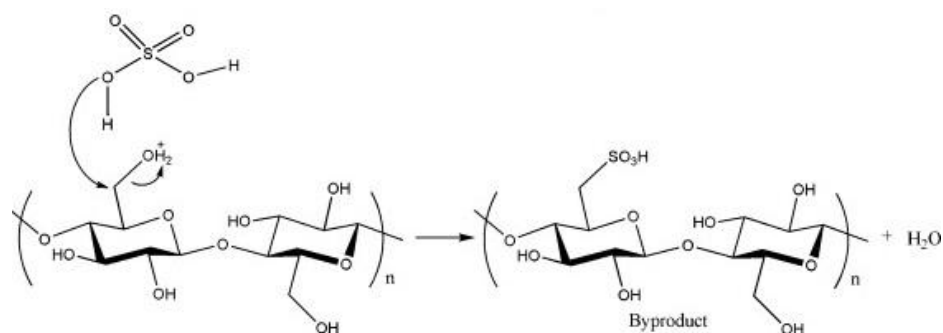
Figure 2.9: Mechanism of Cellulose Nanocrystal Esterification (Adapted from Kargarzadeh et al., 2017)

Post-treatment of cellulose nanocrystal dispersion in a strong acid is commonly diluted with water and washed using successive centrifugations (Shaheen and Emam, 2018). This is to neutralise the suspension and discourage the formation of charges on the surface of cellulose nanocrystals to prevent agglomeration. Agglomeration will enlarge the size of cellulose nanocrystals, thus reduces the dispersion and lower down the values as a composite reinforcing agent. Therefore, post-treatment is a critical step in acid hydrolysis.

2.4.2.2   Ionic Liquid Hydrolysis

In addition, cellulose nanocrystal preparation can proceed via ionic liquid hydrolysis. Ionic liquid is a group of organic salts with a melting point less than 100 °C (Kargarzadeh et al., 2017). It is commonly used due to its valuable properties such as low vapour pressure, non-flammability, chemically and thermally stable and environmental friendly (Shaheen and Emam, 2018). Ionic liquid is generally introduced to microcrystalline cellulose as solvent and catalyst to produce cellulose nanocrystals. Typical ionic liquid utilised is 1-butyl-3-methylimidazolium hydrogen sulphate (bmimHSO$_4$) (Tan et al., 2015a). Studies have found that bmimHSO$_4$ is capable of dissolving cellulose. Specifically, bmimHSO$_4$ causes hydrolytic cleavage of glycosidic bonds between two anhydroglucose units (Tan et al., 2015a). Not to mention that esterification of hydroxyl groups on cellulose chemical structure also can happen due to the presence of sulphate groups in bmimHSO$_4$ (Shaheen and Emam, 2018). Hence, amorphous regions in microcrystalline cellulose are selectively removed, forming highly-crystalline cellulose nanocrystals after several cycles of

centrifugation and sonication. The illustration of bmimHSO$_4$ catalysed hydrolysis is depicted in Figure 2.10.

The main benefit of this treatment is that the ionic liquid will not be consumed in the reactions as it can always be recovered via ion exchange, reverse osmosis and evaporation method (Kargarzadeh et al., 2017). The recovered ionic liquid can be reused for another cycle of microcrystalline cellulose hydrolysis process. This feature exhibits the strength of ionic liquid as an eco-friendly compound with no hazardous product will be synthesized (Tan et al., 2015a). The main disadvantage of the ionic liquid is its time-consuming treatment process, which can decrease the productivity (Salminen et al., 2017).
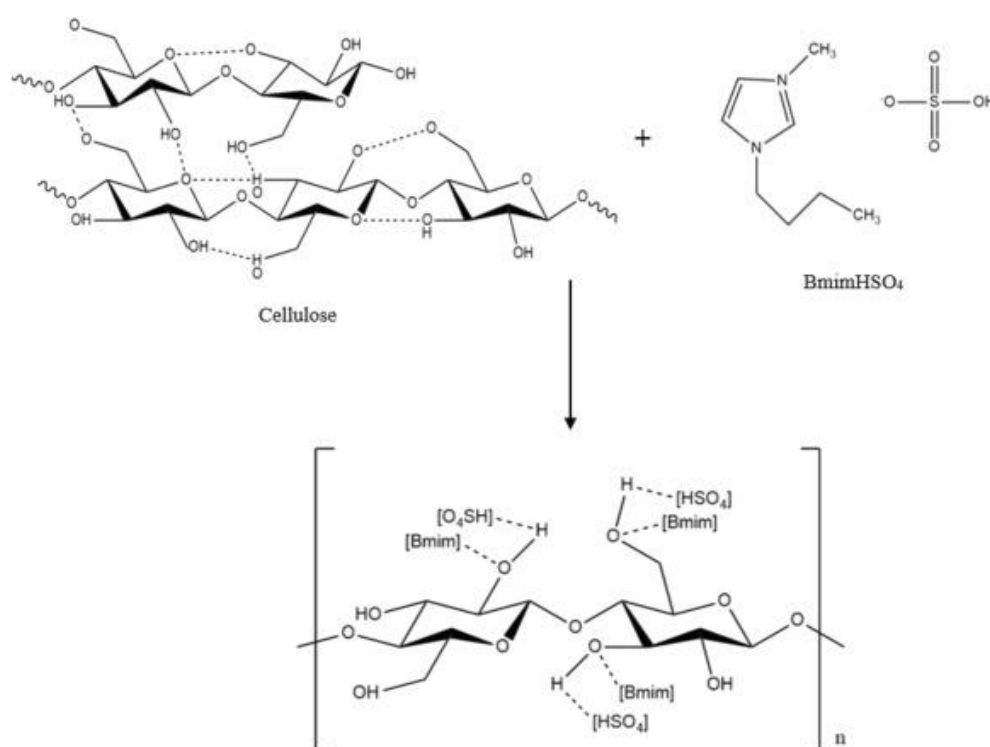
Figure 2.10: Mechanisms of Ionic Liquid Hydrolysis of Cellulose (Adapted from Kargarzadeh et al., 2017)

2.4.2.3 (2,2,6,6-Tetramethylpiperidin-1-yl)oxyl (TEMPO)-Mediated Oxidation

Oxidation is another alternative way to synthesize cellulose nanocrystals. By using microcrystalline cellulose as starting material, the high surface charge of TEMPO exists in carboxylic form is introduced into cellulose chemical structure to disintegrate microcrystalline cellulose to yield cellulose nanocrystals. TEMPO is also known as (2,2,6,6-tetramethylpiperidine-1-yl)oxyl radical (Kargarzadeh et al., 2017). After the

introduction of TEMPO, sodium bromide and sodium hypochlorite solutions are added to initiate the reactions (Salminen et al., 2017). As charges are introduced on the cellulose fibril surface, hydroxylation can take place by displacing sodium ions on the hydroxyl group, which is the main disordered segment in the native cellulose microfibril as shown in Figure 2.11.

This oxidation method must couple with mechanical pre-treatment for cellulose nanocrystal extraction. Mechanical pre-treatment is important because nanoparticles from the fibril matrices will be the key components to produce a high yield of cellulose nanocrystals. Post-treatment such as sonication and centrifugation is necessary in the process, which is similar to acid hydrolysis treatment (Salminen et al., 2017). The benefit of TEMPO-mediated oxidation is low energy consumption as compared with acid hydrolysis and ionic liquid treatment. Also, it can be used to synthesize other types of cellulose such as CMF and CNF combined with high-pressure homogenizer (HPH) (Kargarzadeh et al., 2017). However, the oxidation process also encourages the formation of aldehyde groups, which will reduce the thermal stability and lead to discoloration of the oxidised cellulose after drying (Kargarzadeh et al., 2017).
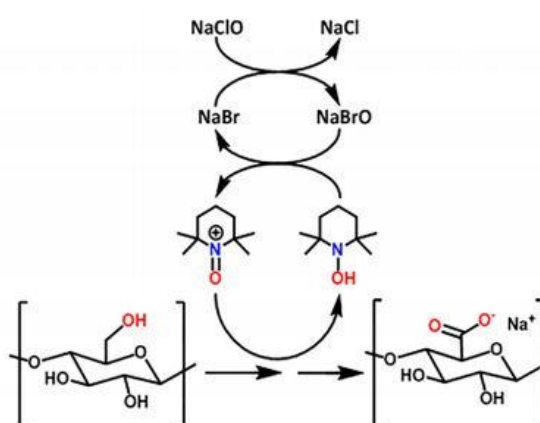
Figure 2.11: Mechanisms of TEMPO-mediated Oxidation of Cellulose (Adapted from Salminen et al., 2017)

2.5   Characterisation of Cellulose Nanocrystals using Different Techniques

In order to investigate the surface morphology, topography, crystallographic structure, elemental and thermal properties of cellulose nanocrystals extracted by acid-hydrolysis from empty fruit bunches, various types of characterisation techniques and instrumentations are introduced. Different characterisation techniques reveal different

information of the analyzed sample. Morphology and topography of the samples can be evaluated using transmission electron microscopy (TEM) and field emission scanning electron microscopy (FESEM) (Asad et al., 2018). As for crystallographic structures and elemental properties, cellulose nanocrystals can be analysed using X-ray diffractometer (XRD) and Fourier transform infrared spectroscopy (FTIR), respectively. The dynamic light scattering (DLS) technique can be used to determine the particle size distribution in cellulose nanocrystals (Naduparambath et al., 2018).

2.5.1   Transmission Electron Microscopy, TEM

Transmission electron microscopy (TEM) is a common technique used to acquire images of cellulose nanocrystals at high magnification (Kumar et al., 2014). It is a microscopy technique that utilises the electron beams to provide morphological, compositional and crystallographic information on samples (Asad et al., 2018). In TEM, a primary electron beam of high energy and intensity passes through a condenser to produce parallel rays that impinge on the ultra-thin sample (Chorkendorff and Niemantsverdriet, 2003). It interacts with the sample as it passes through. The transmitted electrons form a two-dimensional projection of the sample mass. The image is then focused on an imaging device including a layer of photographic film and a fluorescent screen. Therefore, one can determine the sample particle size and inter-layer spacing of nanoparticles at a corresponding diffraction plane from the TEM image.

Due to its small-sized in nature, consisting of hydrogen bonding and low electron density, individual cellulose nanocrystals are difficult to be imaged (Kaushik et al., 2015). Thus, TEM with high resolution and magnification is commonly used to investigate the defined shapes and distribution of cellulose nanocrystals. Apart from that, diameter of cellulose nanocrystals can be determined as well in order to identify the possible occurrence of agglomeration. Morphological characterisation using TEM in previous work revealed the appearance of needle-like shaped cellulose nanocrystals as depicted in Figure 2.12 (Li et al., 2015). Figure 2.12 also compared cellulose nanocrystals prepared by different approaches.
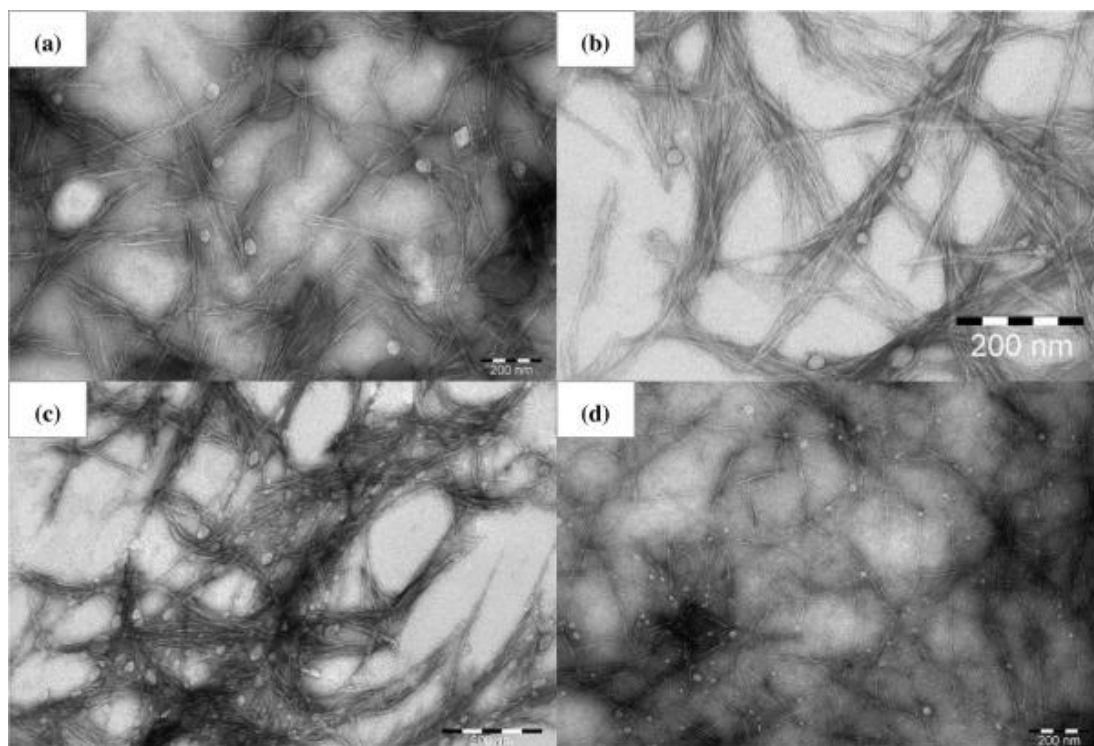
Figure 2.12: TEM Images of (a) Cellulose Nanocrystals Prepared by Sulphuric Acid Hydrolysis, (b) Cellulose Nanocrystals Prepared by Combination of Formic Acid and Hydrochloric Acid Hydrolysis, (c) Cellulose Nanocrystals Prepared by Formic Acid Hydrolysis and (d) Cellulose Nanocrystals Prepared by TEMPO-mediated Oxidation (Adapted from Li et al., 2015)

2.5.2   Field Emission Scanning Electron Microscopy, FESEM

FESEM, unlike normal optical microscope, functions based upon electrons instead of light (Chorkendorff and Niemantsverdriet, 2003). Electrons are negatively charged particles that can be released by emission source field and subsequently accelerated due to high electrical field gradient that is applied to it (Zhang et al., 2009). These liberated primary electrons will focus and deflect by electronic lenses in high vacuum column to produce narrow electron beams that will bombard the sample. As a result, secondary electrons are liberated from the impacted spot on the sample. The angle and velocity of the liberated secondary electrons are then captured, thus, generating an electronic signal that enabling video scan image to be perceived on the monitor (Wijeyesekera et al., 2016). In this way, the surface structures or topography of the cellulose nanocrystals produced can be observed and analysed.

Comparison is made between SEM and FESEM. In terms of resolution, FESEM is far better than SEM due to fact that the beam gun in SEM is thermionic

while the beam gun used in FESEM is electromagnetic (Chorkendorff and Niemantsverdriet, 2003). FESEM is capable of producing low-voltage images with a magnification factor up to 300,000 × and can detect or measure sample as small as 1 nm (Skoog, D. A., Holler, F. J., and Nieman, 1998). As cellulose nanocrystals are in nano-sized range, FESEM could be one of the suitable instruments that can be used to obtain high-resolution images. Example of cellulose nanocrystals observed under FESEM is illustrated in Figure 2.13.
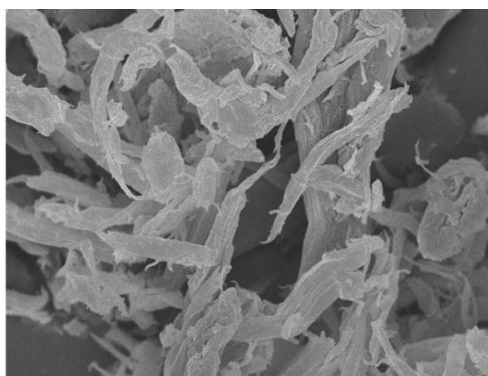
Figure 2.13: Surface Structures of Cellulose Nanocrystals under Field Emission-Scanning Electron Microscopy (Adapted from Yadav and Chiu, 2019)

2.5.3 X-ray Diffraction Analysis, XRD

XRD technology originated from physicist Max Von Laue in 1912. Max Von Laue discovered that crystalline materials can act as three-dimensional diffraction gratings for X-ray, in which the wavelengths are similar to the spacing of planes in a crystal lattice (Eckert, 2012). This discovery leads to the X-ray diffraction technique to characterise the crystallite size and orientation of crystallographic structure in powdered solid samples or polycrystalline. On top of that, X-ray diffraction can observe the variations in crystalline phases of the compound by lattice structural parameters means (Borchert, 2014). Generally, X-rays are produced by cathode ray tube (Chorkendorff and Niemantsverdriet, 2003). It heated up the filament to generate high concentration of electrons. Monochromatic radiation is produced as electrons, which are filtered by using the collimator and the radiation will then pass through the sample (Skoog, D. A., Holler, F. J., and Nieman, 1998). At this state, the electric vector of the radiation interacts with the electrons in the atoms of the sample. When X-rays are scattered by crystals, destructive and constructive interference will result among the scattered rays.

The principles of XRD analysis are founded upon Bragg's Law (Skoog, D. A., Holler, F. J., and Nieman, 1998). As X-ray strikes on crystal structure, part of the beam is scattered, unscattered beam will proceed to next planes and so on. The successive planes are separated by interplanar distance, this will yield constructive interference. Hence, the lattice spacing, *d*, can be measured by angle *2θ* obtained in the diffraction pattern and X-rays with a wavelength, *λ*, leave the crystal by applying the Bragg Equation 2.1.

$$n\lambda = 2d \sin \theta \qquad (2.1)$$

where

λ = Wavelength, nm

d   = Lattice plane distance, nm

θ = Diffraction angle, °

XRD analysis can be used to study the crystallinity of the cellulose nanocrystals by calculating the crystallinity index (CrI) and crystallite size (Kargarzadeh et al., 2015). With these information, the hypothesis of cellulose nanocrystals having a high degree of crystallinity can be verified. A sample spectrum of cellulose nanocrystals analysed by XRD is exhibited in Figure 2.14. It shows XRD spectra of cellulose nanocrystals under different treatments with similar obvious peak angle at approximately 16°, 22° and 34°.
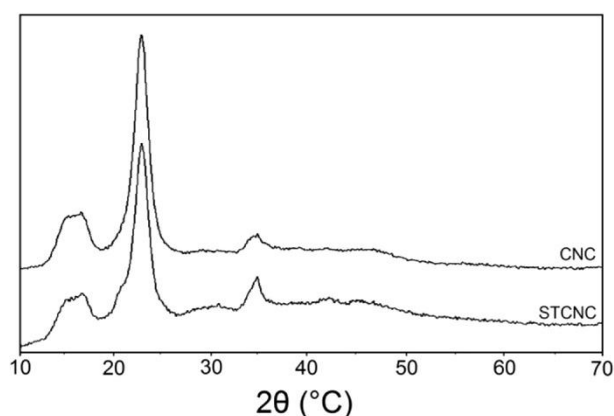
Figure 2.14: XRD Spectra of Cellulose Nanocrystals and Silane-treated Cellulose Nanocrystals (Adapted from Kargarzadeh et al., 2015)

2.5.4   Fourier Transform Infrared Spectrometry, FTIR

FTIR spectrometry is used to study the absorption of infrared radiation (Zhang et al., 2009). Molecular absorption of the radiation will promote the transition between vibrational and rotational energy levels of the ground electronic energy state (Skoog, D. A., Holler, F. J., and Nieman, 1998). This induces molecular vibration catagorised by bending and stretching movement. The absorbed infrared radiation will produce a net change of radiation transmittance that passes through the sample and the changes will be displayed on the spectrum (Jaggi and Vij, 2006). From the spectrum, identification of specific functional group is possible based on the peak observed due to vibrational movement. The variation of FTIR is obtained through the interferometer rather than the grating used in the conventional IR spectrometers (Ismail et al., 1997). Also, FTIR has greater resolution compared to dispersive IR, that allows the characterisation to be performed at a much greater accuracy.

FTIR spectrometry can be used to reveal the presence of lignin and hemicellulose in cellulose nanocrystals prepared by acid hydrolysis (Mazlita et al., 2016). It distinguishes the differences of cellulose nanocrystals extracted from microcrystalline cellulose and cellulose. This can be used to evaluate the production of cellulose nanocrystals. Besides, the transmittance in FTIR spectrum can provide a brief idea about the concentration of the sample (Griffiths, 1978). Figure 2.15 displays various spectra of cellulose nanocrystals that are produced by different treatments.
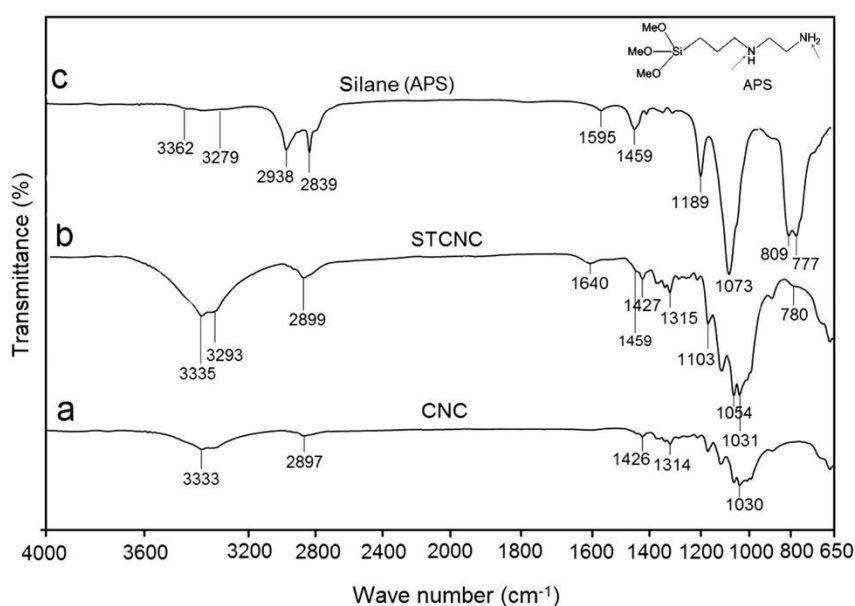
Figure 2.15: FTIR Spectra of Cellulose Nanocrystals Produced by Different Treatments (Adapted from Kargarzadeh et al., 2015)

Figure 2.15 shows various absorbance peaks of different functional groups. Stretching of hydroxyl group of cellulose lies in the wavenumber range of 3350 to 3200 cm^{-1}. Remarkably, the absorbance peak of C-H stretching group is noted around 3000 to 2840 cm^{-1}. The spectra of cellulose nanocrystals displayed the bending variations of C-H and C-O groups of the rings in polysaccharides and symmetrical bending of CH_2 at absorbance peak of 1315 cm^{-1} and 1426 cm^{-1}, respectively.

2.5.5 Dynamic Light Scattering, DLS

DLS is a technique that can be used to determine the average size distribution of particles contained in a sample (Ross Hallett, 1994). DLS technique is founded on light scattered by diffusing particles. In this case, DLS encompasses measurement of Doppler broadening of the Rayleigh-scattered light resulted from particles Brownian motion or translational diffusion (Skoog, D. A., Holler, F. J., and Nieman, 1998). This thermal motion lead to time fluctuation in broadening of Rayleigh line that is depicted as Lorentzian shape and scattering intensity. Concentration of the fluctuation is significant in macromolecular solutions (Skoog, D. A., Holler, F. J., and Nieman, 1998). Under these conditions, Rayleigh line width will be directly proportional to the coefficient of translational diffusion. Subsequently, particle size distribution data can be generated from existing results.

Determination of size distribution of rod-like cellulose nanocrystal particles could be proposed using translational diffusion coefficient (measured by DLS) to obtain dimensional information of cellulose nanocrystals (Boluk and Danumah, 2014). As DLS technique can obtain size information within few minutes for particles with diameters ranging from few nm to 5 μm, it is suitable to be applied on the cellulose nanocrystals for size verification while at the same time it can determine the occurrence of agglomeration between cellulose nanocrystal particles. Besides, DLS technique can be coupled with an electron microscope to determine the length and diameter of the particle in liquid to yield a greater accuracy result (Boluk and Danumah, 2014).

2.6 Summary

Various sources for the production of cellulose nanocrystals are considered in this review such as plants, tunicates, algae and bacteria (George and Sabapathi, 2015). The plant resources are subclassified to woody and non-woody sources, agro-industrial

biomass wastes and etc. Among these sources, oil palm empty fruit bunch has demonstrated its potential value as a viable sustainable source mainly due to its tremendous availability in Malaysia (Chang, 2014). As aforementioned, utilisation of empty fruit bunches is a green approach that unraveled oil palm empty fruit bunch waste disposal problem and by minimising greenhouse gases (Loh, 2017). Hence, this broadens the path to produce cellulose nanocrystals that have higher demand nowadays.

Despite being a promising feedstock for isolation of cellulose nanocrystals, empty fruit bunches possess one major drawback, which is the presence of hemicellulose and lignin together with cellulose in plant fibres (Harmsen et al., 2010). So, pre-treatment step is necessary to obtain final high purity cellulose nanocrystals. Few methods are proposed in this review. Each method has its advantages and disadvantages. Among all of these methods, alkali-based pre-treatment is considered to be one of the most promising pre-treatment methods (Harmsen et al., 2010). Chemical pre-treatment is the most extensively studied pre-treatment techniques. Chemical approach gives rise to high efficiency in the removal of impurities and relatively low energy consumption (Kargarzadeh et al., 2017). Similarly, sulphuric acid hydrolysis exhibits a greater advantage in term of conversion yield compared to other treatments. Yet, sulphuric acid hydrolysis of purified cellulosic material must be conducted under controlled acid concentration, temperature and reaction time to produce a high yield of cellulose nanocrystals (Kargarzadeh et al., 2017). Several researchers have proved that incomplete physical treatments and excessive sulphuric retention time will reduce the cellulose nanocrystals yield and degrade the quality of cellulose nanocrystals. Therefore, proper control of operating parameters must be emphasised.

Characterisation of cellulose nanocrystals extracted needs to be carried out to determine the presence of cellulose nanocrystals as well as its relative abundance, compositions and crystalline structure (Fatah, 2015). This determines the usefulness of cellulose nanocrystals generated for its downstream applications. In order to study the properties of cellulose nanocrystals, various instrumental analyses will be carried out. XRD, FTIR, TEM, FESEM and DLS are the appropriate techniques to characterise cellulose nanocrystals based on their relative integrated roles.

CHAPTER 3

METHODOLOGY AND WORK PLAN

3.1   Introduction

As cellulose nanocrystals have received a great amount of interest in industries and academic study owing to its superior physiochemical characteristics, new treatment and extraction procedures are currently under development to satisfy the increasing demand of manufacturing this bio-based nanomaterial. Cellulose nanocrystals is undoubtedly a promising candidate utilised in membranes, nanocomposites and even biomedical sectors (Trache et al., 2017).

The methodology to isolate cellulose nanocrystals is subdivided into four sections as depicted in Figure 3.1, such as pre-treatment, bleaching, cellulose nanocrystal extraction and post-treatment (Achaby et al., 2018). Role of pre-treatment and bleaching are to selectively dissociate the natural recalcitrance except for cellulose in order to enhance downstream processes in achieving a high purity of cellulose nanocrystals (Jönsson and Martín, 2016). Alkali pre-treatment is prevalent as biological and physical treatment pose few shortcomings. Biological treatment is a complex operation mode as culturing of bacteria or fungi is tedious and requires long residence time (Xu et al., 2016). Besides, physical treatment is usually associated with high energy demand that increases the overall cost of productions. Next, extraction of cellulose nanocrystals is performed by sulphuric acid hydrolysis (Achaby et al., 2018). In this case, the effectiveness to isolate crystalline domains of the cellulose microfibrils from amorphous domain is considered. Despite being a conventional approach, sulphuric acid hydrolysis is still relatively advantageous compared to new emerging technologies such as sub-critical water hydrolysis in terms of yield and cellulose nanocrystals properties (Trache et al., 2017). Ease of preparation is also considered for cellulose nanocrystal extraction from empty fruit bunches.
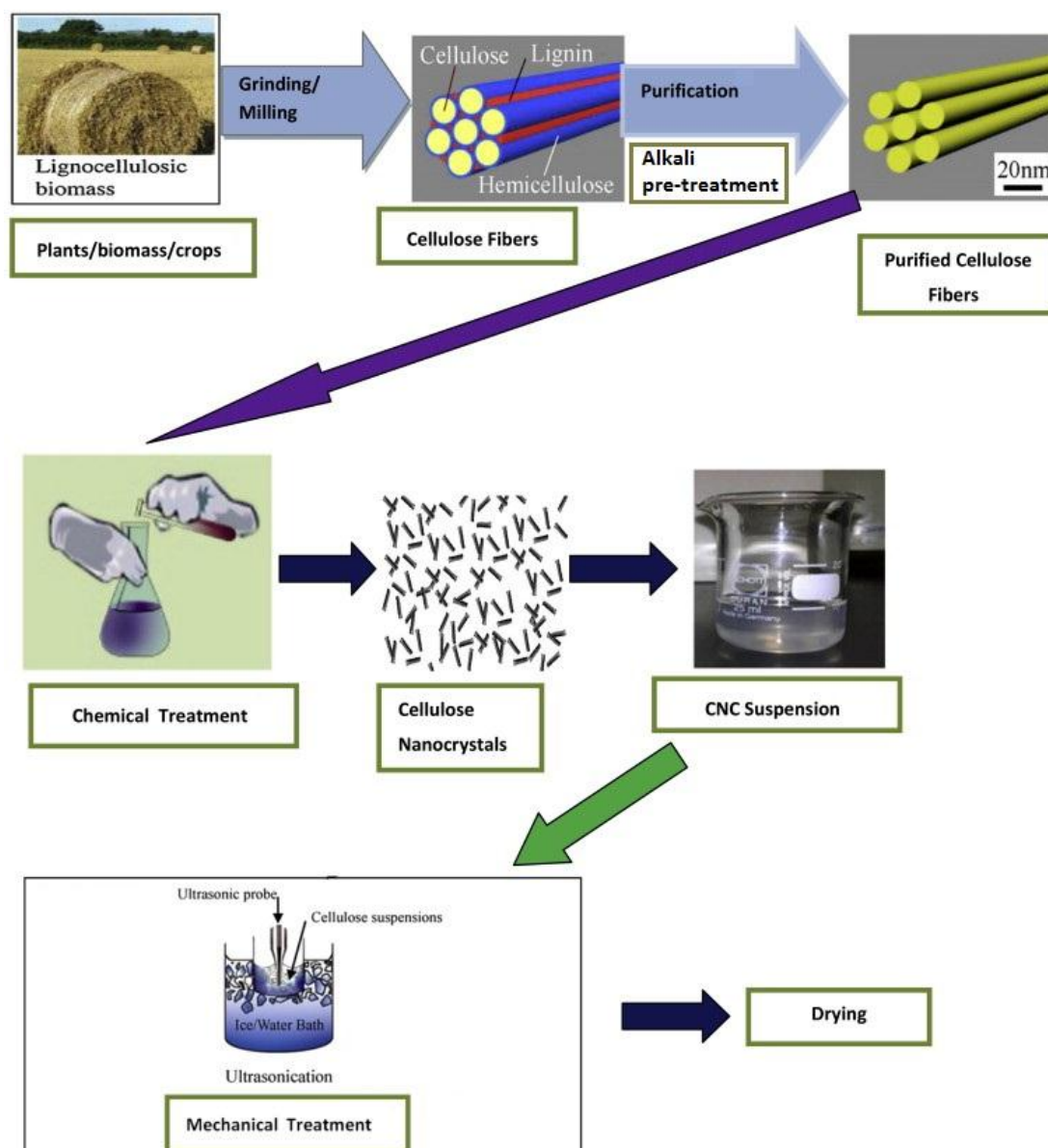
Figure 3.1: Step-by-step Cellulose Nanocrystal Preparation (Adapted from Ng et al., 2015)

After the extraction of cellulose nanocrystals, characterisation will be carried out. The objective of this work is mainly to identify the products generated via procedures described above, in both qualitative and quantitative means. Size, crystallinity, appearances, chemical structures and intensity are obtained through characterisation of cellulose nanocrystals (Budhi et al., 2018). With all of these criterions identified, results can be compared to previous studies to gauge the successfulness and applicability of experiment to produce high purity of cellulose nanocrystals.

3.2 Materials

The chemicals used throughout the study are listed in Table 3.1.

Table 3.1: Chemicals for the Synthesis of Cellulose Nanocrystals

Chemicals Reagent	Purity (%)	Molecular weight (g/mol)	Source	Usage
Sodium hydroxide pellets	85	60.052	Qrec	Alkali pre-treatment of empty fruit bunches
Glacier acetic acid	99.7	39.997	RCI Labscan	Bleaching of empty fruit bunches
Sodium chlorite powder	80	90.442	R & M Chemicals	Bleaching of empty fruit bunches
Sulphuric acid	95 – 97	98.078	Chemolab	Hydrolysis of empty fruit bunches
Hydrochloric acid	37	36.460	Sigma-Aldrich	Hydrolysis of holocellulose

3.3 Pre-treatment of Fibres

A proper pre-treatment is necessary to fully break down the empty fruit bunches before being used in the hydrolysis. As standard empty fruit bunches composition is 50 % cellulose, 25 % lignin and 25 % hemicellulose, degradation of hemicellulose is necessary to optimise cellulose nanocrystal extraction from empty fruit bunches (Abdul et al., 2012). Empty fruit bunch fibres used in this work had been dried and stored at room temperature (Sudiyani, Styarini, Triwahyuni, Sudiyarmanto, et al., 2013). First, empty fruit bunch fibres will subject to grinding that causes empty fruit bunch fibres to pulverise into slightly larger particles than powder form (Achaby et al., 2018). Next, ground empty fruit bunch fibres will be treated in distilled water for 1 hour at 60 °C. The resulting empty fruit bunch fibres were subjected to alkali pre-treatment by using sodium hydroxide solution. The alkali pre-treatment was completed by heating the mixture of empty fruit bunch and 4 wt% sodium hydroxide solution to 80 °C under mechanical stirring for 2 hours (Achaby et al., 2018). The product was washed several times using distilled water. The purpose of this process is to partially

eliminate the impurities contained in the empty fruit bunch fibres (Derman et al., 2018). The residue will be dried in an oven at 100 °C for 12 hours (Abdullah et al., 2016). Washing and drying processes will be repeated for three times to ensure a higher degree of hemicellulose and lignin degradation (Achaby et al., 2018).

3.4 Bleaching

Bleaching treatment comes after alkali pre-treatment. The resulting solid products from previous treatment was mixed with a solution consisting of equal parts of acetic acid buffer and aqueous sodium chlorite solution (Achaby et al., 2018). Acetic acid buffer comprises 75 mL of glacial acetic acid and 27 g of sodium hydroxide will then be subjected to dilution using approximately 1 litre of distilled water. On the other hand, aqueous sodium chlorite is prepared by mixing sodium chlorite pellets with distilled water to produce 1.7 wt% of aqueous solution with an estimated pH ranging from 3.6 to 4 (Achaby et al., 2018). Subsequently, the mixture will be heated at a temperature of 80ºC for 3 hours under continuous stirring (Achaby et al., 2018). Bleached empty fruit bunch fibres will be filtered and washed using deionized water. Washing of bleached empty fruit bunch fibres will proceed until pH of the sample is neutral. After that, drying of bleached and washed empty fruit bunch fibres will be carried out in an oven at 105 °C for 8 hours (Sudiyani, Styarini, Triwahyuni, Sudiyarmanto, et al., 2013). Similar to alkali pre-treatment, bleaching will also be performed thrice to ensure complete removal of rigid lignin layers to enhance cellulose nanocrystal extraction. Pure white coloured cellulose microfibres will be generated after this process (Achaby et al., 2018).

3.5 Extraction of Cellulose Nanocrystals by Acid Hydrolysis

Acidic agent employed in this treatment is concentrated sulphuric acid (Xing et al., 2018). White cellulose microfibres isolated from empty fruit bunch fibres are hydrolysed using 64 wt% sulphuric acid (Achaby et al., 2018). At this stage, the microcrystalline cellulose and concentrated sulphuric acid mixture will be preheated until it reaches a temperature of 50 °C for 30 minutes consecutively. Simultaneously, the mixture will be continuously stirred to enhance heat and mass transfer. Soon after acid hydrolysis, addition of ice-cubes and distillate water into the microcrystalline cellulose mixture will be carried out to halt the reaction. Amount of ice cubes and distilled water is about ten times the mass of the microcrystalline cellulose mixture

(Achaby et al., 2018). The requirement of rapid cooling to inhibit the reaction is because future reaction of sulphuric acid hydrolysis may not only break down the amorphous region of the microcrystalline cellulose but also deteriorate some crystalline parts of cellulose where the yield of cellulose nanocrystals will be lowered (Lu and Hsieh, 2010). Hence, sufficient and controlled retention time is a highly important parameter in cellulose nanocrystals conversion.

In order to prepare 64 wt% sulphuric acid solution, appropriate amount of concentrated sulphuric acid with concentration of 95 to 97 wt% has to be precisely determined. The calculation of volume of 95 to 97 wt% sulphuric acid required is shown in Equation 3.1.

$$V = \frac{m}{\rho} / \left(\frac{C_{SA}}{100}\right) \qquad (3.1)$$

where

V = Volume of sulphuric acid required, ml

m = Mass of sulphuric acid in 100 g of 64 wt% sulphuric acid solution, g

ρ = Density of sulphuric acid, g/ml

C_{SA} = Concentration of sulphuric acid available in laboratory, wt%

By taking a basis of total 100 ml of sulphuric acid solution, the volume of sulphuric acid required to produce 64 wt% sulphuric acid solution is shown in Appendix A.

3.6   Post-treatment

The resulting cellulose nanocrystals suspension will immediately proceed to centrifugation for phase separation. Conditions for centrifugation are at 12000 rpm for 15 minutes at room temperature (Achaby et al., 2018). The supernatant produced from centrifugation will be discarded while distilled water will be added into the heavier substances and continued with another cycle of centrifugation (Chieng et al., 2017) Centrifugation will be stopped when the supernatant produced becomes turbid (Pirich et al., 2015). This indicates the presence of trace amount of cellulose nanocrystals in the supernatant. The supernatant at this stage will be mixed again with the heavier substances and proceeded to the dialysis process (Kang et al., 2018). The mixture of

cellulose nanocrystals suspension will be placed in the dialysis tubing and immersed into distilled water for a few days (Achaby et al., 2018). This is to ensure complete removal of acid to achieve a near-neutral pH. Subsequently, cellulose nanocrystals suspension will be homogenised by a probe-type ultrasonic homogenizer in an ice bath to establish a well-dispersed cellulose nanocrystals suspension (Achaby et al., 2018). This step can also discourage the formation of aggregates that will deteriorate the value of cellulose nanocrystals (Naduparambath et al., 2018). After homogenisation, white stable cellulose nanocrystals suspension in the form of gel will be produced. Last but not least, the drying process of cellulose nanocrystals suspension will be carried out using freeze dryer (Achaby et al., 2018). The freeze drying will proceed at a temperature of -90 °C under vacuum condition. This purpose of this process is to dehydrate cellulose nanocrystals suspension under low pressure and temperature. In this process, cellulose nanocrystals suspension will be converted into solid material for characterisations.

3.7 Characterisation of Cellulose Nanocrystals

3.7.1 Chemical Composition Analysis

Chemical composition analysis plays a significant role in determining the content of biomass samples. Designer Energy Ltd method (DE) is one of the appropriate methods to identify the composition of lignin, hemicellulose and cellulose in empty fruit bunches. It is also a modified alternative of TAPPI standard that is generally accepted and recognised by researchers (Ioelovich, 2015). Via this approach, it can test and distinguish the physical and chemical content in each type of cellulose samples. The main components that can be identified by Designer Energy Ltd method are alpha cellulose and hemicellulose that is also known as collective term of beta and gamma cellulose (Ioelovich, 2015).

Generally, lignocellulosic biomass consists of majorly two types of polysaccharides namely, cellulose and hemicellulose (Chen, 2014). These two types of polysaccharides have different chemical structures but consist of three common elements, which are carbon, oxygen and hydrogen (Yeo et al., 2019). These three elements are the fundamental backbone of lignocellulose biomass. By comparing cellulose and hemicellulose, cellulose possesses a greater degree of polymerisation owning to its un-branched structure while hemicellulose is highly branched that forms short chain of polymer (Chen, 2014). Due to these properties, cellulose has greater

advantages in strength and more stable as compared to hemicellulose. Moreover, cellulose has a higher resistance to chemical attack. This is the reasons why cellulose is utilised as major component in paper fabrication as it lasts longer than hemicellulose (Li et al., 2019). Therefore, Designer Energy Ltd method can differentiate the cellulose from hemicellulose due to their differences in resistivity in chemical treatment.

The first step of Designer Energy Ltd method is to remove the lignin content in empty fruit bunch samples. Bleaching agent will be applied as an effective approach to delignify the samples that have abundant lignin content such as raw empty fruit bunches and alkali-treated empty fruit bunches. Suitable bleaching agent used in this method is sodium chlorite (Agustin-Salazar et al., 2018). The bleached product, or better known as holocellulose, comprises of cellulose and hemicellulose (Álvarez et al., 2018).

Next, the bleached products will be subjected to acid hydrolysis to remove less soluble hemicellulose. Generally, hemicellulose will be more vulnerable in less concentrated acid. Product remained after acid hydrolysis will be cellulose (Agustin-Salazar et al., 2018). The differences in weight before and after treatment was recorded to calculate respective composition of cellulose and hemicellulose.

3.7.2 Scanning Electron Microscopy Coupled with Energy Dispersive X-ray, SEM-EDX

Scanning Electron Microscope (SEM) utilises electron beam to scan samples by providing images of the samples (Vernon-Parry, 2000). Precisely, a beam of electrons that is illuminated from the radiation source passes through the magnetic lens and focuses on the sample. This action will induce interactions between atoms of the sample and electrons to cause secondary electrons, backscattered electrons and X-ray to be deflected from the sample (Singh, 2016). These signals carried information such as morphology, composition, crystallographic and topography (Singh, 2016). In this study, the morphology and structure of cellulose nanocrystals are analysed by Hitachi S-3400N Scanning electron microscopy.

Hitachi S-3400N Scanning electron microscopy is equipped with Tungsten Filament that allows accelerating voltages up to 30 kV (Stanford University, 2018). The pressure control for backscattered electrons observation is ranged from 6 to 270 Pa. Moreover, moisture loss in low vacuum condition is controlled under Deben Peltier Coolstage (Stanford University, 2018).

Cellulose sample needs to be fixed or denatured for plant tissues to proceed to next stages (Pathan et al., 2010). In order to examine the native structure of the cellulose nanocrystals, cellulose nanocrystals must be in dehydrated form (Pathan et al., 2010). This is because the scanning electron microscope and coating system will operate under extremely low pressure or high vacuum condition. In these conditions, most of the samples will be distorted as it cannot withstand the water removal under vacuum system (Pathan et al., 2010). Many techniques have been devised to eliminate water compound from the sample. Examples of drying techniques including critical point, freeze and air drying (Pathan et al., 2010). Coincidentally, cellulose nanocrystals suspension is generated in freeze-dried form after the extraction process. Thus, dehydration requirement is met to visualise the cellulose nanocrystals scanning through SEM.

Next, freeze-dried cellulose nanocrystals may proceed to specimen mounting (Ngoc et al., 2017). Cellulose nanocrystals will be mounted on the stubs that are suitable for viewing using SEM. Cellulose nanocrystals are mounted on a stub of metal with adhesive carbon tape in this case due to its electrically conductive properties (Samuel Roberts Noble Microscopy Laboratory, 2018). Then, it is coated with 40 to 60 nm of metal such as gold or platinum before the samples can be observed under the microscope. Coating will be performed by sputter coater. Sputter coater is plasma chamber that uses argon ions to peel gold or palladium atoms off from gold or platinum plate to coat the surface of the sample to produce a conductive gold coating (Ngoc et al., 2017).

Subsequently, the gold or palladium coated cellulose nanocrystals are readied to be analysed in SEM. Few images will be taken and the sizes of cellulose nanocrystals can be measured. In order to estimate an average grain size of cellulose nanocrystals, intercept technique can be applied (Spaulding et al., 2010). First, random straight line is drawn across the micrograph with specific magnification. Amount of grain boundaries that are intersecting the line will be recorded. The average size of cellulose nanocrystals is determined by dividing the number of intersections by the actual line length (Spaulding et al., 2010).

Furthermore, SEM was equipped with EDX which can be used to generate chemical and elemental data of the cellulose samples. The presence of certain elements on the surface of cellulose such as carbon (C) and oxygen (O) can be revealed.

3.7.3   Crystallinity Study

Crystallite size and crystallinity of cellulose nanocrystals were analysed by Shimadu XRD-6000 type X-ray diffractometer using the Cu Kα radiation (λ = 1.54184 nm) in the 2θ range of 2° to 60° at room temperature (Mat Zain et al., 2014). Applied current and accelerating voltage are 30 mA and 40 kV, respectively (Budhi et al., 2018). For analytical diffraction studies, the cellulose nanocrystal samples will be ground to a fine homogeneous powder. At this state, a tremendous number of small crystallites existed in cellulose nanocrystals could be oriented in all possible directions (Skoog, D. A., Holler, F. J., and Nieman, 1998). Hence, significant number of particles oriented in a way that can satisfy the Bragg's law for the deflection from countless interplanar spacing when X-ray beam strikes and passes through the cellulose nanocrystal specimens.

First, cellulose nanocrystals dried powder was placed in a sample holder that uses a depression or cavity to mount the sample (Skoog, D. A., Holler, F. J., and Nieman, 1998). In order to produce a flat upper surface, compression needs to be performed with great care to produce virtually no scratch or dent on the powder surface as the groove will greatly affect the analysed results. These mounts are commonly made of aluminium (Skoog, D. A., Holler, F. J., and Nieman, 1998). Cavity mounts are most commonly backloaded or sideloaded. Frosted glass surface, cardboard or ceramics is purposely placed over the front and the cellulose nanocrystals dried powder is gingerly top up via the open side or back. Prepared cellulose nanocrystals dried powder sample can place into X-ray diffractometer and subject to X-ray radiation at different angles (Mat Zain et al., 2014). After characterisation, diffraction peaks of cellulose nanocrystals can be pinpointed on the XRD spectrum.

From the analysis, crystallinity index can be calculated from the equation of crystallinity that as shown in Equation 3.2 (Mat Zain et al., 2014).

$$Crystalline\ index,\ CrI\ (\%) = \frac{I_{002} - I_{am}}{I_{002}} \times 100 \qquad (3.2)$$

where

I_{002} = Maximum intensity of the diffraction peak, count

I_{am} = Intensity of diffraction attributed to amorphous cellulose, count

The crystallinity indices were calculated and compared to Joint Committee on Power Diffraction Standard (JCPDS) to verify the unique lattice structure of cellulose nanocrystals.

3.7.4   Functional Group Determination

The presence of the functional groups (such as O-H and C=C) can be validated by the FT-IR analysis using a Nicolet IS10 FT-IR Spectrometer over a Mid-IR range of 4000-500 cm^{-1} (Anwar et al., 2015). The default resolution of FT-IR Spectrometer is 4 (Wang et al., 2015). Greater resolution of FT-IR Spectrometer can resolve closely-packed peak better compare to low resolution version. A higher degree of resolution is manifested in lower numerical number.

Infrared spectrum was collected after an average of 32 scans in transmittance mode (Aracri et al., 2014). Higher number of scans can raise the signal-to-noise ratio; however, the collection time of cellulose nanocrystal samples will be lengthened. In short, the structure of the cellulose nanocrystals will be determined using FTIR by displaying unique vibrational wavenumbers of cellulose nanocrystals (Aracri et al., 2014). As a result, the FTIR spectra are compared with Joint Committee on Power Diffraction Standard (JCPDS) and other research papers to show that cellulose nanocrystals existed with common spectra patterns and similar wavenumber produced.

3.7.5   Dynamic Light Scattering, DLS

In this study, DLS was carried out on Malvern Zetasizer Nano ZS90 to determine the size distribution of cellulose nanocrystals particles. Cellulose nanocrystal samples were collected and suspended in deionised water directly to observe. Appropriate conditions for analysis to carry on is essential. Analysis was carried out at temperature 24.9 °C with particle absorption coefficient of 0.01 and particle refractive index of 1.40. The solvent or dispersant that are compatible with cellulose nanocrystals is water. In this case, deionised water prevailed as it contained literally no impurities (such as ions). The sample will be measured in three and the duration allocated for each cycle is ten seconds. Approximately 1.5 mL of solvent containing cellulose nanocrystals 1.5 ml was placed in a glass cuvette and placed in the instrument.

The hydrodynamic diameter of the cellulose nanocrystals can be correlated to translational diffusion coefficient, Boltzmann's constant, temperature and viscosity of

the dispersant by Stokes-Einstein equation (Oliveira et al., 2017). The formula of Stokes-Einstein is depicted in Equation 3.3.

$$d_H = \frac{k_B T}{3\pi D \eta_o}$$
(3.3)

where

d_H = Hydrodynamic diameter of particles, m

k_B = Boltzmann's constant, J/K

T = Temperature of solvent, K

D = Translational diffusion coefficient, m^2/s

η_o = Viscosity of the solvent, kg/(m·s)

3.7.6 Thermogravimetric Analysis, TGA

Thermogravimetric analysis (TGA) or thermal gravimetric analysis is a method to analyse the change in chemical and physical properties of substances under thermal conditions (Betie et al., 2018). The differences are measured and evaluated with increasing temperature. The heating rate applied is constant, which is 10 °C per minute in this case. Pyrolysis or thermogravimetric experiments will be carried out using a thermogravimetric analyser, TA Instrument Q5000IR (Zhezi Zhang et al., 2018). First, five to eight milligrams of cellulose nanocrystal samples were prepared to be placed in the thermogravimetric analyser. Next, it will be heated at a constant heating rate around 10 °C per minute from room temperature to approximately 105 °C. The moisture that resides in the samples will be vaporised at this stage. Then, the temperature increases until it reaches at about 800 °C. This temperature is also known as final pyrolysis temperature. Simultaneously, the change in mass of the samples were continuously recorded as a function of time or temperature. Highly pure nitrogen gas will sweep through the internal environment of the thermogravimetric analyser at a constant flow rate of 150 cm^3 per minute. The purpose of this step was to support the pyrolysis process by providing inert environment and also to remove the volatile substances released during the reaction (Fernandez et al., 2019).

The changes in term of mass of cellulose nanocrystal samples will be recorded and analysed to determine the thermal resistance and degradation of the samples. The changes in mass might due to several thermal events, namely, vaporisation, oxidation,

desorption, reduction, absorption, decomposition and sublimation (Barneto et al., 2016). These possible events are investigated to evaluate the thermal properties of cellulose nanocrystal samples. During the pyrolysis process, mass losses event will inevitably occur and the losses might appear in gaseous forms. This implied that greater mass loss can be attributed by higher content of volatile species in the samples (Shen and Gu, 2009). Thermal degradation of cellulose nanocrystal samples can give rise to a few products, namely hydroxyacetaldehyde, 5-hydroxymethyl-furfural and hydroxyacetone (Shen and Gu, 2009).

Feature of thermogravimetric analyser allowed it to determine different species that contained in a single sample as each species has its own distinct onset degradation temperature and maximum decomposition rate point. Thus, TGA can be used to analyse the thermal stability of the cellulose nanocrystals prepared by a few stages of chemical treatment.

3.8   Summary

Briefly, the production of cellulose nanocrystals will undergo four major steps, which are alkali pre-treatment, bleaching, cellulose nanocrystal extraction and post-treatment in chronologically order (Achaby et al., 2018). The steps selected are based on the comparison made between applicability, complexity, effectiveness and environmental-friendliness of different methods (Kargarzadeh et al., 2015). Great care and delicacy are necessary conditions when executing the experiment to minimise the errors.

Characterisation of cellulose nanocrystals will be performed in different perspectives. Morphology, topography and dimensions of cellulose nanocrystals are observed by SEM (Fatah, 2015). In the meantime, crystallinity properties were evaluated by XRD analysis using Bragg's law equation. FTIR spectroscopy can be used to support the presence of lignin and hemicellulose after the cellulose nanocrystal isolation (Fatah, 2015). It identifies specific functional groups that belong to cellulose nanocrystals via absorption wavenumbers. DLS can be used to identify the size distribution of nanocellulose particles in the sample and TGA investigated the thermal behaviour of the cellulose nanocrystal samples. The collection and tabulation of characterisation results will be specified and discussed in the next chapter.

CHAPTER 4

RESULTS AND DISCUSSIONS

4.1   Introduction

Since the empty fruit bunches used in this study were prepared with different chemical treatments as alkaline treatment, bleaching process and acid hydrolysis chronologically, characterisation was conducted to study their differences in physical and chemical aspects. Besides, the purpose of characterisation is also to study their effects after each succeeding treatment. The changes in chemical composition of samples before and after treatment were conducted to evaluate the effectiveness of chemical treatment to remove unwanted hemicellulose and lignin to acquire cellulose for numerous applications as mentioned in Chapter 1.

Chemical composition analysis, however, is not sufficient to prove the formation of cellulose nanocrystals during experiment. More analytical tools are required to demonstrate and convince the usefulness of chemical treatments in terms of cellulose nanocrystal extraction from empty fruit bunches. This was performed by implementing various types of analytical instruments, namely X-ray diffractometer (XRD), Fourier transform infrared spectroscopy (FTIR), scanning electron microscope equipped with energy dispersive X-ray (SEM-EDX) and thermogravimetric analysis (TGA). Implementation of these analytical instruments simultaneously might increase the reliability of the results and also acknowledge the weaknesses and shortcomings of the experiments.

4.2   Extraction of Cellulose Nanocrystals from Empty Fruit Bunches

Several treatment steps have to be carried out in order to successfully extract cellulose nanocrystals from the empty fruit bunches. In brief, the necessary treatment steps are washing, alkaline treatment, bleaching treatment and acid hydrolysis. First and foremost, blended empty fruit bunches will be washed by using distilled water in 60℃ with continuous magnetic stirring for an hour (Achaby et al., 2018). Size of blended empty fruit bunches are less than 300 microns. The purpose of this washing process is to remove soluble impurities mixed with the empty fruit bunch fibres (such as inorganic fertilizer). After the reaction time has been finished, the mixture solution will be decanted and the remaining samples will be filtered off by using vacuum pump.

After the washing process, the samples will proceed to alkaline treatment by using sodium hydroxide in order to remove majority of the hemicellulose and lignin resided in the samples. The sample will be immersed into a 4 wt% sodium hydroxide solution with continuous stirring at a temperature of 80℃ for 2 hours (Sudiyani, Styarini, Triwahyuni, Sudiyarmanto, et al., 2013). 4 wt% sodium hydroxide was chosen because it can remove impurities embedded with empty fruit bunches without damaging the surface of fibre. The biomass sample will be washed attentively by using distilled water for about 5 to 6 times in order to remove the suspended mixture solution that contains the biomass sample. The biomass sample will be transferred into a petri dish and heated in the oven at 105 °C.

Subsequently, the samples will be immersed into a mixture of 1.7 wt% sodium chlorite solution with little amount of acetic acid under continuous stirring at a temperature of 80 ℃ for 2 hours, which is intended to ensure that the samples are totally in contact with the mixture solution (Achaby et al., 2018). The purpose of using sodium chlorite mixture solution is to remove the impurities such as lignin and hemicellulose from the EFB before going through further treatment process. This treatment process will be carried out thrice to make sure that the reaction is complete and can achieve higher efficiency in the removal of lignin and hemicellulose.

Lastly, the dried sample will be immersed into a sulphuric acid solution to obtain nanocrystalline cellulose by breaking down the β-1,4-glycosidic bonds via acid hydrolysis process. The sample will be immersed into the sulphuric acid solution with continuous stirring at 50 ℃ for 30 minutes. Sulphuric acid solution prepared must be highly concentrated up to 64 wt% to encourage the degradation of cellulose microfibres (Meng et al., 2019). After the process, H_2SO_4 solution will be decanted and the remaining samples will be filtered off by using Buchner porcelain funnel. The imitative biomass was rough enough to use these filters. Then, the sulphuric acid solution will be removed out from the filters. The biomass sample will be washed attentively by using distilled water several times until the pH value has reached 5 in order to remove the suspended mixture solution that contained inside the biomass sample (Achaby et al., 2018).

The weight loss of each treatment step has been recorded. Initially, the weight of samples will reduce tremendously due to the removal of the wax, oil, lignin, hemicellulose and other extractives that may be able to be eliminated by the treatment process (Taflick et al., 2017). Based on Table 4.1, the effect of weight loss is obvious.

The weight of the dried cellulose nanocrystals was 1.0090 g from the original weight of 40.1961 g, which makes a weight loss of 39.1871 g. There are a few possibilities that might contribute to significant weight loss of empty fruit bunches. First, some infinitesimal particles from the samples might be able to pass through the filter paper during the filtration process by diffusing through the pores of filter paper. Next, degradation or dissolution of cellulose into the chemical solution is also conceivable. Optimum temperature, concentration and treatment duration are the main factors to maximise the production of cellulose nanocrystals (Meng et al., 2019). Last but not least, some samples that tend to deposit onto the filter paper after drying are tenacious and irretrievable.

Table 4.1: Weight of Empty Fruit Bunches After Each Processing Steps

Process	Number	Weight of Empty Fruit Bunches (g)	
		Average weight (g)	Standard Deviation
Untreated EFB	1	40.1961	0.0032
Washing	1	38.5284	0.0079
Alkaline treatment	1	34.2306	0.0026
	2	29.2563	0.0045
	3	26.8994	0.0090
Extracted alkali-treated EFB	1	25.3872	0.0043
Bleaching	1	21.1399	0.0113
	2	16.7869	0.0064
	3	15.1176	0.0095
Extracted bleached CMF	1	13.6089	0.0022
Acid Hydrolysis	1	1.0090	0.0064

The yield of alkali-treated empty fruit bunches obtained from washing and alkaline treatment compared to raw empty fruit bunches can be calculated using Equation 4.1.

$$Yield\ (\%) = \frac{W_f}{W_i} \times 100\ \% \tag{4.1}$$

where

W_i = Weight of untreated empty fruit bunch sample before treatment, g

W_f = Weight of empty fruit bunch sample after washing and alkaline treatment, g

Calculation of yield of alkali-treated empty fruit bunches obtained from washing and alkaline treatment is shown in Appendix B.

A small portion of the alkali-treated empty fruit bunches will be utilised in characterisation. Hence, the yield of bleached cellulose microfibres obtained from bleaching treatment compared to raw empty fruit bunches will be reformulated as depicted in Equation 4.2.

$$Yield\ (\%) = Y_{ATEFB} \times (\frac{W_f}{W_i} \times 100\ \%) \tag{4.2}$$

where

Y_{ATEFB} = Yield of third alkali-treated empty fruit bunches

W_i = Weight of cellulose sample before bleaching, g

W_f = Weight of cellulose sample after bleaching, g

Calculation of yield of bleached cellulose microfibres compared to raw empty fruit bunches is shown in Appendix C.

Correspondingly, small portion of the bleached cellulose microfibres, CMF will be utilised in characterisation. The yield of cellulose nanocrystals obtained from acid hydrolysis compared to raw empty fruit bunches can be calculated using Equation 4.3.

$$Yield\ (\%) = \ Y_{ATEFB} \times Y_{CMF} \times (\frac{W_f}{W_i} \times 100\ \%) \tag{4.3}$$

where

Y_{ATEFB} = Yield of third alkali-treated empty fruit bunches

Y_{CMF} = Yield of third bleached cellulose microfibres

W_i = Weight of cellulose sample before acid hydrolysis, g

W_f = Weight of cellulose sample after acid hydrolysis, g

Calculation of yield of cellulose nanocrystals compared to raw empty fruit bunches is shown in Appendix C and the yield of alkali-treated empty fruit bunches, bleached cellulose microfibres and cellulose nanocrystals after each processing steps were summarised in Table 4.2.

Table 4.2: Yield of Alkali-treated Empty Fruit Bunches, Bleached Cellulose Microfibres and Cellulose Nanocrystals After Each Processing Steps

Cellulose samples	Yield (%)
Washed empty fruit bunches	95.8511
First alkali-treated empty fruit bunches (ATEFB)	85.1590
Second alkali-treated empty fruit bunches (ATEFB)	72.7839
Third alkali-treated empty fruit bunches (ATEFB)	66.9204
First bleached cellulose microfibres (CMF)	55.7245
Second bleached cellulose microfibres (CMF)	44.2501
Third bleached cellulose microfibres (CMF)	39.8499
Acid-hydrolysed cellulose nanocrystals (CNC)	2.9282

As shown in Table 4.2, the yield of cellulose dwindled gradually at alkaline treatment and bleaching process. Evidently, after third alkaline treatment and bleaching, the yield of alkali-treated empty fruit bunches and bleached cellulose microfibres were 66.92 % and 39.85 %, respectively. Under weak alkaline environment, it disrupts the lignin structure in empty fruit bunches, thus improving the susceptibility of the remaining polysaccharides, namely cellulose and hemicellulose, for other treatment. Besides, the effectiveness of this treatment can be considered low as compared to other types of pretreatment technologies. Therefore, the degradation of

cellulose from biomass can be attenuated to prevent excessive weight loss of cellulose via the processes. The percentages of cellulose obtained from other sources such as wheat straw and white cotton are 34 to 40 % and 35 to 40 %, respectively. By comparing to this study, cellulose obtained from empty fruit bunches displayed a higher cellulose yield at 39.85 %, which is in good agreement with a reported work of 37.5 to 45 % (Sudiyani, Styarini, Triwahyuni, Sembiring, et al., 2013).

On the other hand, the yield of cellulose reduced tremendously to 1 % after acid hydrolysis. This can be explained by high degree deconstruction of natural recalcitrance in empty fruit bunches (Xie et al., 2018). The matrix of empty fruit bunches is segregated into two main parts, which are the crystalline and amorphous that are randomly distributed along its length. Highly acidic condition disintegrates amorphous structure of cellulose thoroughly. The consequence of acid hydrolysis is that only highly crystalline nanocellulose structure will remain after the treatment (Xie et al., 2018). By comparison, the yield obtained from other sources such as alfa fiber is 21 %, the yield of empty fruit bunches acquired in this study is exceptionally low at 3 % (Achaby et al., 2018). Normally, the yield of CNC in empty fruit bunches varies between 6 to 24 % (Xie et al., 2018). Manifestly, the experimental data in this study exhibited a lower yield. There are several reasons that might lead to this outcome. First, the reaction persisted after an optimum duration of 30 minutes for acid hydrolysis. As reaction time is one of the significant parameters affecting the crystallinity and yield of cellulose nanocrystals, it should be ideally controlled within the range (Afiq bin Jumhuri et al., 2017). The methodology utilised in this study is by using ice bath to reduce the reaction temperature and adding distilled water to the solution to decrease the concentration of sulphuric acid that leads to the continuous degradation of cellulose, however, this might be not sufficient to completely alter the reaction. Next, the losses of cellulose might happen during centrifugation. It is highly possible that tiny cellulose nanocrystals were wasted during the decantation of clear solution from the turbid masses of cellulose nanocrystals.

4.3   Chemical Composition Analysis

The composition of the plant fibres after various chemical treatment can be determined by various testing methods, which are Designer Energy Ltd. method that is similar to TAPPI methods generally recognized as a good indication of alpha cellulose content. TAPPI method, however, has one major shortcoming, which is only applicable to

extractive-free and delignified biomass samples (Ioelovich, 2015). Therefore, the modified TAPPI method or also known as Designer Energy Ltd. method (DE) that has been established by Design Energy Ltd. is more suitable to determine the hemicellulose, cellulose, physical and chemical compositions in raw empty fruit bunch fibres.

4.3.1 Holocellulose

Empty fruit bunch fibres are made up of various lignocellulosic materials. In order to determine the percentage of holocellulose in empty fruit bunch samples, other recalcitrant such as lignin, ashes and water reside in the empty fruit bunch fibres must be eliminated. One of the renowned methods for lignin removal is bleaching technology. Bleaching is a chemical process to decolorize and brighten the plant fibres (John and Anandjiwala, 2009). Decolorisation of plant fibres is a clear indication of lignin removal. There are few chemicals classified as oxidants for bleaching process. For instance, chlorine, hypochlorite and chlorite. Similarly to TAPPI T9 wd-75 method, it utilises sodium chlorite and acetic acid as bleaching agent for holocellulose determination (Casillas et al., 2018). The role of sodium chlorite is to oxidise and solubilise lignin that enables it to dissolve in solution.

Figure 4.1: Determination of Holocellulose Content Using Mixture of Glacial Acetic Acid and Sodium Chlorite Solution for 90 Minutes at 90 °C

The holocellulose was prepared from 500 mg of biomass samples after various chemical treatment processes. Next, the samples were added to 40 mL of distilled water, 1 mL of glacial acetic acid and 0.5 g of sodium chlorite in 100 mL beaker. After mixing, the samples will be immersed in a water bath at 90 °C for 45 minutes with continuous stirring at 800 rpm by magnetic stirrer. Subsequently, an additional 0.5 g of sodium chlorite and 1 mL of acetate buffer were added to 100 mL beaker, the reaction will be continued for another 45 minutes at 90 °C. After that, the samples were allowed to cool down to room temperature for 30 minutes. In order to reduce weight loss of the samples, it was centrifuged for 10 minutes to remove the supernatant that contained lignin. Next, holocellulose samples obtained were washed with 50 °C distilled water to remove the impurities deposited onto the holocellulose samples. Correspondingly, holocellulose samples were washed by distilled water several times until the pH of washed solution reached 7. Lastly, the holocellulose samples will be dried at 105 °C to a constant weight. The remaining weight represents the content of holocellulose (Ioelovich, 2015). Holocellulose content in empty fruit bunches can be calculated by Equation 4.4.

$$Holocellulose\ content\ (\%) = \frac{W_{HP} - W_P}{W_S} \times 100\ \%$$ (4.4)

where

W_{HP} = Weight of dry holocellulose and petri dish, g

W_P = Weight of petri dish, g

W_S = Weight of dried biomass samples, g

The holocellulose content of raw empty fruit bunches, alkali-treated empty fruit bunches, bleached cellulose microfibres and cellulose nanocrystals obtained in this study were calculated as shown in Appendix D and the values were summarised in Table 4.3.
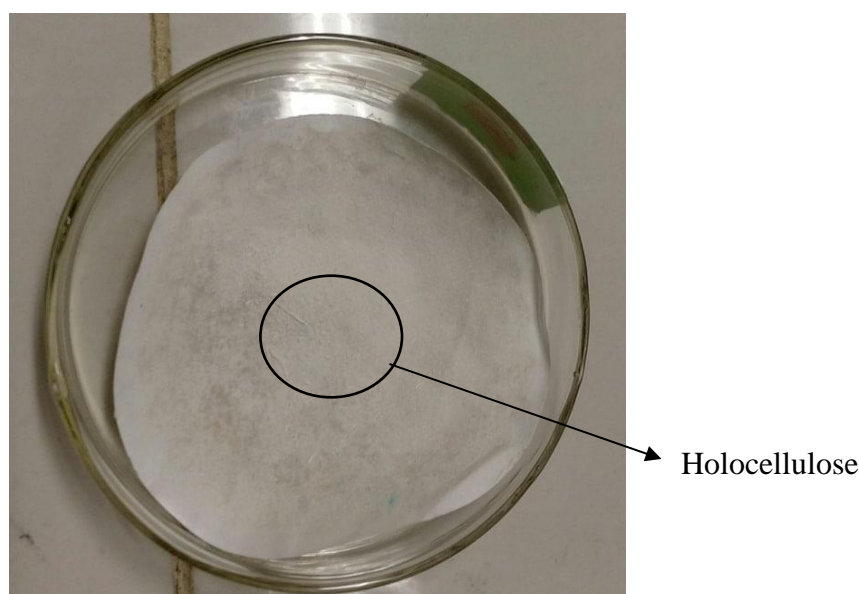
Figure 4.2: Holocellulose Deposited on Filter Paper

Table 4.3: Holocellulose Content of Raw Empty Fruit Bunches, Alkali-treated Empty Fruit Bunches, Bleached Cellulose Microfibres and Cellulose Nanocrystals

Content	Raw empty fruit bunches (%)	Alkali-treated empty fruit bunches (%)	Bleached cellulose microfibres (%)	cellulose nanocrystals (%)
Holocellulose	41.00	48.16	63.06	85.94

4.3.2   Hemicellulose and Cellulose

Holocellulose is total polysaccharide fraction that exists in the wood or plant fibres. In other words, holocellulose comprises of hemicellulose and cellulose (Burhani and Septevani, 2018). Thus, segregation of hemicellulose and cellulose must be carried out in order to determine its composition in empty fruit bunch fibres. In order to separate hemicellulose and cellulose, one must recognise their differences in terms of molecular structure. Hemicellulose is a branched polymer consists of carbon, hydrogen and oxygen with shorter chain length compared to cellulose (Chen, 2014). On the other hand, cellulose is a linear and unbranched polymer that consists of repeating units of glucose. Based on the molecular structure differences, researchers have developed a way to separate hemicellulose and cellulose. In this case, hemicellulose is identified as amorphous structure polymer that has low strength and it is highly vulnerable to acid hydrolysis, even at low acid concentration (Ioelovich, 2015). In contrast, cellulose

is a crystalline structured polymer that can withstand acid hydrolysis up to certain extent. Therefore, acid hydrolysis can be considered as one of the effective methods to alleviate hemicellulose and cellulose.

First and foremost, holocellulose samples acquired from the bleaching treatment were hydrolysed by 45 mL of 2 wt% hydrochloric acid solution. The experiment was setup in the reflux condenser and round-bottomed flask to minimise the losses of water as vapour. Simultaneously, the samples were continuously stirred by magnetic stirrer and the process was carried out at 50 °C for 2 hours. Similarly, the samples were allowed to cool for 30 minutes after acid hydrolysis. The samples were then centrifuged for 10 minutes. The settlement would be collected while supernatant was discarded. Next, cellulose samples obtained will be washed with 50 °C of distilled water, followed by 1 wt% sodium bicarbonate solution and distilled water. Lastly, the cellulose samples were dried at 105 °C to a constant weight (Ioelovich, 2015).

Figure 4.3: Determination of Cellulose Content by Acid Hydrolysis Using Dilute Hydrochloric Acid Solution for 2 Hours at 50 °C
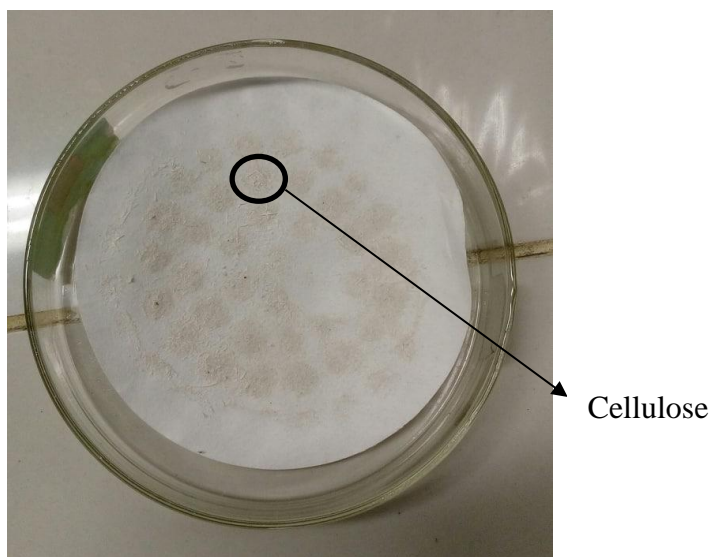
Figure 4.4: Cellulose Deposited on Filter Paper

Cellulose content in empty fruit bunches can be calculated by Equation 4.5.

$$Cellulose\ content\ (\%) = HC \times \left(\frac{W_{CP} - W_P}{W_H}\right) \tag{4.5}$$

where

HC = Holocellulose content in samples, %

W_{CP} = Weight of dry cellulose and petri dish, g

W_P = Weight of petri dish, g

W_H = Weight of dried holocellulose samples, g

Cellulose content of raw empty fruit bunches, alkali-treated empty fruit bunches, bleached cellulose microfibres and cellulose nanocrystals were calculated as shown in Appendix E. Hemicellulose content in empty fruit bunches can be calculated by Equation 4.6.

$$Hemicellulose\ content\ (\%) = HC - C \tag{4.6}$$

where

HC = Holocellulose content in samples, %

C = Cellulose content in samples, %

Calculation of hemicellulose content of raw EFB, alkali-treated empty fruit bunches, bleached cellulose microfibres and cellulose nanocrystals are shown in Appendix F. Subsequently, the overall content of raw EFB, alkali-treated empty fruit bunches, bleached cellulose microfibres and cellulose nanocrystals are summarised in Table 4.4.

Table 4.4: Overall Content of Raw Empty Fruit Bunches, Alkali-treated Empty Fruit Bunches, Bleached Cellulose Microfibres and Cellulose Nanocrystals

Content	Raw empty fruit bunches (%)	Alkali-treated empty fruit bunches (%)	Bleached cellulose microfibres (%)	cellulose nanocrystals (%)
Cellulose	20.28	30.06	46.68	73.74
Hemicellulose	20.72	18.10	16.38	12.20
Others	59.00	51.84	36.94	14.06
Total	100.00	100.00	100.00	100.00

Table 4.4 shows the overall content of raw EFB, alkali-treated empty fruit bunches, bleached cellulose microfibres and cellulose nanocrystals. Based on the cellulose composition of raw empty fruit bunches, alkali-treated empty fruit bunches, bleached cellulose microfibres and cellulose nanocrystals, the cellulose content are 20.28 %, 30.06 %, 46.68 % and 73.74 %, respectively. As postulated, cellulose content increased after each treatment process. Simultaneously, hemicellulose and lignin content dropped after each successive treatment as shown in Table 4.4. Raw empty fruit bunches existed in the form of lignocellulose that comprised of cellulose, lignin and hemicellulose (Akhtar et al., 2016). The pre-treatment can effectively deconstruct lignin and hemicellulose barriers on empty fruit bunches. In other words, the accessibility and detectability of cellulose become greater after different pre-treatments as higher amount of lignin and hemicellulose have been dissolved and eliminated in acid and alkaline solutions (Bali et al., 2015).

The cellulose content in cellulose nanocrystals reported by previous work was higher than the results obtained in this study, which is around 94 % (Casillas et al., 2018). There are several rationales that can lead to this outcome. First, it might due to leftover impurities after the acid hydrolysis, which alter the quantity of soluble samples in the solution. Nevertheless, the possibility of this occurrence is fairly low as the

sulphuric acid utilised was highly concentrated and would disintegrate most of the amorphous structure in cellulose. Additionally, if the substances contained in the cellulose is not degradable by highly concentrated sulphuric acid, it will not be easily dissolved in the solution. Therefore, weight losses might be another reason that lead to this outcome. As cellulose determination requires several handling steps to transfer the cellulose from solution to solution. Hence, it is justifiable for the occurrences of weight losses during the centrifugation and washing steps.

4.4 Functional Group Determination

The functional groups present on the empty fruit bunches were identified using FTIR analysis with the wavenumber range of 400 to 4000 cm^{-1}. In this study, changes in chemical composition of empty fruit bunch fibres after underwent different chemical treatments were identified. Commonly, empty fruit bunch fibres possess several functional groups such as carboxylic acid (-COOH), hydroxyl (-OH), alkyl (C-H) and pyranose ring skeletal (C-O-C) (Osman et al., 2016). Figure 4.5 shows the infrared spectra of raw empty fruit bunches and final cellulose nanocrystals extracted whereas Figure 4.6 depicted the infrared spectra of alkali-treated empty fruit bunches, bleached cellulose microfibres and cellulose nanocrystals to compare and study the effect of various pre-treatment and hydrolysis on the empty fruit bunches.
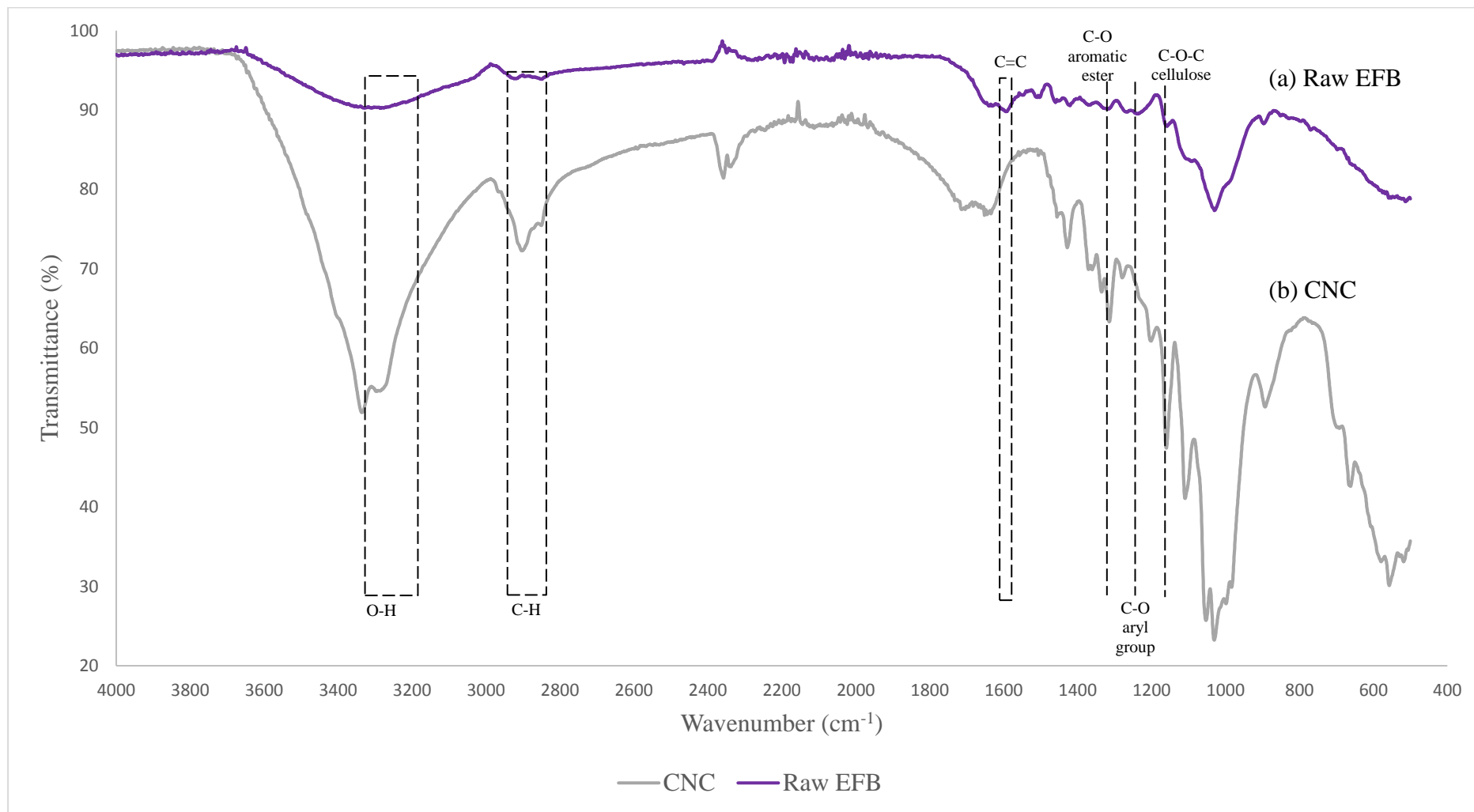
Figure 4.5: FTIR Spectra of Raw Empty Fruit Bunches and Cellulose Nanocrystals
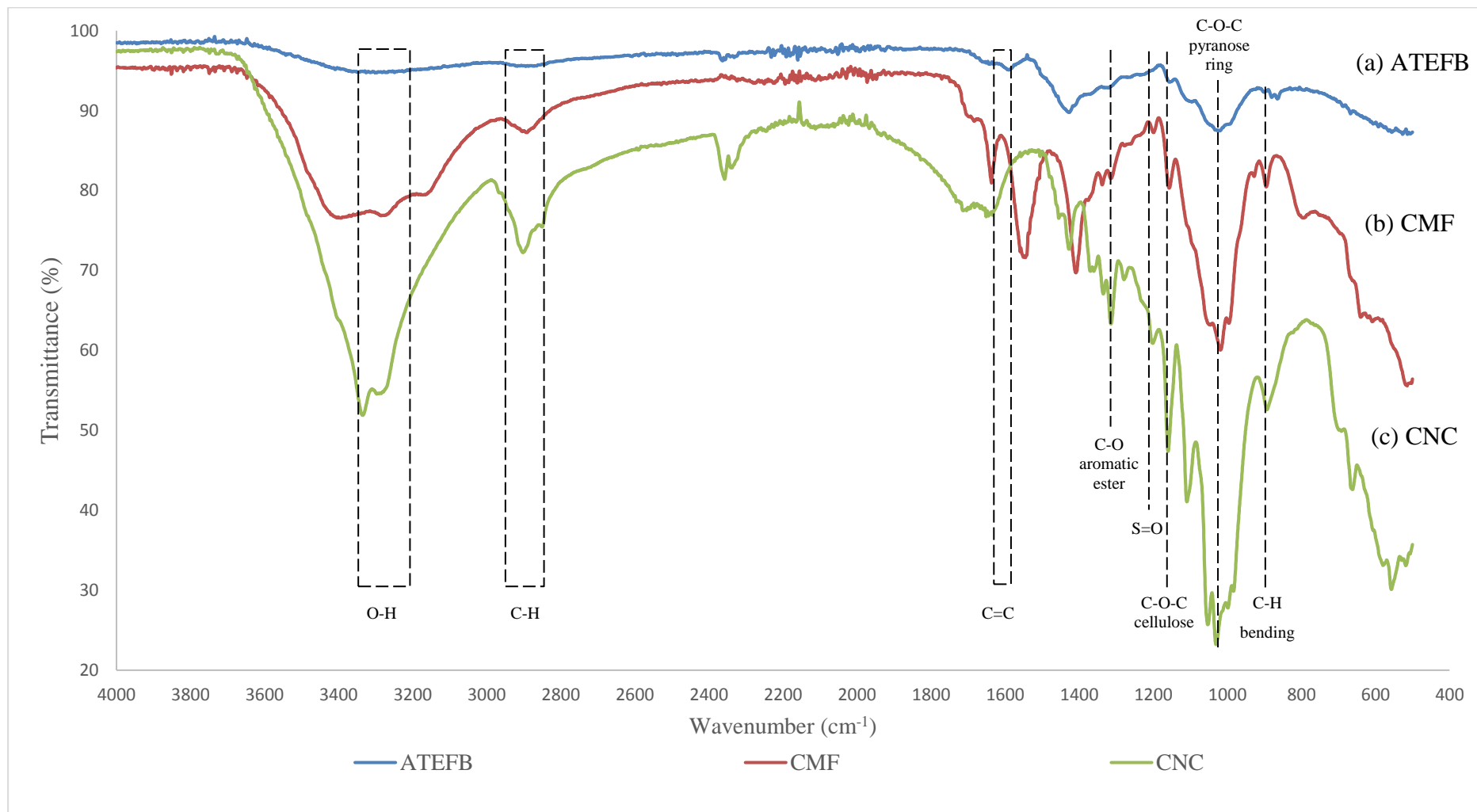
Figure 4.6: FTIR Spectra of Alkali-treated Empty Fruit Bunches, Bleached Cellulose Microfibres and Cellulose Nanocrystals

Table 4.5: Infrared Stretching Frequencies (Sigma-Aldrich, 2019)

Group	Compound class	Wavenumber (cm^{-1})
O-H stretching	Alcohol	3200 - 3350
C-H stretching	Alkane	2840 - 3000
C=C stretching	Alkene	1600 - 1678
C-O stretching	Aromatic ester	1240 - 1315
C-O stretching	Tertiary alcohol	1124 - 1205
S=O stretching	Sulphate	1185 - 1200
C-O stretching	Primary alcohol	1050 - 1085
C-H bending	Trisubstituted hydrocarbon	800 - 900

It can be seen from Figure 4.5 that the overall transmittance of raw empty fruit bunches is lower than the spectrum displayed by cellulose nanocrystals. Transmittance measures the extent of infrared at a certain wavelength to pass through a species. In other words, a greater transmittance percent indicates that the species absorbs less amount of radiation. Table 4.5 displays various functional groups detected at different wavenumber ranges. In this study, cellulose nanocrystals absorbed more amount of radiation and contained more intensified peaks as compared to raw empty fruit bunches. This means that the amount of chemical functional groups increased after several chemical treatments. The major difference between raw empty fruit bunches and cellulose nanocrystals are exhibited in the spectra. First, the peaks at 1600 cm^{-1} and 1240 cm^{-1} are attributed to C=C stretching vibration of aromatic components and C-O stretching of aryl group. These two peaks indicate the presence of hemicellulose and lignin molecules in raw empty fruit bunches before chemical treatment (Achaby et al., 2018). Consequently, these two peaks do not appear in purified cellulose nanocrystals after the removal of lignin and hemicellulose compounds.

As shown in Figure 4.6, well-defined peaks were detected from the empty fruit bunch fibres after various chemical treatments. A deep band ranging from 3200 to 3350 cm^{-1} appeared in the FTIR spectra of all samples, which indicates the stretching vibration of O-H group present in asymmetrical and symmetrical forms of lignocellulosic biomass (Achaby et al., 2018). Next, band around 2840 to 3000 cm^{-1} was attributed to the C-H group that is present in all organic-made substances (Prado and Spinacé, 2019). Additionally, peaks at 893 cm^{-1} and 1031 cm^{-1} demonstrate the existence of the glycosidic deformation of C_1-H with trisubstituted ring skeletal

bending and C-O functional groups that exist in the form of C-O-C pyranose ring skeletal stretching, respectively. These two peaks are the major characteristics of cellulose derived from oil palm empty fruit bunches, which comprises of β-glycosidic linkages between reducing sugar glucose. Apart from that, the asymmetric stretching mode of C-O-C bond at 1160 cm^{-1} was attributable to the aliphatic ring contained in cellulose (Achaby et al., 2018). This peak was gradually increased in terms of intensity after successive chemical treatments, which constitute of alkaline treatment, bleaching and acid hydrolysis. This signifies the increasing cellulose content and accessibility in cellulose nanocrystals derived from empty fruit bunches. The observed transmittance peaks at 1315 cm^{-1}, 1370 cm^{-1} and 1426 cm^{-1} were attributed to the C-O symmetric stretching of aromatic ester in cellulose, C-H and CH$_2$ symmetrical bending of methyl group in cellulose, respectively (Okahisa et al., 2018). Similarly, intensities of these observed peaks escalated after each successive chemical treatment. The increasing of intensities these peaks were observed in bleached cellulose microfibres and cellulose nanocrystals.

Subsequently, the presence of sulphate group, S=O, incorporated in cellulose nanocrystals is determined by the observed transmittance peak at 1201 cm^{-1}, which distinguished the cellulose nanocrystals from cellulose microfibres and alkali-treated empty fruit bunches (Achaby et al., 2018).

4.5   Crystallinity Study

The XRD patterns in Figure 4.7 shows the characteristic reflection of the crystalline structures of cellulose samples extracted from empty fruit bunches under three various chemical treatments. The three types of chemical treatments implemented were alkaline treatment by sodium hydroxide, bleaching process (by glacial acetic acid and sodium chlorite) and acid hydrolysis (by sulphuric acid). These cellulose samples provided two main cellulose I characteristic peaks. First, the peak for 2θ around 22.5° is the maximum intensity of lattice diffraction correspond to cellulose crystallographic plane at [0 0 2] (Salari et al., 2019). Next, the peak for 2θ around 16 to 18° is the minimum intensity of lattice diffraction correspond to cellulose crystallographic plane at [1 1 0] (Vanitjinda et al., 2019).
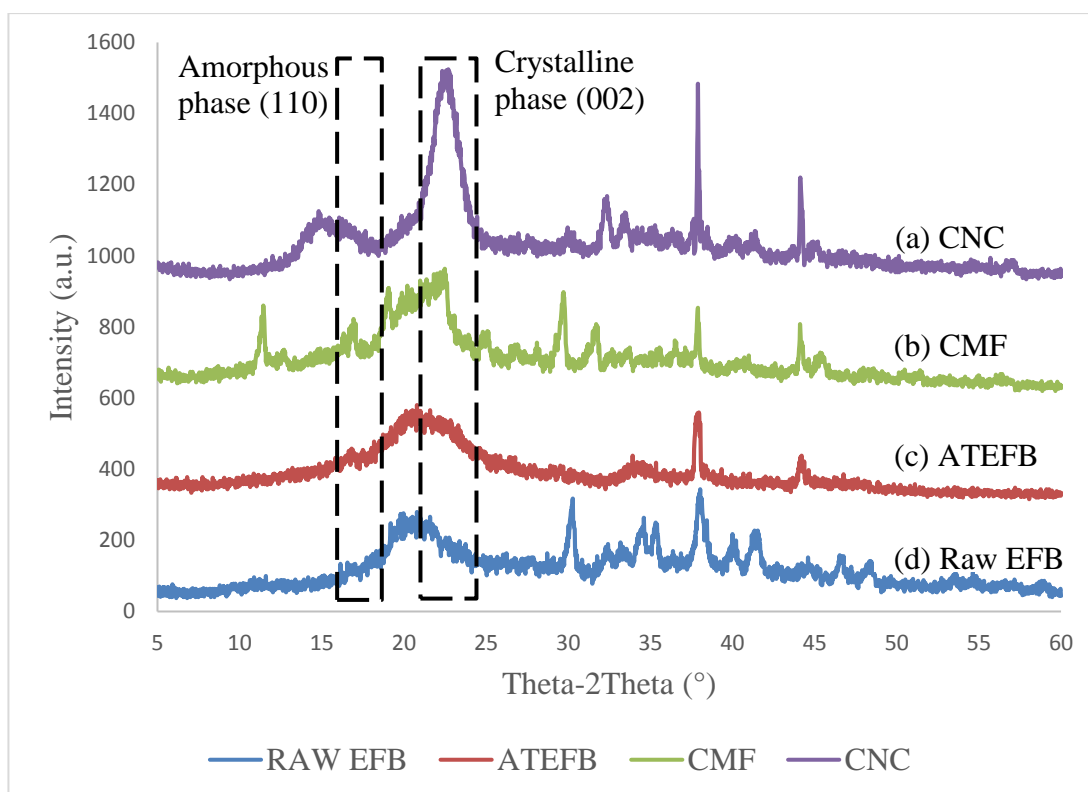
Figure 4.7: XRD Patterns of Alkali-treated Empty Fruit Bunches, Bleached Cellulose Microfibres and Cellulose Nanocrystals

By comparing the crystallinity peaks from the alkali-treated empty fruit bunches to cellulose microfibres, diffraction peak at around $2\theta = 22.5°$ has been amplified after bleaching process, representing an increase in the cellulose crystallinity. The Crystallinity Index (CrI) can be computed using Equation 4.7 (Prado and Spinacé, 2019).

$$CrI\ (\%) = \frac{I_{002} - I_{am}}{I_{002}} \times 100 \tag{4.7}$$

where

I_{002} = maximum intensity of (002) lattice diffraction, count

I_{am} = Intensity of (am) lattice diffraction due to amorphous cellulose, count

In this study, the calculation of crystallinity indices (CrI) of raw empty fruit bunches, alkali-treated empty fruit bunches, cellulose microfibres and cellulose nanocrystals will be shown in Appendix H. The crystallinity indices of different samples were summarised in Table 4.6.

Table 4.6: Crystallinity Indices at Different Stages of Treatment Using XRD

Components	Peak	2θ (°)	Intensity (count)	Crystallinity, CrI (%)
Raw empty fruit bunches	1	22.58	42	45.2381
	2	17.82	23	
Alkali-treated empty fruit bunches	1	22.84	52	57.6923
	2	16.84	22	
Bleached Cellulose microfibres	1	22.34	142	68.3099
	2	16.80	45	
Cellulose nanocrystals	1	22.54	327	83.4862
	2	16.30	54	

The crystallinity of raw empty fruit bunches, alkali-treated empty fruit bunches, bleached cellulose microfibres and cellulose nanocrystals were determined to be 45.2381, 57.6923, 68.3099 and 83.4862 %, respectively. Obviously, the crystallinity indices increase tremendously after series of chemical treatments. This signifies the successful removal of hemicellulose and lignin from the raw empty fruit bunches (Naduparambath et al., 2018). Crystallinity indicates the degree of ordered structure in an object, which is the extent of atomic arrangement in regular and ordered manner (Skoog, D. A., Holler, F. J., and Nieman, 1998). Antithetically, low crystallinity indicates an amorphous object, which has random atomic arrangement and lower strength compared to highly crystalline object. In this context, hemicellulose and lignin are regarded as amorphous objects. This is because hemicellulose and lignin have shorter chains and they are highly branched compared to linear chain of cellulose (Chen, 2014). Branched polysaccharides contribute to the formation of random atomic or amorphous structure. Hence, the increment of crystallinity index is one of the effective ways to verify the removal of lignin and hemicellulose from raw empty fruit bunches. Besides, this can be compared and supported by the data obtained from FTIR analysis, with the absence of characteristic peaks of lignin and hemicellulose from the bleached cellulose microfibres and cellulose nanocrystals spectra.

Raw empty fruit bunches as the starting material for cellulose extraction exhibited crystallinity index of 45.2381 %, which is the lowest value among the samples tested such as alkali-treated empty fruit bunches, bleached cellulose microfibres and cellulose nanocrystals. This demonstrated the presence of greater content of amorphous lignocellulosic substances. Coincidentally, the crystallinity index of raw empty fruit bunches obtained in this study was in good agreement with other crystallinity indices that were reported from other journals at around 48.6 %. Thus, it evinces highly-amorphous properties of empty fruit bunches before treatment (Choong et al., 2018). The crystallinity index of alkali-treated empty fruit bunches acquired in this study was 57.6923 %, which is in good agreement with other crystallinity indices that were reported from other journals at around 56 % (Achaby et al., 2018). This revealed that the method and concentration of sodium hydroxide solution used to prepare the alkali-treated empty fruit bunches were effective and appropriate. Similarly, the crystallinity index of bleached cellulose microfibres was measured to be 68.3099 %. The result reported from other journals displayed 71 % of crystallinity index (Achaby et al., 2018). Experimental results in this study depicted a slightly lower degree of crystallinity index compared to the value reported from other journals. Remarkably, the crystallinity indices between alkali-treated empty fruit bunches and bleached cellulose microfibres were fairly obvious, which indicates the necessity of bleaching treatment as the modus operandi to further remove lignin and hemicellulose from raw empty fruit bunches.

Subsequently, cellulose nanocrystals showed a greater value of crystallinity index compared to alkali-treated empty fruit bunches and bleached cellulose microfibres. This was mainly due to the reaction of concentrated sulphuric acid solution that penetrated into the amorphous region of the cellulose. This contributed to the hydrolytic cleavage of glycosidic bonds in the cellulose and encouraged the liberation of ester group (Cheng et al., 2017). Furthermore, an increase in crystallinity of cellulose indicates the modification of the cellulose structure that can contribute to higher tensile strength and improved structural stability when compared to cellulose structure prior to the acid hydrolysis. From other work, nano-crystalline cellulose samples that were produced from similar technique yielded a crystallinity index up to 90 % (Achaby et al., 2018). High crystallinity signifies the complete removal of lignin and hemicellulose from cellulose nanocrystal samples. The experimental results in this study, however, obtained slightly lower crystallinity index of 83.4862 % compared to

the results obtained from other studies. Despite this, it shows a great advancement in crystallinity index from 68.3099 % to 83.4862 % after a series of alkaline treatment, bleaching and acid hydrolysis. Therefore, acid hydrolysis treatment can be considered to be an effective method in producing nano-crystalline cellulose sample.

4.6 Microstructural Analysis of Cellulose

4.6.1 Scanning Morphological Analysis

Scanning Electron Microscopy (SEM) can be used to examine the surface morphology, structural properties and topography of alkali-treated empty fruit bunches, bleached cellulose microfibres and cellulose nanocrystals at different magnifications. Figure 4.8 shows the SEM images of the alkali-treated empty fruit bunches and bleached cellulose microfibres at a magnification of 650 $\times$ and 1600 $\times$. In this study, the effects of chemical treatments towards the sample surface morphology and structure can be evaluated by analysing the data obtained from SEM.

SEM images of raw empty fruit bunches contained rather smooth and flat surfaces compared to alkali-treated empty fruit bunches and bleached cellulose microfibres (Sellappah et al., 2016). Fibres are bound to each other and form a big lump of masses with estimated diameter at around 20 to 45 µm based on Figure 4.8 (a) and 4.8 (b). The smooth surfaces on the raw empty fruit bunches are probably due to the wax coated on the surface of empty fruit bunches. This layer of wax will eventually be eliminated by chemical treatments. Next, it can be seen that for alkali-treated empty fruit bunches, long and thick fibre-like structures are clearly represented in Figure 4.8 (a) and 4.8 (b). Fissures are quite obvious in alkali-treated empty fruit bunches, forming alternating lamellar structures that deposit on the long fibres. As the magnification increases, more crevices and cracks are becoming more visible. Results reported from other study has suggested that raw empty fruit bunches display a relatively smooth and even topography compared to post-treated empty fruit bunch fibres (Sellappah et al., 2016). This implies that the alkaline treatment has contributed to reduce lignin linkages with other cellulosic substances, which is an important indication of lignin removal after the alkaline treatment (Khalili et al., 2018). Moreover, the sizes of alkali-treated empty fruit bunches are relatively small, in which the diameter discerned from SEM images at around 20 to 70 µm. This is mainly due to mechanical grinding of the raw empty fruit bunches prior to the chemical treatments and also the effectiveness of alkaline treatment itself.
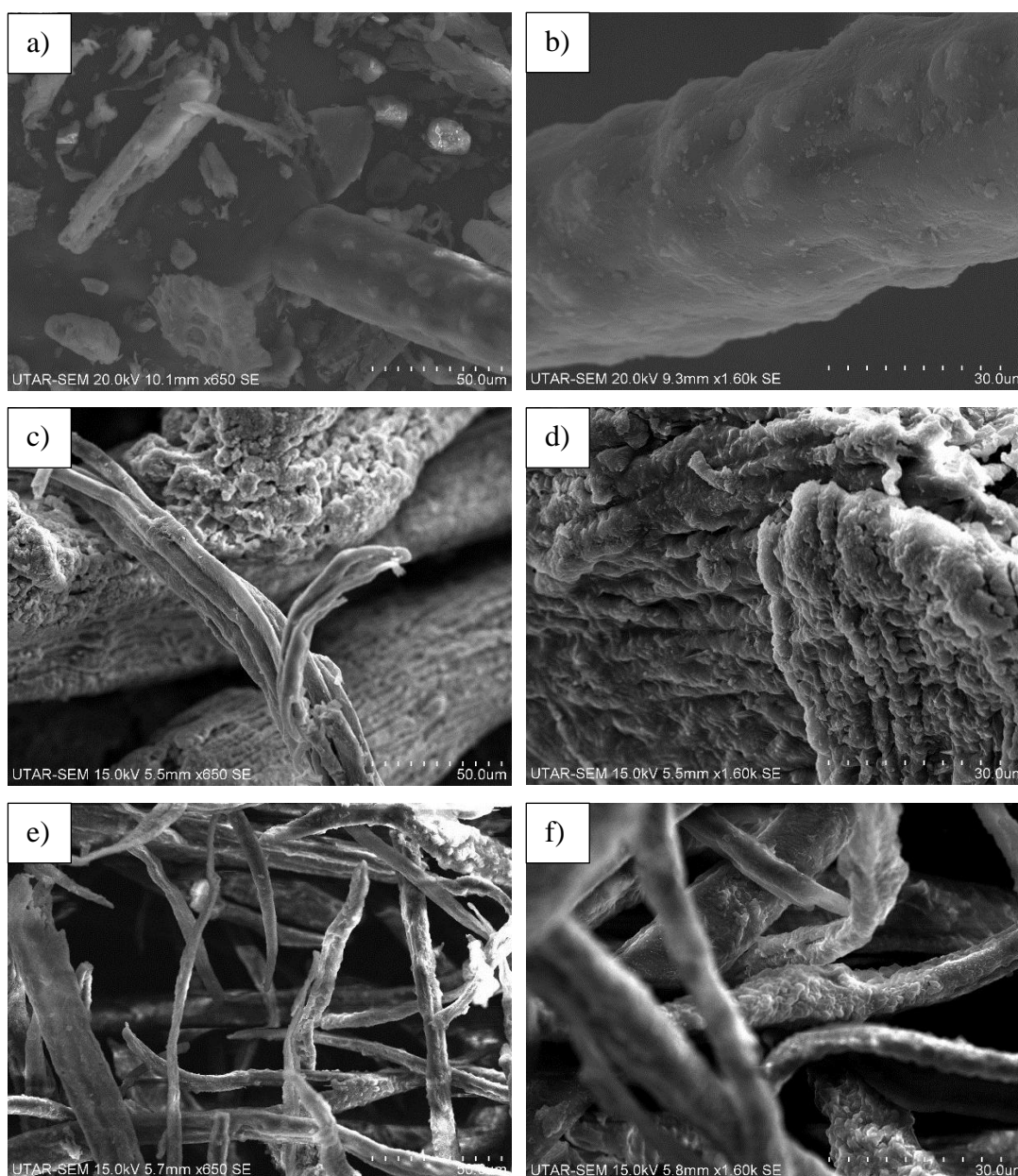
Figure 4.8: SEM Images of (a) Raw Empty Fruit Bunches at a Magnification of 650 ×, (b) Raw Empty Fruit Bunches at a Magnification of 1600 ×, (c) Alkali-treated Empty Fruit Bunches at a Magnification of 650 ×, (d) Alkali-treated Empty Fruit Bunches at a Magnification of 1600 ×, (e) Bleached Cellulose Microfibres at a Magnification of 650 × and (f) Bleached Cellulose Microfibres at a Magnification of 1600 ×

Apart from that, bleached cellulose microfibres showed similar outer appearance as compared to alkali-treated empty fruit bunches. Surface roughness increased steadily after the bleaching process which was in good agreement with a previously reported work (Sellappah et al., 2016). Small pores and uneven surfaces

were detected after bleaching process in this study. This proved that the bleaching process assisted in porosity development, thus, increased the total surface area exposed. In scientific context, alkali-treated empty fruit bunches are deemed as semi-treated biomass products as it requires further processes to complete the pre-treatment of lignocellulosic biomass (Ng et al., 2015). In this study, greater extent of lignin removal was shown by bleached cellulose microfibres based on more uneven surfaces observed. This can be explained by defibrillation of fibres in which the labile linkages between lignin and other cellulosic substances, and between lignin monomers, have been severed (Achaby et al., 2018). In term of sizes, there is a huge difference of bleached cellulose microfibres as compared to alkali-treated empty fruit bunches noticeable from the SEM images. The SEM images revealed that the diameter of bleached cellulose microfibres were around 5 to 20 μm, indicating the importance and necessity of bleaching treatment as part of hemicellulose and lignin removal schemes. The diameter of similar products after underwent bleaching treatment was reported to be 10 μm (Achaby et al., 2018), which is in good agreement with the result obtained in the current work. After bleaching treatment, semi-treated empty fruit bunches are ready and available for cellulose nanocrystal extraction.
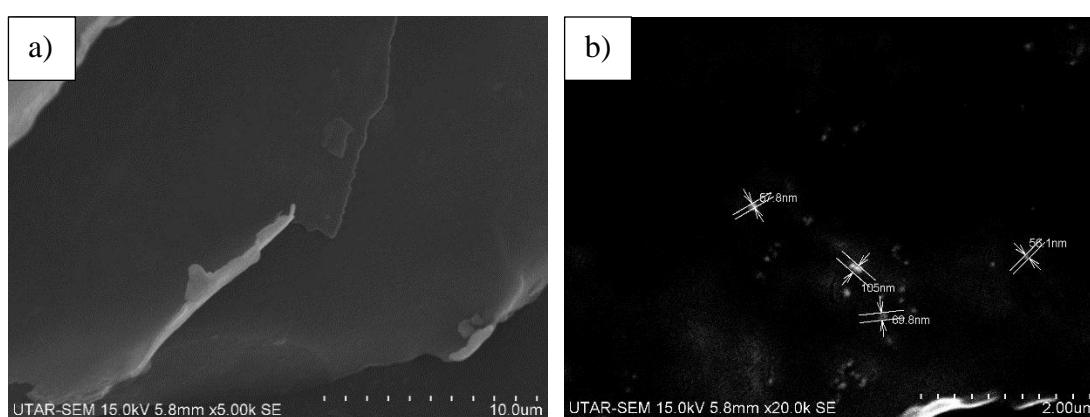

Figure 4.9: SEM Images of (a) Cellulose Nanocrystals at a Magnification of 5000 × and (b) Cellulose Nanocrystals at a Magnification of 20000 ×

Subsequently, the bleached cellulose microfibres will undergo acid hydrolysis process to yield the final nanoscale product. In the acid hydrolysis process, duration of the process, sizes of cellulosic materials and concentration of acid are the significant parameters to be considered to produce highly-crystalline cellulose nanocrystals (Lu and Hsieh, 2010). The acid hydrolysis condition is more critical than alkaline treatment

and bleaching process as it needs to completely remove the amorphous structure of cellulose. Consequently, the size of cellulose nanocrystals produced was significantly smaller than bleached cellulose microfibres. For this reason, the magnification level of SEM used for cellulose nanocrystals characterisation was much higher than alkali-treated cellulose nanocrystals and bleached cellulose microfibres, which was conducted at $5000 \times$ and $20000 \times$ to detect the nanoparticles present in the samples. From Figure 4.9 (a), the SEM image at a magnification power of $5000 \times$ showed that the cellulose nanocrystals agglomerated to form a big lump of structure. Aggregation of nanocellulose particles is a common phenomenon that has been reported by many studies due to the strong interfibrillar attraction of hydrogen bonding (Tan et al., 2019). Presence of negatively-charged sulphate group, however, can repel and diminish those attraction forces to certain extent (Kargarzadeh et al., 2017). In term of size, the diameters of cellulose nanocrystals observed were ranged from 56.1 to 105.0 nm, which can be used to confirm the successful extraction of cellulose nanocrystals after the acid hydrolysis.

4.6.2   Energy Dispersive X-ray Analysis

Table 4.7 shows the overall elements that are present in empty fruit bunch fibres after various stages of chemical treatment. Based on the EDX data collected, the raw empty fruit bunches contain 57.38 wt% and 42.62 wt% of carbon atom (C) and oxygen atom (O), respectively. On the other hand, hydrogen atom (H) cannot be detected by EDX analysis. EDX analysis is detecting elements based on the electrons occupying the K-shells. Since hydrogen does not have a K shell as it consists only single electron, which is too light to be detected by EDX (Stojilovic, 2012). As hydrogen atom is undetectable by energy dispersive X-ray equipment, chemical composition of carbon and oxygen elements in the samples become significant. As aforementioned, raw empty fruit bunch is lignocellulosic biomass that mainly comprises of lignin, cellulose and hemicellulose. These three components are organic compounds. In other words, carbon, oxygen and hydrogen are the main elements forming the frameworks of the empty fruit bunches. Apparently, cellulose constitutes of polysaccharide with repeating units of $(C_6H_{10}O_5)_n$ or $\beta-1,4$ linked glucose units (Mariano et al., 2014).

Table 4.7: Elements Detected in Samples After Different Chemical Treatment

Elements	Raw empty fruit bunches		Alkali-treated fruit bunches		Bleached cellulose microfibres		Cellulose nanocrystals	
	wt%	at%	wt%	at%	wt%	at%	wt%	at%
C	57.38	64.20	53.11	60.14	52.97	60.01	49.17	57.63
O	42.62	35.80	46.89	39.86	47.03	39.99	45.48	40.02
S	-	-	-	-	-	-	5.35	2.35

Apart from that, the compositions of carbon atom of various samples as shown in Table 4.7 are varied around 50 wt%. The carbon content is expected to be gradually decreased due to the removal of hemicellulose and lignin (Khalili et al., 2018). The purpose of pre-treatments is to obtain the cellulose contained in fiber matrix, whereas lignin and hemicellulose are removed via dissolution in chemicals. Therefore, it is reasonable that loss of carbon element in this study was due to the removal of hemicellulose and lignin in the chemical solution. On the contrary, oxygen atom depends on the adsorption of water molecules onto the cellulose samples. Thus, effect of lignin and hemicellulose removal towards oxygen content in empty fruit bunches is insignificant (Tan et al., 2015b). Based on Table 4.7, the sodium atom (Na) and chlorine atom (Cl) atoms were not detected, indicates the sodium hydroxide and sodium chlorite solution are completely removed from the samples via washing process. Thus, the results obtained by energy dispersive X-ray analysis exhibited favorable results that the composition of carbon atom and oxygen atom in various samples prepared by different pre-treatments are accurate and reliable.

Ideally, chemical composition of cellulose nanocrystals for carbon atom (C), oxygen atom (O) and sulphur atom (S) are 47.69 wt%, 51.63 wt% and 0.68 wt%, respectively (Man et al., 2011). Based on the results obtained from EDX analysis, chemical composition of CNC for carbon atom (C), oxygen atom (O) and sulphur atom (S) were 49.17 wt%, 45.48 wt% and 5.35 wt%, respectively. The chemical composition of carbon atom and oxygen atom were in good agreement with the previously reported study. This indicates that the preparation methods of cellulose nanocrystals were adequate and decent. Conversely, content of sulfur atom obtained in this study showed a slight difference with findings reported by other work. Low amount of sulfur atom contained in the cellulose nanocrystals would be mainly due to

the reaction with sulphuric acid during the hydrolysis that causes the incorporation of sulfur ester group into the cellulose nanocrystals (Rahimi Kord Sofla et al., 2016). Excessive amount of sulfur atom was discovered via EDX analysis demonstrated incomplete washing of cellulose nanocrystals produced and minor amount of sulphuric acid might remain on cellulose nanocrystal samples.

4.7 Dynamic Light Scattering

Dynamic light scattering was employed to study the particles size distribution of cellulose nanocrystals. It utilised a beam of monochromatic laser light to radiate on a biomolecule solution containing the sample to be analysed (Oliveira et al., 2017). The intensity of laser light scattered by molecules in the solution will be quantified. Light intensities scattered is related to the hydrodynamic radius of the samples. Thus, different ranges of size distribution of cellulose nanocrystals can be evaluated and displayed in the form of chart as shown in Figure 4.10.
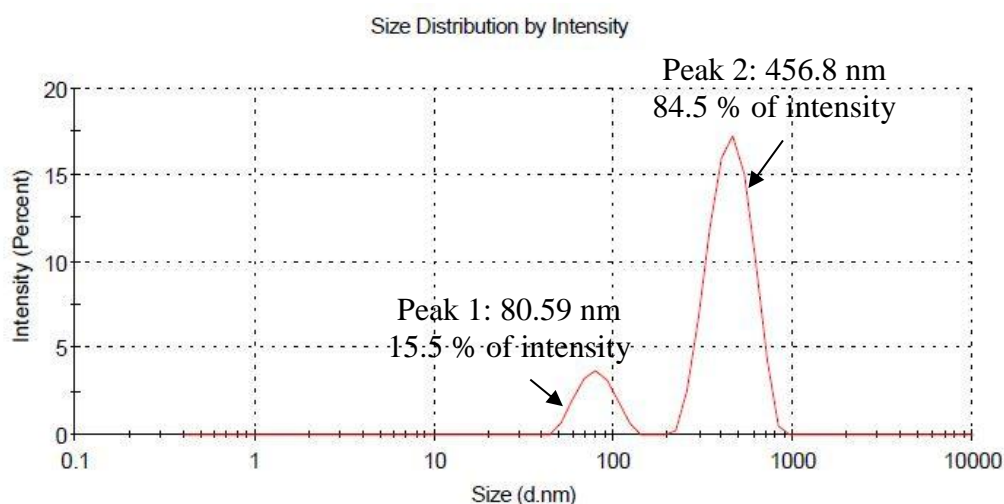

Figure 4.10: Size Distribution of Cellulose Nanocrystals Analysed Using Dynamic Light Scattering

From Figure 4.10, it can be clearly seen that the particle size distribution resulted in two main population groups. 15.5 % and 84.5 % of the nanocellulose particles were having average sizes of 80.59 nm and 456.8 nm, respectively. The size detected for 15.5 % of the nanocellulose particles in this study was in good agreement with the results obtained from SEM analysis, which ranged between 56.1 to 105.0 nm. On the contrary, the size detected for 84.5 % of the nanocellulose particles in this study

was greater than the sizes obtained through SEM analysis. This might due to the circumstance that the particle sizes of cellulose nanocrystals in dynamic light scattering were augmented considerably by the solvation effects. Solvation effect is a process of surrounding solute particles with solvent owing to polarity of the substances. Solvation effect can decrease the diffusion coefficient of the nanocellulose particles. As the hydrodynamic diameter is inversely proportional to the diffusion coefficient, reduction of diffusion coefficient increases the hydrodynamic diameter of cellulose nanocrystals (Oliveira et al., 2017). Consequently, the hydrodynamic diameters of cellulose nanocrystals can be amplified to 1.3 times of the original diameters of the cellulose nanocrystals without incorporated in the water (Srivastava et al., 2019).

It is important to ensure that the sizes of cellulose nanocrystal samples are compatible to nanoscale particles, which is ranged below 1 μm (Novo et al., 2016). Surface charge is also an important parameter to determine the stability and dispersion state of aqueous cellulose nanocrystals suspension (Morais et al., 2013). A stable nanocellulose particles have negatively-charged surface as reported by other studies (Choong et al., 2018). Negatively-charged surface of cellulose nanocrystals can create sufficient electrostatic repulsion to overcome the agglomeration force between nanocellulose particles (Achaby et al., 2018). The electrostatic repulsion is also applicable to particle with positively-charged surface. On the contrary, presence of positive and negative surface charge simultaneously on surface of nanocellulose particles can create attraction forces between nanocellulose particles, which induce particle aggregation. Therefore, enlargement of nanoparticles with bigger hydrodynamic diameter in this study might be due to greater particle aggregation (Cheng et al., 2014). The aggregated particles can be observed under dynamic light scattering technique as a single particle.

4.8   Thermogravimetric Analysis

Thermal stability of the cellulose nanocrystals was evaluated using thermogravimetric analysis under inert nitrogen atmosphere. The acquired thermogravimetric analysis (TGA) and derivative thermogravimetry (DTG) curves demonstrate the specific degradation temperatures and rates of degradation via mass losses as shown in Figure 4.11 (a) and (b), respectively.
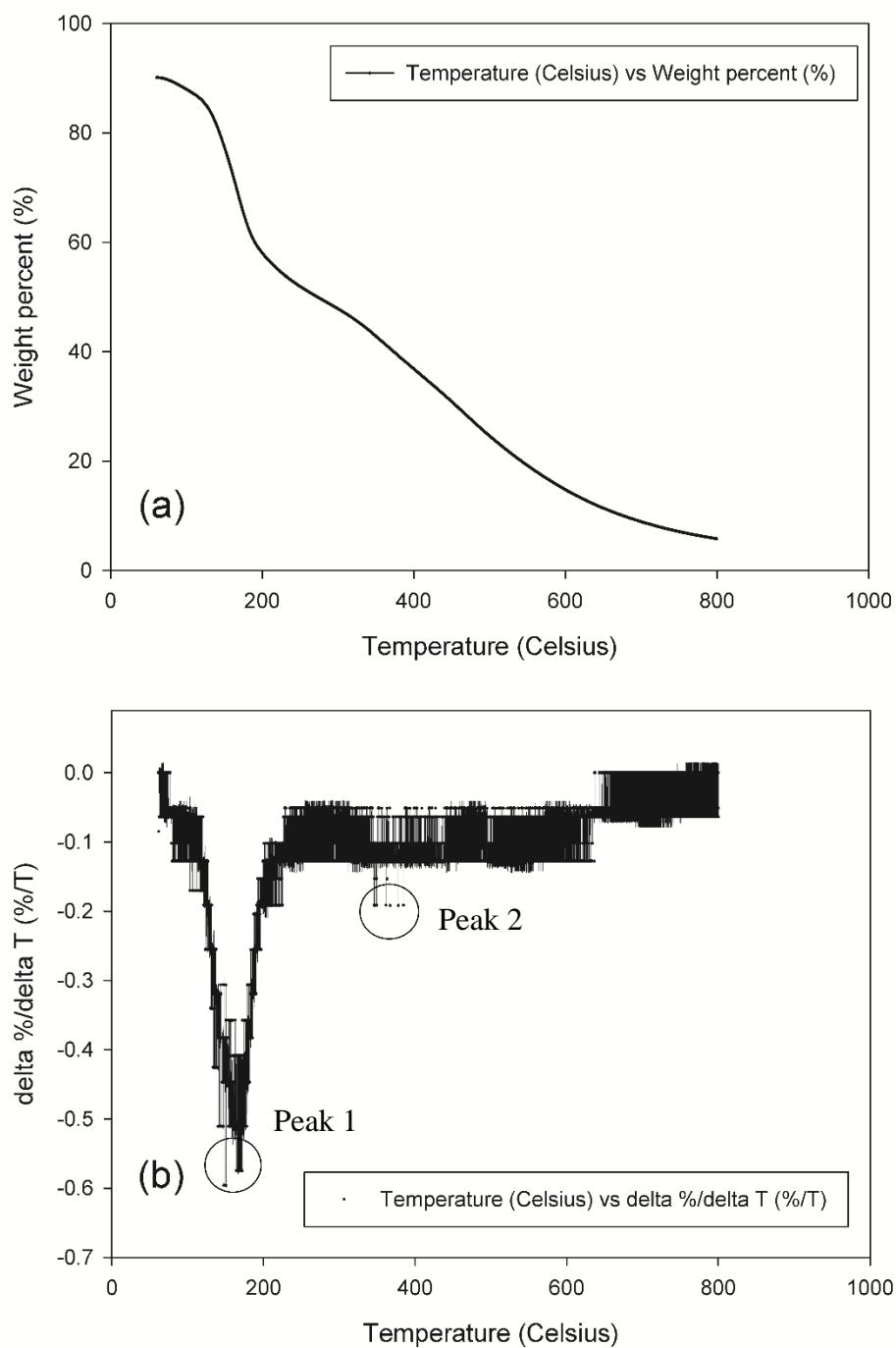
Figure 4.11: (a) Thermogravimetric Analysis (TGA) Curve of Cellulose Nanocrystals and (b) Derivative Thermogravimetry (DTG) Curve of Cellulose Nanocrystals

In this study, decomposition of the samples was observed between 60 to 800 °C. Mass loss of cellulose nanocrystal samples at temperature below 100 °C was attributable to the evaporation of low molecular weight substances such as adsorbed

water. The mass reduction, however, is relatively small before 100 °C due to highly crystalline structure of cellulose nanocrystals that are stable below this temperature (Mondragon et al., 2014). The onset temperature for the degradation of cellulose nanocrystal samples occurred at a temperature of 150 °C based on Figure 4.11 (a). This is probably due to the cleavage of β-(1/4)-glycosidic bonds linked D-anhydroglucopyranose that present in cellulose nanocrystals. The formation of β-(1/4)-glycosidic bonds linked D-anhydroglucopyranose can be attributed to the acid hydrolysis. Subsequently, two obvious degradation stages for cellulose nanocrystals were detected in this study, which can be confirmed by the presence of two peaks as shown in DTG curve. The first degradation stage of mass loss at temperature around 170 to 250 °C was induced by the presence of sulphate group on the surface of cellulosic materials, which was in good agreement with the presence of sulphate group peak at 1201 cm^{-1} obtained in FTIR spectra in this study (Mondragon et al., 2014). Degradation processes occurred at this stage including depolymerisation and dehydration of cellulose nanocrystals (Choong et al., 2018).

The second degradation stage occurred at around 350 to 380 °C in this study can be correlated to the degradation of ordered and packed cellulose regions (Luzi et al., 2019). As cellulose nanocrystals consist of highly crystalline domains, they have greater thermal stability as compared to other lignocellulosic materials. Pectin, lignin and hemicellulose for examples, have degradation temperature of 207 °C, 217 °C and 308 °C, respectively, as reported by other works (Mondragon et al., 2014). Therefore, the absence of degradation peaks at these temperatures implied that the multistep processes of pre-treatment and acid hydrolysis in this study have successfully eliminated the hemicellulose and lignin in the cellulose nanocrystal samples.

4.9   Summary

In this chapter, it recapitulated all the results obtained by physical and chemical means. Cellulose-based products synthesised at different stages are characterised by additional treatment and analytical instruments such as X-ray diffraction (XRD), scanning electron microscopy (SEM), Fourier transform infrared spectroscopy (FTIR), dynamic light scattering (DLS) and thermogravimetric analysis (TGA). In order to examine the effectiveness of the approach selected to achieve the objectives, the results obtained are analysed and interpreted to compare with the literatures. Each analytical instrument plays a significant role to determine the existence of cellulose nanocrystals. For

instance, X-ray diffraction (XRD) determined the crystallinity index of samples, Fourier transform infrared spectroscopy (FTIR) verified the presence of unique functional groups in samples, scanning electron microscopy (SEM) dealt with the topography, morphology and size of samples produced, dynamic light scattering (DLS) determined the size distribution of cellulose nanocrystal samples in order to strengthen the fact that cellulose nanocrystals produced in this study lies in nano-scale range and thermogravimetric analysis (TGA) discovered the thermal degradation pattern of samples. All of these characterisation methods provide reliable and plausible information to confirm the characteristics of cellulose nanocrystals.

Apart from that, some uncertainties were addressed and investigated to determine the possible reasons that lead to these outcomes. Nonetheless, the overall results are favourable and are able to meet with the expectations of this study.

CHAPTER 5

CONCLUSIONS AND RECOMMENDATIONS

5.1   Conclusions

The present work highlighted the isolation of cellulose nanocrystals from biomass waste of empty fruit bunches. Several characterisation techniques such as XRD, SEM-EDX, FTIR and TGA were carried out on the samples produced. Alkali-treated empty fruit bunches and bleached cellulose microfibres have porous and rough surfaces with a diameter at around 20 to 70 μm and 5 to 20 μm, respectively. After subjecting the bleached cellulose nanocrystals to acid hydrolysis, cellulose nanocrystals can be successfully obtained with a crystallinity index of 83. 4862 %, diameter at around 56.1 to 105.0 nm and a yield of 2.93 % with respect to the total weight of raw empty fruit bunches used. The onset degradation temperature and maximum degradation temperature range of cellulose nanocrystals are 150 °C and 350 to 380 °C, respectively. On the other hand, based on the results of FTIR analysis, the presence of sulphate group stretching peaks proved its successful incorporation onto the cellulose nanocrystals.

The chemical composition analysis confirmed the increasing trend of cellulose content and decreasing trend of hemicellulose content in empty fruit bunches after successive treatment steps. Based on the experimental results, raw empty fruit bunches, alkali-treated empty fruit bunches, bleached cellulose microfibres and cellulose nanocrystals comprise of 20.28 %, 30.06 %, 46.68 % and 73.74 % of cellulose, respectively. The cellulose content in cellulose nanocrystals obtained in this study is lower than cellulose content as reported by other researchers, which was around 90 %. This can be explained by the losses in the middle of handling processes throughout series of chemical treatments.

In brief, all the established objectives in this study were accomplished. The presented outcomes were able to confirm that the approach selected can be used to extract cellulose nanocrystals from empty fruit bunches effectively. In addition, it assures the reduction of empty fruit bunches biomass waste by utilising chemo-mechanical treatment and acid hydrolysis to convert empty fruit bunches into useful

product. Therefore, it can be concluded that the empty fruit bunches are the suitable and sustainable sources for cellulose nanocrystal extraction.

5.2 Recommendations for Future Work

Throughout this study, experimental works were carried out as stated in the scope of study but errors and anomalies occurred and led to considerable consumption of time. In order to produce more accurate and reliable results, repetition of similar experimental work is inevitable. This main repercussion will limit the exploration of study on other possible parameters to yield a better result. The deviations might due to differences in every batch of samples fabricated, either in the processing conditions or external factors. Few improvements are suggested in the future related project work in order to enhance the consistency, reliability and precision of the data obtained from laboratory work. Various recommendations related to the study are summarised as follows:

(i) After the cellulose samples are produced, the samples should be sent for chemical analysis and characterisation as soon as possible to prevent oxidation, contamination and degradation of the final products.

(ii) Parameter studies on the extraction of cellulose nanocrystals such as concentration of sulphuric acid, duration of hydrolysis as well as appropriate operating temperature must be evaluated in order to determine the optimum operating conditions for higher yield if cellulose nanocrystals are targeted to be produced in large scale.

(iii) Field emission scanning election microscope (FESEM) can be used in the future for better understanding on the morphology of cellulose nanocrystals as it can be easily observed under greater magnification. This is especially useful for samples in nanoscale.

(iv) Dialysis tubing should be encouraged to be employed in the washing of cellulose nanocrystals suspension that is produced after acid hydrolysis to eliminate the remnant acid resides in the suspension to a greater extent.

(v) Addition of appropriate stabiliser or dispersant in cellulose nanocrystal suspension is should be suggested in order to prevent the aggregation of cellulose nanocrystals.

REFERENCES

Abdul, H.P.S., Jawaid, M., Hassan, A., Paridah, M.T. and Zaido, A., 2012. Oil Palm Biomass Fibres and Recent Advancement in Oil Palm Biomass Fibres Based Hybrid Biocomposites. *Composites and Their Applications*, 8, pp.187–220.

Abdullah, M.A., Nazir, M.S., Raza, M.R., Wahjoedi, B.A. and Yussof, A.W., 2016. Autoclave and ultra-sonication treatments of oil palm empty fruit bunch fibers for cellulose extraction and its polypropylene composite properties. *Journal of Cleaner Production*, 126, pp.686–697.

Abdulrazik, A., Elsholkami, M., Elkamel, A. and Simon, L., 2017. Multi-products productions from Malaysian oil palm empty fruit bunch (EFB): Analyzing economic potentials from the optimal biomass supply chain. *Journal of Cleaner Production*, 168, pp.131–148.

Abraham, E., Deepa, B., Pothan, L.A., Jacob, M., Thomas, S., Cvelbar, U. and Anandjiwala, R., 2011. Extraction of nanocellulose fibrils from lignocellulosic fibres: A novel approach. *Carbohydrate Polymers*, 86(4), pp.1468–1475.

Achaby, M. El, Kassab, Z., Barakat, A. and Aboulkas, A., 2018. Alfa fibers as viable sustainable source for cellulose nanocrystals extraction: Application for improving the tensile properties of biopolymer nanocomposite films. *Industrial Crops and Products*, 112, pp.499–510.

Afiq bin Jumhuri, A., Nur Elleina binti Fatanah, D., Husaini bin Mohamed, A., Rohaida binti Che Hak, C., bin Mohamed Sapari, J. and Nadia binti Dzulkifli, N., 2017. Characterization of cellulose nanocrystal isolated from oil palm empty fruit bunch using formic acid hydrolysis. *International Journal of Agriculture*, 5, pp.52–59.

Agustin-Salazar, S., Cerruti, P., Medina-Juárez, L.Á., Scarinzi, G., Malinconico, M., Soto-Valdez, H. and Gamez-Meza, N., 2018. Lignin and holocellulose from pecan nutshell as reinforcing fillers in poly (lactic acid) biocomposites. *International Journal of Biological Macromolecules*, 115, pp.727–736.

Akhtar, M.N., Sulong, A.B., Radzi, M.K.F., Ismail, N.F., Raza, M.R., Muhamad, N. and Khan, M.A., 2016. Influence of alkaline treatment and fiber loading on the physical and mechanical properties of kenaf/polypropylene composites for variety of applications. *Progress in Natural Science: Materials International*, 26(6), pp.657–664.

Alemdar, A. and Sain, M., 2008. Isolation and characterization of nanofibers from agricultural residues – Wheat straw and soy hulls. *Bioresource Technology*, 99(6), pp.1664–1671.

Álvarez, A., Cachero, S., González-Sánchez, C., Montejo-Bernardo, J., Pizarro, C. and Bueno, J.L., 2018. Novel method for holocellulose analysis of non-woody biomass wastes. *Carbohydrate Polymers*, 189, pp.250–256.

Anwar, B., Bundjali, B. and Arcana, I.M., 2015. Isolation of Cellulose nanocrystals from Bacterial Cellulose Produced from Pineapple Peel Waste Juice as Culture Medium. *Procedia Chemistry*, 16, pp.279–284.

Anyaoha, K.E., Sakrabani, R., Patchigolla, K. and Mouazen, A.M., 2018. Critical evaluation of oil palm fresh fruit bunch solid wastes as soil amendments: Prospects and challenges. *Resources, Conservation and Recycling*, 136, pp.399–409.

Aracri, E., Díaz Blanco, C. and Tzanov, T., 2014. An enzymatic approach to develop a lignin-based adhesive for wool floor coverings. *Green Chemistry*, 16(5), p.2597–2603.

Asad, M., Saba, N., Asiri, A.M., Jawaid, M., Indarti, E. and Wanrosli, W.D., 2018. Preparation and characterization of nanocomposite films from oil palm pulp nanocellulose/poly (Vinyl alcohol) by casting method. *Carbohydrate Polymers*, 191, pp.103–111.

Athinarayanan, J., Periasamy, V.S. and Alshatwi, A.A., 2018. Fabrication and cytotoxicity assessment of cellulose nanofibrils using Bassia eriophora biomass. *International Journal of Biological Macromolecules*, 117, pp.911–918.

Bali, G., Meng, X., Deneff, J.I., Sun, Q. and Ragauskas, A.J., 2015. The effect of alkaline pretreatment methods on cellulose structure and accessibility. *ChemSusChem*, 8(2), pp.275–279.

Barneto, A.G., Carmona, J.A. and Garrido, M.J.F., 2016. Thermogravimetric assessment of thermal degradation in asphaltenes. *Thermochimica Acta*, 627–629, pp.1–8.

Betie, A., Meghnefi, F., Fofana, I. and Yeo, Z., 2018. Thermogravimetric Analyses. *Energies*, 11(3), pp.162–186.

Bhatnagar, A. and Sain, M., 2005. Processing of cellulose nanofiber-reinforced composites. *Journal of Reinforced Plastics and Composites*, 24(12), pp.1259–1268.

Bittar, K., 2012. *Cellulose*. Available through: <http://wwwcourses.sens.buffalo.edu/ce435/Cellulose_CB.pdf.> [Accessed 24 June 2018].

Boluk, Y. and Danumah, C., 2014. Analysis of cellulose nanocrystals rod lengths by dynamic light scattering and electron microscopy. *Journal of Nanoparticle Research*, 16(1), p.2174–2180.

Borchert, H., 2014. X-ray Diffraction. *Solar Cells Based on Colloidal Nanocrystal*, Springer, Cham, 5, pp.79–94.

Budhi, Y.W., Fakhrudin, M., Culsum, N.T.U., Suendo, V. and Iskandar, F., 2018. Preparation of cellulose nanocrystals from empty fruit bunch of palm oil by using phosphotungstic acid. *IOP Conference Series: Earth and Environmental Science*, 105(1), pp.1–6.

Burhani, D. and Septevani, A.A., 2018. Isolation of nanocellulose from oil palm empty fruit bunches using strong acid hydrolysis. *AIP Conference Proceedings*, 2024, pp.1–9.

Casillas, R., Rodríguez, K., Cruz-Estrada, R., Dávalos-Olivares, F., Navarro-Arzate, F., and Satyanarayana, K., 2018. Isolation and Characterization of Cellulose nanocrystals Created from Recycled Laser Printed Paper. *BioResources*, 13(4), pp.7404–7429.

Chang, S.H., 2014. An overview of empty fruit bunch from oil palm as feedstock for bio-oil production. *Biomass and Bioenergy*, 62, pp.174–181.

Chen, H., 2014. *Chemical Composition and Structure of Natural Lignocellulose. In: Biotechnology of Lignocellulose*. Dordrecht, Netherlands: Springer Netherlands.

Chen, Y.W., Lee, H.V., Juan, J.C. and Phang, S.-M., 2016. Production of new cellulose nanomaterial from red algae marine biomass Gelidium elegans. *Carbohydrate Polymers*, 151, pp.1210–1219.

Cheng, M., Qin, Z., Chen, Y., Hu, S., Ren, Z. and Zhu, M., 2017. Efficient Extraction of Cellulose nanocrystals through Hydrochloric Acid Hydrolysis Catalyzed by Inorganic Chlorides under Hydrothermal Conditions. *ACS Sustainable Chemistry & Engineering*, 5(6), pp.4656–4664.

Cheng, M., Qin, Z., Liu, Y., Qin, Y., Li, T., Chen, L. and Zhu, M., 2014. Efficient extraction of carboxylated spherical cellulose nanocrystalss with narrow distribution through hydrolysis of lyocell fibers by using ammonium persulfate as an oxidant. *Journal of Material Chemistry A*, 2(1), pp.251–258.

Cherian, B.M., Leão, A.L., de Souza, S.F., Thomas, S., Pothan, L.A. and Kottaisamy, M., 2010. Isolation of nanocellulose from pineapple leaf fibres by steam explosion. *Carbohydrate Polymers*, 81(3), pp.720–725.

Chieng, B., Lee, S., Ibrahim, N., Then, Y. and Loo, Y., 2017. Isolation and Characterization of Cellulose nanocrystals from Oil Palm Mesocarp Fiber. *Polymers*, 9(8), p.355–365.

Choong, T.S., Chew, I.M., Shanmugarajah, B., Mubarak, N.M., Tan, K. and Yoo, C., 2018. Valorization of palm oil agro-waste into cellulose biosorbents for highly effective textile effluent remediation. *Journal of Cleaner Production*, 210, pp.697–709.

Chorkendorff, I. and Niemantsverdriet, J.W., 2003. *Concepts of Modern Catalysis and Kinetics*. Weinheim, Germany: John Wiley & Sons.

Cudjoe, E., Hunsen, M., Xue, Z., Way, A.E., Barrios, E., Olson, R.A., Hore, M.J.A. and Rowan, S.J., 2017. Miscanthus Giganteus: A commercially viable sustainable source of cellulose nanocrystals. *Carbohydrate Polymers*, 155, pp.230–241.

Derman, E., Abdulla, R., Marbawi, H. and Sabullah, M.K., 2018. Oil palm empty fruit bunches as a promising feedstock for bioethanol production in Malaysia. *Renewable Energy*, 129, pp.285–298.

Dong, S., Bortner, M.J. and Roman, M., 2016. Analysis of the sulphuric acid hydrolysis of wood pulp for cellulose nanocrystals production: A central composite design study. *Industrial Crops and Products*, 93, pp.76–87.

Dowling, A.P., 2004. Development of nanotechnologies. *Materials Today*, 7(12), pp.30–35.

Eckert, M., 2012. Max von Laue and the discovery of X-ray diffraction in 1912. *Annalen der Physik*, 524(5), pp.83–85.

Fatah, I.Y.B.A., 2015. *Cellulose From oil palm empty fruit bunch and its influence as reinforcement agent in epoxy based nanobiocomposite*. Available through: <http://eprints.usm.my/31868/1/Ireana_Yusra_Bt_Abdul_Fatah_(HJ).pdf> [Accessed 26 June 2018].

Fernandez, A., Soria, J., Rodriguez, R., Baeyens, J. and Mazza, G., 2019. Macro-TGA steam-assisted gasification of lignocellulosic wastes. *Journal of Environmental Management*, 233, pp.626–635.

Gao, Y., Wang, H., Guo, J., Peng, P., Zhai, M. and She, D., 2016. Hydrothermal degradation of hemicelluloses from triploid poplar in hot compressed water at 180–340 °C. *Polymer Degradation and Stability*, 126, pp.179–187.

George, J. and Sabapathi, S.N., 2015. Cellulose nanocrystals: synthesis, functional properties, and applications. *Nanotechnology, science and applications*, 8, pp.45–54.

Griffiths, P.R., 1980. *Basic Theory and Instrumentation for FT-IR Spectrometry. In: Analytical Applications of FT-IR to Molecular and Biological Systems*. Dordrecht, Netherlands: Springer Netherlands.

Harmsen, P.F.H., Huijgen, W.J.J., Lopez, L.M.B., Bakker, R.R.C., 2010. *Literature review of physical and chemical pretreatment processes for lignocellulosic biomass*. Wageningen, Netherlands: Wageningen UR, Food & Biobased Research.

Hassan, M.L., Mathew, A.P., Hassan, E.A., El-Wakil, N.A. and Oksman, K., 2012. Nanofibers from bagasse and rice straw: process optimization and properties. *Wood Science and Technology*, 46(1–3), pp.193–205.

Hwang, K.-L., Choi, S.-M., Kim, M.-K., Heo, J.-B. and Zoh, K.-D., 2017. Emission of greenhouse gases from waste incineration in Korea. *Journal of Environmental Management*, 196, pp.710–718.

Ioelovich, M., 2015. Methods For Determination of Chemical Composition of Plant Biomass. *Journal Scientific Israel-Technological Advantages*, 17(4), pp.208–214.

Ismail, A.A., van de Voort, F.R. and Sedman, J., 1997. Chapter 4 Fourier transform infrared spectroscopy: Principles and applications. *Techniques and Instrumentation in Analytical Chemistry*, 18, pp.93–139.

Jaggi, N. and Vij, D.R., 2006. *Fourier Transform Infrared Spectroscopy. In: Handbook of Applied Solid State Spectroscopy*. Boston, United States: Springer US.

John, M.J. and Anandjiwala, R.D., 2009. Surface modification and preparation techniques for textile materials. In: *Surface Modification of Textiles*. Cambridge, England: Woodhead Publishing.

Jonoobi, M., Oladi, R., Davoudpour, Y., Oksman, K., Dufresne, A., Hamzeh, Y. and Davoodi, R., 2015. Different preparation methods and properties of nanostructured cellulose from various natural resources and residues: a review. *Cellulose*, 22(2), pp.935–969.

Jönsson, L.J. and Martín, C., 2016. Pretreatment of lignocellulose: Formation of inhibitory by-products and strategies for minimizing their effects. *Bioresource Technology*, 199, pp.103–112.

Kang, X., Kuga, S., Wang, C., Zhao, Y., Wu, M. and Huang, Y., 2018. Green Preparation of Cellulose nanocrystals and Its Application. *ACS Sustainable Chemistry & Engineering*, 6(3), pp.2954–2960.

Kargarzadeh, H., Ioelovich, M., Ahmad, I., Thomas, S. and Dufresne, A., 2017. Methods for Extraction of Nanocellulose from Various Sources. *Handbook of Nanocellulose and Cellulose Nanocomposites*, 1, pp.1–49.

Kargarzadeh, H., M. Sheltami, R., Ahmad, I., Abdullah, I. and Dufresne, A., 2015. Cellulose nanocrystals: A promising toughening agent for unsaturated polyester nanocomposite. *Polymer*, 56, pp.346–357.

Kaushik, M., Fraschini, C., Chauve, G., Putaux, J.-L. and Moores, A., 2015. *Transmission Electron Microscopy for the Characterization of Cellulose nanocrystals. In: The Transmission Electron Microscope - Theory and Applications*. InTech. Available through: <http://www.intechopen.com/books/the-transmission-electron-microscope-theory-and-applications/transmission-electron-microscopy-for-the-characterization-of-cellulose-nanocrystal> [Accessed 5 July 2018].

Khalili, P., Tshai, K.Y. and Kong, I., 2018. Comparative Thermal and Physical Investigation of Chemically Treated and Untreated Oil Palm EFB Fiber. *Materials Today: Proceedings*, 5(1), pp.3185–3192.

Kumar, A., Negi, Y.S., Choudhary, V. and Bhardwaj, N.K., 2014. Characterization of Cellulose nanocrystals Produced by Acid-Hydrolysis from Sugarcane Bagasse as Agro-Waste. *Journal of Materials Physics and Chemistry*, 2(1), pp.1–8.

Li, B., Xu, W., Kronlund, D., Määttänen, A., Liu, J., Smått, J.-H., Peltonen, J., Willför, S., Mu, X. and Xu, C., 2015. Cellulose nanocrystals prepared via formic acid hydrolysis followed by TEMPO-mediated oxidation. *Carbohydrate Polymers*, 133, pp.605–612.

Li, Z., Yang, X., Li, W. and Liu, H., 2019. Stimuli-responsive cellulose paper materials. *Carbohydrate Polymers*, 210, pp.350–363.

Liu, H., Pang, B., Zhao, Y., Lu, J., Han, Y. and Wang, H., 2018. Comparative study of two different alkali-mechanical pretreatments of corn stover for bioethanol production. *Fuel*, 221, pp.21–27.

Loh, S.K., 2017. The potential of the Malaysian oil palm biomass as a renewable energy source. *Energy Conversion and Management*, 141, pp.285–298.

Lu, P. and Hsieh, Y.-L., 2010. Preparation and properties of cellulose nanocrystals: Rods, spheres, and network. *Carbohydrate Polymers*, 82(2), pp.329–336.

Luzi, F., Puglia, D., Sarasini, F., Tirillò, J., Maffei, G., Zuorro, A., Lavecchia, R., Kenny, J.M. and Torre, L., 2019. Valorization and extraction of cellulose nanocrystals from North African grass: Ampelodesmos mauritanicus (Diss). *Carbohydrate Polymers*, 209, pp.328–337.

Machado, R.T.A., Gutierrez, J., Tercjak, A., Trovatti, E., Uahib, F.G.M., Moreno, G. de P., Nascimento, A.P., Berreta, A.A., Ribeiro, S.J.L. and Barud, H.S., 2016. Komagataeibacter rhaeticus as an alternative bacteria for cellulose production. *Carbohydrate Polymers*, 152, pp.841–849.

Man, Z., Muhammad, N., Sarwono, A., Bustam, M.A., Kumar, M.V. and Rafiq, S., 2011. Preparation of Cellulose Nanocrystals Using an Ionic Liquid. *Journal of Polymers and the Environment*, 19(3), pp.726–731.

Mat Zain, N.F., Yusop, S.M. and Ahmad, I., 2014. Preparation and Characterization of Cellulose and Nanocellulose From Pomelo (Citrus grandis) Albedo. *Journal of Nutrition & Food Sciences*, 5(1), pp.10–13.

Mazlita, Y., Lee, H. V and Hamid, S.B.A., 2016. Preparation of Cellulose nanocrystals Bio-Polymer From Agro- Industrial Wastes : Separation and Characterization. *Polymers & Polymer Composites*, 24(9), pp.719–728.

Meng, F., Wang, G., Du, X., Wang, Z., Xu, S. and Zhang, Y., 2019. Extraction and characterization of cellulose nanofibers and nanocrystal from liquefied banana pseudo-stem residue. *Composites Part B: Engineering*, 160, pp.341–347.

Mondragon, G., Fernandes, S., Retegi, A., Peña, C., Algar, I., Eceiza, A. and Arbelaiz, A., 2014. A common strategy to extracting cellulose nanoentities from different plants. *Industrial Crops and Products*, 55, pp.140–148.

Montafia, P. and Gnansounou, E., 2017. *Life Cycle Assessment of Thermochemical Conversion of Empty Fruit Bunch of Oil Palm to Bio-Methane BT In: Life-Cycle Assessment of Biorefineries.* Amsterdam, Netherlands: Elsevier.

Morais, J.P.S., Rosa, M. de F., de Souza Filho, M. de sá M., Nascimento, L.D., do Nascimento, D.M. and Cassales, A.R., 2013. Extraction and characterization of nanocellulose structures from raw cotton linter. *Carbohydrate Polymers*, 91(1), pp.229–235.

Naduparambath, S., Jinitha, T.V., Shaniba, V., Sreejith, M.P., Balan, A.K. and Purushothaman, E., 2018. Isolation and characterisation of cellulose nanocrystals from sago seed shells. *Carbohydrate Polymers*, 180, pp.13–20.

Ng, H.M., Lee, T.S., Tee, T.T., Bee, S.T., Hui, D., Low, C.Y. and Rahmat, A.R., 2015. Extraction of cellulose nanocrystals from plant sources for application as reinforcing agent in polymers. *Composites Part B: Engineering*, 75, pp.176–200.

Nguyen, J.N.T. and Harbison, A.M., 2017. *Scanning Electron Microscopy Sample Preparation and Imaging*, New York: Humana Press.

Novo, L.P., García, A., Belgacem, N. and Curvelo, A.A. da S., 2016. A study of the production of cellulose nanocrystals through subcritical water hydrolysis. *Industrial Crops and Products*, 93, pp.88–95.

Ofori-Boateng, C. and Lee, K.T., 2014. Sono-assisted organosolv/H2O2 pretreatment of oil palm (Elaeis guineensis Jacq.) fronds for recovery of fermentable sugars: Optimization and severity evaluation. *Fuel*, 115, pp.170–178.

Okahisa, Y., Furukawa, Y., Ishimoto, K., Narita, C., Intharapichai, K. and Ohara, H., 2018. Comparison of cellulose nanofiber properties produced from different parts of the oil palm tree. *Carbohydrate Polymers*, 198, pp.313–319.

Oliveira, O., Marystela, F., Leite, F. and Róz, A., 2017. *Nanocharacterization techniques*. Norwich, United States: William Andrew Publishing.

Opon, J. and Henry, M., 2019. An indicator framework for quantifying the sustainability of concrete materials from the perspectives of global sustainable development. *Journal of Cleaner Production*, 218, pp.718–737.

Osman, N., Shamsuddin and Uemura, 2016. ScienceDirect Activated Carbon of Oil Palm Empty Fruit Bunch (EFB); Core and Shaggy. *Procedia Engineering*, 148, pp.758–764.

Palamae, S., Dechatiwongse, P., Choorit, W., Chisti, Y. and Prasertsan, P., 2017. Cellulose and hemicellulose recovery from oil palm empty fruit bunch (EFB) fibers and production of sugars from the fibers. *Carbohydrate Polymers*, 155, pp.491–497.

Patel, B., Guo, M., Izadpanah, A., Shah, N. and Hellgardt, K., 2016. A review on hydrothermal pre-treatment technologies and environmental profiles of algal biomass processing. *Bioresource Technology*, 199, pp.288–299.

Pathan, A.K., Bond, J. and Gaskin, R.E., 2010. Sample preparation for SEM of plant surfaces. *Materials Today*, 12, pp.32–43.

Pirich, C.L., de Freitas, R.A., Woehl, M.A., Picheth, G.F., Petri, D.F.S. and Sierakowski, M.R., 2015. Bacterial cellulose nanocrystals: impact of the sulfate content on the interaction with xyloglucan. *Cellulose*, 22(3), pp.1773–1787.

Prado, K.S. and Spinacé, M.A.S., 2019. Isolation and characterization of cellulose nanocrystals from pineapple crown waste and their potential uses. *International Journal of Biological Macromolecules*, 122, pp.410–416.

Rahimi Kord Sofla, M., Brown, R.J., Tsuzuki, T. and Rainey, T.J., 2016. A canofibres extracted from bagasse using acid and ball milling methodsomparison of cellulose nanocrystals and cellulose n. *Advances in Natural Sciences: Nanoscience and Nanotechnology*, 7(3), pp.1–9.

Ross Hallett, F., 1994. Particle size analysis by dynamic light scattering. *Food Research International*, 27(2), pp.195–198.

Salari, M., Sowti Khiabani, M., Rezaei Mokarram, R., Ghanbarzadeh, B. and Samadi Kafil, H., 2019. Preparation and characterization of cellulose nanocrystals from bacterial cellulose produced in sugar beet molasses and cheese whey media. *International Journal of Biological Macromolecules*, 122, pp.280–288.

Salminen, R., Reza, M., Pääkkönen, T., Peyre, J. and Kontturi, E., 2017. TEMPO-mediated oxidation of microcrystalline cellulose: limiting factors for cellulose nanocrystals yield. *Cellulose*, 24(4), pp.1657–1667.

Samuel Roberts Noble Microscopy Laboratory, 2018. *SEM Preparatory Equipment.* Available through: <http://www.microscopy.ou.edu/sem-prep.shtml> [Accessed 8 Jul. 2018].

Sellappah, V., Uemura, Y., Hassan, S., Sulaiman, M.H. and Lam, M.K., 2016. Torrefaction of Empty Fruit Bunch in the Presence of Combustion Gas. *Procedia Engineering*, 148, pp.750–757.

Shaheen, T.I. and Emam, H.E., 2018. Sono-chemical synthesis of cellulose nanocrystals from wood sawdust using Acid hydrolysis. *International Journal of Biological Macromolecules*, 107, pp.1599–1606.

Shen, D.K. and Gu, S., 2009. The mechanism for thermal decomposition of cellulose and its main products. *Bioresource Technology*, 100(24), pp.6496–6504.

Sigma-Aldrich, 2019. *IR Spectrum Table and Chart*. Available through: <https://www.sigmaaldrich.com/technical-documents/articles/biology/ir-spectrum-table.html> [Accessed 2 Feb. 2019].

Singh, A.K., 2016. *Engineered Nanoparticles: Structure, Properties and Mechanisms of Toxicity.* Massachusetts, United States: Academic Press.

Skoog, D. A., Holler, F. J., and Nieman, 1998. *Principles of instrumental analysis*, Philadelphia, Pennsylvania: Saunders College Pub.

Song, Y.K., Leng Chew, I.M., Yaw Choong, T.S., Tan, J. and Tan, K.W., 2016. Isolation of Nanocrystalline Cellulose from oil palm empty fruit bunch − A response surface methodology study. *MATEC Web of Conferences*, 60, pp.1–5.

Spaulding, N.E., Meese, D.A., Baker, I., Mayewski, P.A. and Hamilton, G.S., 2010. A new technique for firn grain-size measurement using SEM image analysis. *Journal of Glaciology*, 56(195), pp.12–19.

Srivastava, S., Bhargava, A., Pathak, N. and Srivastava, P., 2019. Production, characterization and antibacterial activity of silver nanoparticles produced by Fusarium oxysporum and monitoring of protein-ligand interaction through in-silico approaches. *Microbial Pathogenesis*, 129, pp.136–145.

Stanford University, 2018. *SEM: Hitachi S-3400N VP | Stanford Microscopy Facility.* Available through: <https://microscopy.stanford.edu/sem-hitachi-s-3400n-vp-0> [Accessed 8 Jul. 2018].

Stojilovic, N., 2012. Why Can't We See Hydrogen in X-ray Photoelectron Spectroscopy? *Journal of Chemical Education*, 89(10), pp.1331–1332.

Sudiyani, Y., Styarini, D., Triwahyuni, E., Sudiyarmanto, Sembiring, K.C., Aristiawan, Y., Abimanyu, H. and Han, M.H., 2013. Utilization of Biomass Waste Empty Fruit Bunch Fiber of Palm Oil for Bioethanol Production Using Pilot–Scale Unit. *Energy Procedia*, 32, pp.31–38.

Sun, Y. and Cheng, J., 2002. Hydrolysis of lignocellulosic materials for ethanol production : a review q. *Bioresource technology*, 83(1), pp.1–11.

Taflick, T., Schwendler, L.A., Rosa, S.M.L., Bica, C.I.D. and Nachtigall, S.M.B., 2017. Cellulose nanocrystals from acacia bark–Influence of solvent extraction. *International Journal of Biological Macromolecules*, 101, pp.553–561.

Tan, K., Heo, S., Foo, M., Chew, I.M. and Yoo, C., 2019. An insight into nanocellulose as soft condensed matter: Challenge and future prospective toward environmental sustainability. *Science of The Total Environment*, 650, pp.1309–1326.

Tan, X.Y., Abd Hamid, S.B. and Lai, C.W., 2015. Preparation of high crystallinity cellulose nanocrystals (CNCs) by ionic liquid solvolysis. *Biomass and Bioenergy*, 81, pp.584–591.

Trache, D., Hussin, M.H., Haafiz, M.K.M. and Thakur, V.K., 2017. Recent progress in cellulose nanocrystals: sources and production. *Nanoscale*, 9(5), pp.1763–1786.

Vasconcelos, N.F., Feitosa, J.P.A., da Gama, F.M.P., Morais, J.P.S., Andrade, F.K., de Souza Filho, M. de S.M. and Rosa, M. de F., 2017. Bacterial cellulose nanocrystals produced under different hydrolysis conditions: Properties and morphological features. *Carbohydrate Polymers*, 155, pp.425–431.

Vaskan, P., Pachón, E.R. and Gnansounou, E., 2018. Techno-economic and life-cycle assessments of biorefineries based on palm empty fruit bunches in Brazil. *Journal of Cleaner Production*, 172, pp.3655–3668.

Vernon-Parry, K.D., 2000. Scanning electron microscopy: an introduction. *III-Vs Review*, 13(4), pp.40–44.

Vanitjinda, G., Nimchua, T. and Sukyai, P., 2019. Effect of xylanase-assisted pretreatment on the properties of cellulose and regenerated cellulose films from sugarcane bagasse. *International Journal of Biological Macromolecules*, 122, pp.503–516.

Wang, B., Sain, M. and Oksman, K., 2007. Study of Structural Morphology of Hemp Fiber from the Micro to the Nanoscale. *Applied Composite Materials*, 14(2), pp.89–103.

Wang, Y., Xu, K., Li, Y. and Feng, Q., 2015. Fourier transform infrared spectroscopy analysis of the active components in serum of rats treated with Zuogui Pill. *Journal of Traditional Chinese Medical Sciences*, 2(4), pp.264–269.

Wijeyesekera, D.C., Ho, M.H., Bai, X. and Bakar, I., 2016. Strength and Stiffness Development in Soft Soils: A FESEM aided Soil Microstructure Viewpoint. *Materials Science and Engineering*, 136(1), p.1-11.

Wu, Q., Qiang, T.C., Zeng, G., Zhang, H., Huang, Y. and Wang, Y., 2017. Sustainable and renewable energy from biomass wastes in palm oil industry: A case study in Malaysia. *International Journal of Hydrogen Energy*, 42(37), pp.23871–23877.

Xie, H., Du, H., Yang, X. and Si, C., 2018. Recent Strategies in Preparation of Cellulose nanocrystals and Cellulose Nanofibrils Derived from Raw Cellulose Materials. *International Journal of Polymer Science*, 2018(5), pp.1–25.

Xie, J., Hse, C.-Y., De Hoop, C.F., Hu, T., Qi, J. and Shupe, T.F., 2016. Isolation and characterization of cellulose nanofibers from bamboo using microwave liquefaction combined with chemical treatment and ultrasonication. *Carbohydrate Polymers*, 151, pp.725–734.

Xing, L., Gu, J., Zhang, W., Tu, D. and Hu, C., 2018. Cellulose I and II nanocrystal produced by sulphuric acid hydrolysis of Tetra pak cellulose I. *Carbohydrate Polymers*, 192, pp.184–192.

Xu, H., Li, B. and Mu, X., 2016. Xu, H., Li, B. and Mu, X., 2016. Review of Alkali-Based Pretreatment To Enhance Enzymatic Saccharification for Lignocellulosic Biomass Conversion. *Industrial & Engineering Chemistry Research*, 55(32), pp.8691–8705.

Yadav, M. and Chiu, F.C., 2019. Cellulose nanocrystals reinforced κ-carrageenan based UV resistant transparent bionanocomposite films for sustainable packaging applications. *Carbohydrate Polymers*, 211, pp.181–194.

Yeo, J.Y., Chin, B.L.F., Tan, J.K. and Loh, Y.S., 2019. Comparative studies on the pyrolysis of cellulose, hemicellulose, and lignin based on combined kinetics. *Journal of the Energy Institute*, 92(1), pp.27–37.

Ying, T.Y., Teong, L.K., Abdullah, W.N.W. and Peng, L.C., 2014. The Effect of Various Pretreatment Methods on Oil Palm Empty Fruit Bunch (EFB) and Kenaf Core Fibers for Sugar Production. *Procedia Environmental Sciences*, 20, pp.328–335.

Yu, H., Qin, Z., Liang, B., Liu, N., Zhou, Z. and Chen, L., 2013. Facile extraction of thermally stable cellulose nanocrystals with a high yield of 93 % through hydrochloric acid hydrolysis under hydrothermal conditions. *Journal of Materials Chemistry A*, 1(12), p.3938–3944.

Zeng, X., Small, D.P. and Wan, W., 2011. Statistical optimization of culture conditions for bacterial cellulose production by Acetobacter xylinum BPR 2001 from maple syrup. *Carbohydrate Polymers*, 85(3), pp.506–513.

Zhang, S., Lin, L. and Kumar, A., 2009. *Materials Characterization Techniques.* Boca Raton, United States: CRC Press.

Zhang, Z., Harrison, M.D., Rackemann, D.W., Doherty, W.O.S. and O'Hara, I.M., 2016. Organosolv pretreatment of plant biomass for enhanced enzymatic saccharification. *Green Chemistry*, 18(2), pp.360–381.

Zhang, Z., He, F., Zhang, Y., Yu, R., Li, Y., Zheng, Z. and Gao, Z., 2018. Experiments and modelling of potassium release behavior from tablet biomass ash for better recycling of ash as eco-friendly fertilizer. *Journal of Cleaner Production*, 170, pp.379–387.

Zhang, Z., Zhu, M. and Zhang, D., 2018. A Thermogravimetric study of the characteristics of pyrolysis of cellulose isolated from selected biomass. *Applied Energy*, 220, pp.87–93.

Zhao, X., Cheng, K. and Liu, D., 2009. Organosolv pretreatment of lignocellulosic biomass for enzymatic hydrolysis. *Applied Microbiology and Biotechnology*, 82(5), pp.815–827.

Zhao, Y., Zhang, Y., Lindström, M.E. and Li, J., 2015. Tunicate cellulose nanocrystals: Preparation, neat films and nanocomposite films with glucomannans. *Carbohydrate Polymers*, 117, pp.286–296.

APPENDICES

APPENDIX A: Calculation of Volume of Sulphuric Acid

Volume of sulphuric acid required to prepare 100 ml of 64 wt% sulphuric acid solution

Basis: Density of water = 1 g/ml. 100 g of water is equivalent to 100 ml of water

By taking the average value of 96 wt% as the concentration of sulphuric acid available in laboratory with density of 1.84 g/ml, the volume of sulphuric acid required in 100 ml of 64 wt% sulphuric acid solution is

$$V = \frac{64 \, g}{1.84 \frac{g}{ml}} \Big/ \left(\frac{96}{100}\right)$$

$$= 36.23 \, ml$$

At the same time, the volume of water required in 100 g or 100 ml of 64 wt% sulphuric acid solution is calculated by assuming the water density to be 1 g/ml at ambient temperature.

$$V = \frac{36 \, g}{1.00 \frac{g}{ml}}$$

$$= 36.00 \, ml$$

Hence, in order to prepare 100 ml of sulphuric acid solution, the amount required for concentration sulphuric acid and water is displayed in calculation below.

Amount of sulphuric acid required,

$$V = 100 \, ml \times \frac{36.23 \, ml}{(36.23 \, ml + 36.00 \, ml)}$$

$$= 50.16 \, ml$$

Amount of water required,

$$V = 100 \, ml \times \frac{36.00 \, ml}{(36.23 \, ml + 36.00 \, ml)}$$

$$= 49.84 \, ml$$

APPENDIX B: Calculations of Yield for ATEFB

<u>Yield of alkali-treated empty fruit bunches obtained from washing and alkaline treatment:</u>

Washed empty fruit bunches:

$$Yield \; (\%) = \frac{38.5284}{40.1961} \times 100 \; \%$$
$$= 95.8511 \; \%$$

First alkali-treated empty fruit bunches (ATEFB):

$$Yield \; (\%) = \frac{34.2306}{40.1961} \times 100 \; \%$$
$$= 85.1590 \; \%$$

Second alkali-treated empty fruit bunches (ATEFB):

$$Yield \; (\%) = \frac{29.2563}{40.1961} \times 100 \; \%$$
$$= 72.7839 \; \%$$

Third alkali-treated empty fruit bunches (ATEFB):

$$Yield \; (\%) = \frac{26.8994}{40.1961} \times 100 \; \%$$
$$= 66.9204 \; \%$$

APPENDIX C: Calculations of Yield for CMF and CNC

Yield of bleached cellulose microfibres compared to raw empty fruit bunches

First bleached cellulose microfibres (CMF):

$$Yield\ (\%) = \ 66.9204\ \% \times \frac{21.1399}{25.3872} \times 100\ \%$$
$$= 55.7245\ \%$$

Second bleached cellulose microfibres (CMF):

$$Yield\ (\%) = \ 66.9204\ \% \times \frac{16.7869}{25.3872} \times 100\ \%$$
$$= 44.2501\ \%$$

Third bleached cellulose microfibres (CMF):

$$Yield\ (\%) = \ 66.9204\ \% \times \frac{15.1176}{25.3872} \times 100\ \%$$
$$= 39.8499\ \%$$

Yield of cellulose nanocrystals compared to raw empty fruit bunches

Acid-hydrolysed cellulose nanocrystals (CNC):

$$Yield\ (\%) = \ 39.8499\ \% \times \frac{15.1176}{25.3872} \times \frac{1.0090}{13.6089} \times 100\ \%$$
$$= 2.9282\ \%$$

APPENDIX D: Calculations of Holocellulose Content for Various Samples

Holocellulose content of raw EFB, alkali-treated empty fruit bunches and bleached cellulose microfibres and cellulose nanocrystals.

Raw EFB:

$$Holocellulose\ content\ (\%) = \frac{51.0065 - 50.8015}{0.5} \times 100\ \%$$
$$= 41.00\ \%$$

Alkali-treated empty fruit bunches:

$$Holocellulose\ content\ (\%) = \frac{47.3202 - 47.0794}{0.5} \times 100\ \%$$
$$= 48.16\ \%$$

Bleached cellulose microfibres:

$$Holocellulose\ content\ (\%) = \frac{46.3566 - 46.0513}{0.5} \times 100\ \%$$
$$= 63.06\ \%$$

Cellulose nanocrystals:

$$Holocellulose\ content\ (\%) = \frac{51.2311 - 50.8014}{0.5} \times 100\ \%$$
$$= 85.94\ \%$$

APPENDIX E: Calculations of Cellulose Content for Various Samples

<u>Cellulose content of raw EFB, alkali-treated empty fruit bunches and bleached cellulose microfibres and cellulose nanocrystals</u>

Raw EFB:

$$Cellulose\ content\ (\%) = 41.00 \times \left(\frac{48.6684 - 48.5970}{0.2050}\right)$$
$$= 20.28\ \%$$

Alkali-treated empty fruit bunches:

$$Cellulose\ content\ (\%) = 48.16 \times \left(\frac{46.0324 - 45.8921}{0.2408}\right)$$
$$= 30.06\ \%$$

Bleached cellulose microfibres:

$$Cellulose\ content\ (\%) = 63.06 \times \left(\frac{49.2675 - 49.0341}{0.3153}\right)$$
$$= 46.68\ \%$$

Cellulose nanocrytals:

$$Cellulose\ content\ (\%) = 85.94 \times \left(\frac{54.9900 - 54.6213}{0.4297}\right)$$
$$= 73.74\ \%$$

APPENDIX F: Calculations of Hemicellulose Content for Various Samples

Hemicellulose content of raw EFB, alkali-treated empty fruit bunches and bleached cellulose microfibres and cellulose nanocrystals

Raw EFB:

$$Hemicellulose\ content\ (\%) = 41.00\ \% - 20.28\ \%$$
$$= 20.72\ \%$$

Alkali-treated empty fruit bunches:

$$Hemicellulose\ content\ (\%) = 48.16\ \% - 30.06\ \%$$
$$= 18.10\ \%$$

Bleached cellulose microfibres:

$$Hemicellulose\ content\ (\%) = 63.06\ \% - 46.68\ \%$$
$$= 16.38\ \%$$

Cellulose nanocrystals:

$$Hemicellulose\ content\ (\%) = 85.94\ \% - 73.74\ \%$$
$$= 12.20\ \%$$

APPENDIX G: FTIR Report
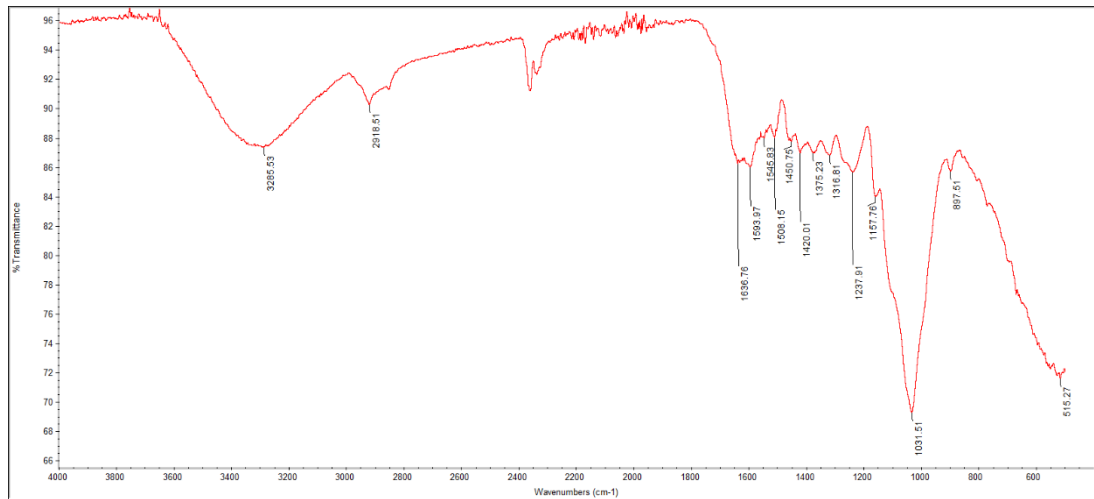
Figure G- 1: FTIR Spectra of Raw Empty Fruit Bunches
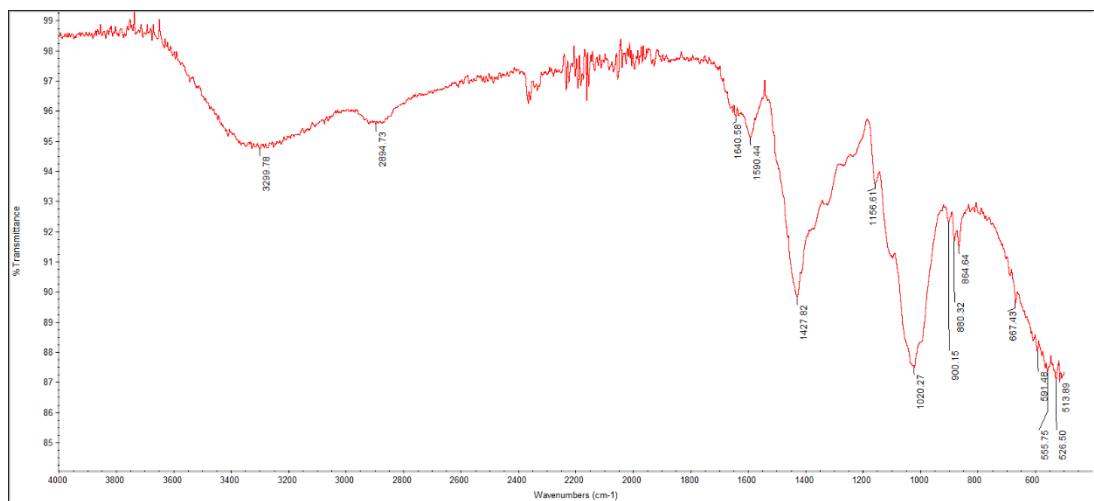
Figure G- 2: FTIR Spectra of Alkali-treated Empty Fruit Bunches
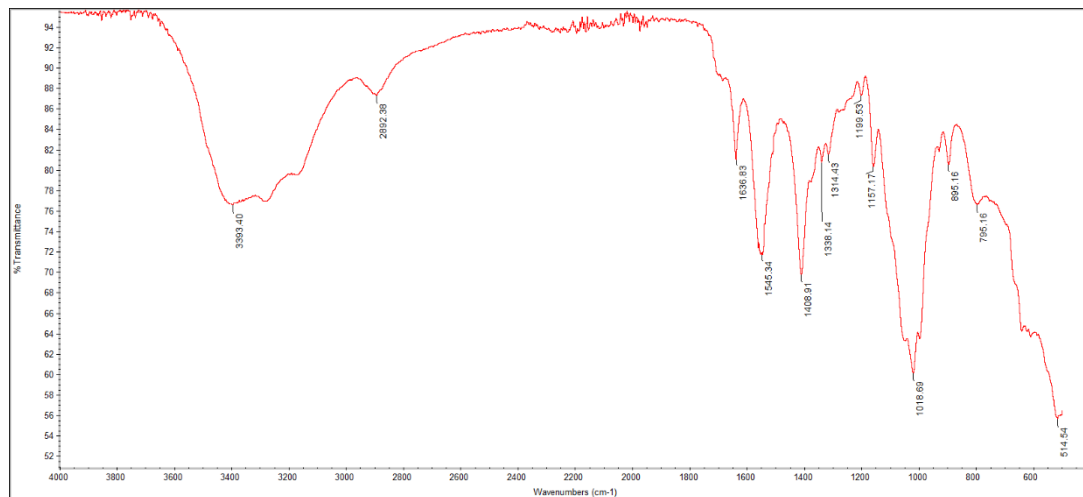
Figure G- 3: FTIR Spectra of Bleached Cellulose Microfibres
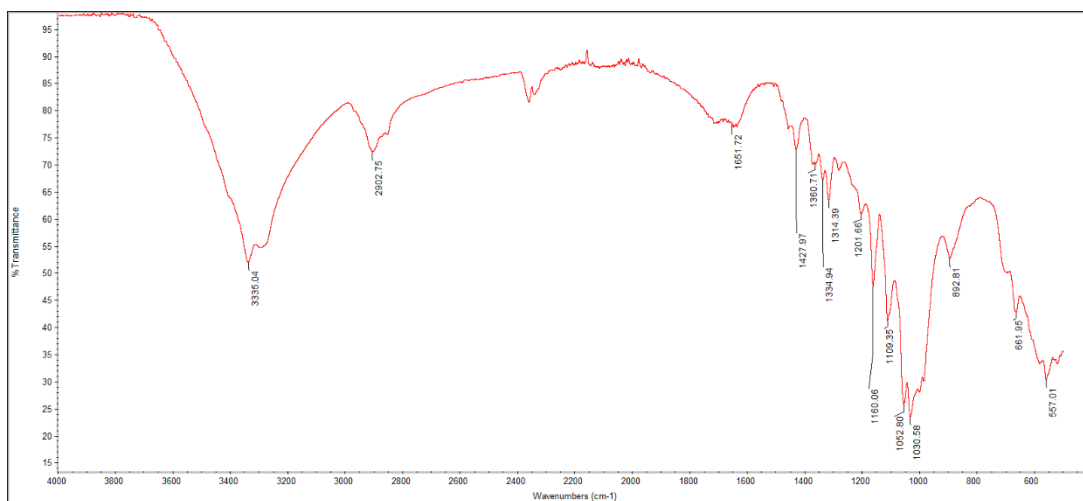
Figure G- 4: FTIR Spectra of Cellulose Nanocrystals

APPENDIX H: Calculation of Crystallinity Indices for Various Samples

Crystallinity indices (Crl) of raw empty fruit bunches, alkali-treated empty fruit bunches, cellulose microfibres and cellulose nanocrystals

Raw empty fruit bunches:

$$CrI = \frac{42 - 23}{42} \times 100$$
$$= 45.2381\ \%$$

Alkali-treated empty fruit bunches:

$$CrI = \frac{52 - 22}{52} \times 100$$
$$= 57.6923\ \%$$

Cellulose microfibres:

$$CrI = \frac{142 - 45}{142} \times 100$$
$$= 68.3099\ \%$$

Cellulose nanocrystals:

$$CrI = \frac{327 - 54}{327} \times 100$$
$$= 83.4862\ \%$$

APPENDIX I: Sem Images of Cellulose Nanocrystals
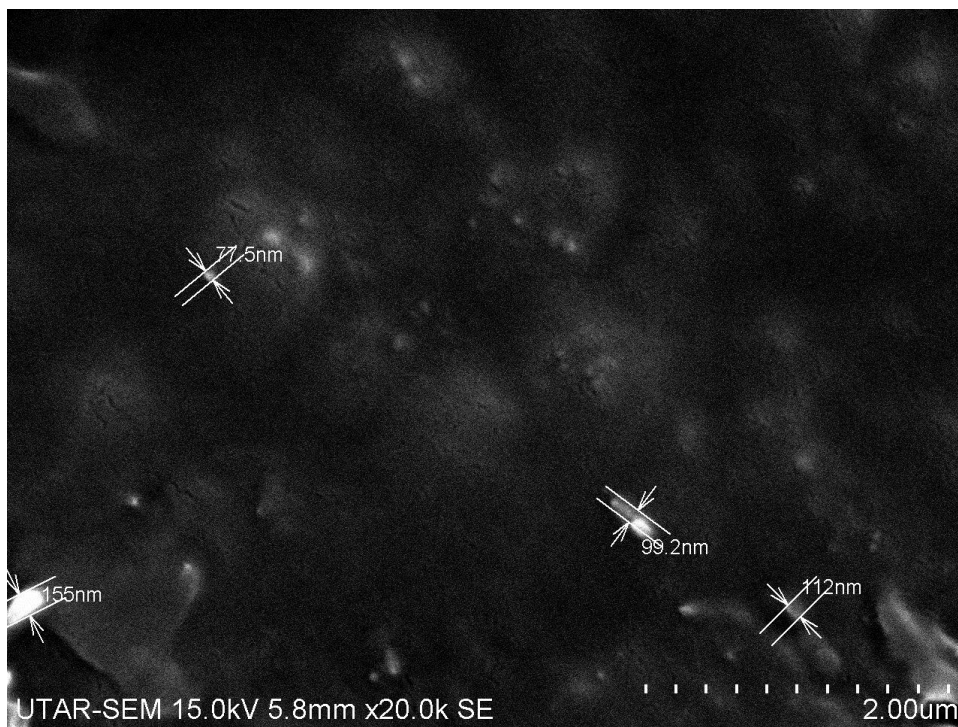
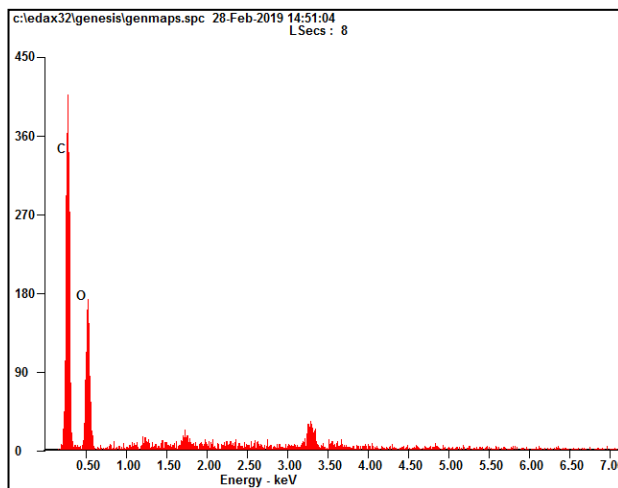Figure I- 1: Sem Image of CNC at a Magnification of 20000 ×
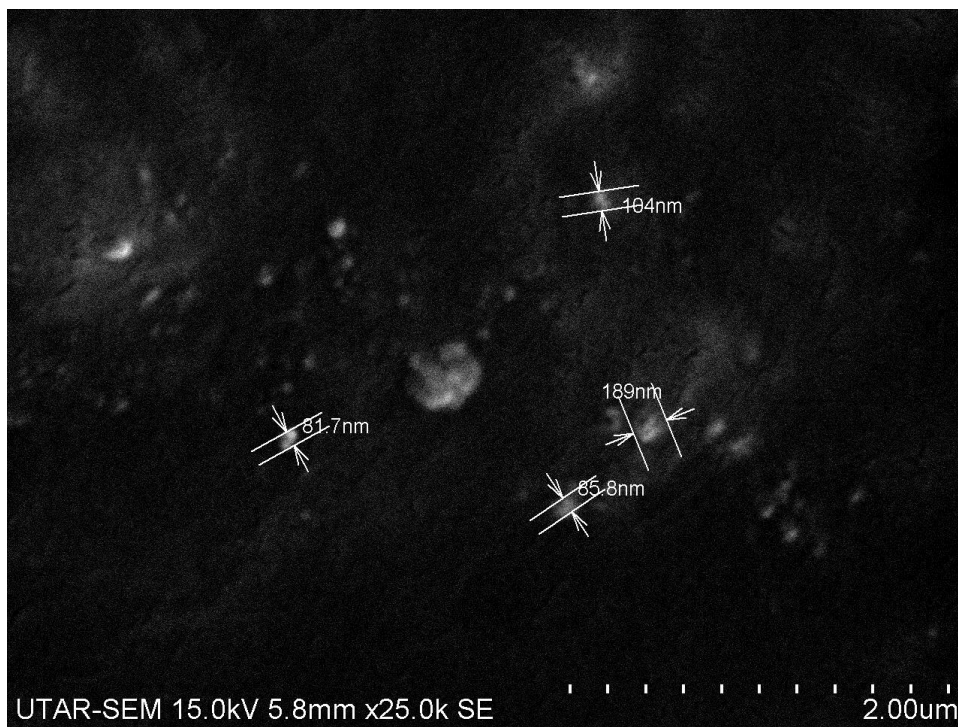
Figure I- 2: Sem Image of CNC at a Magnification of 25000 ×

APPENDIX J: EDX Report
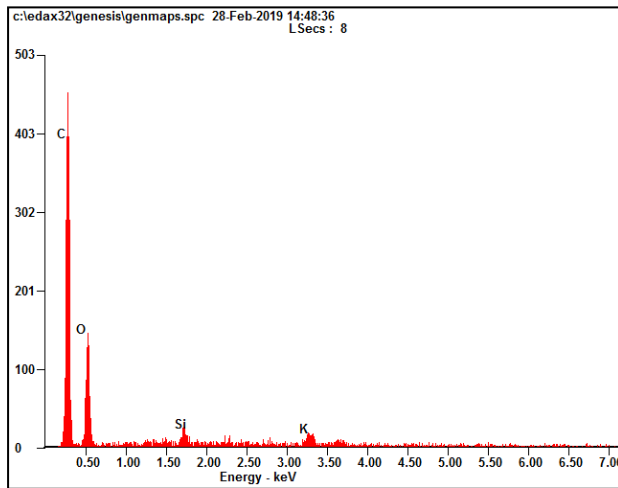
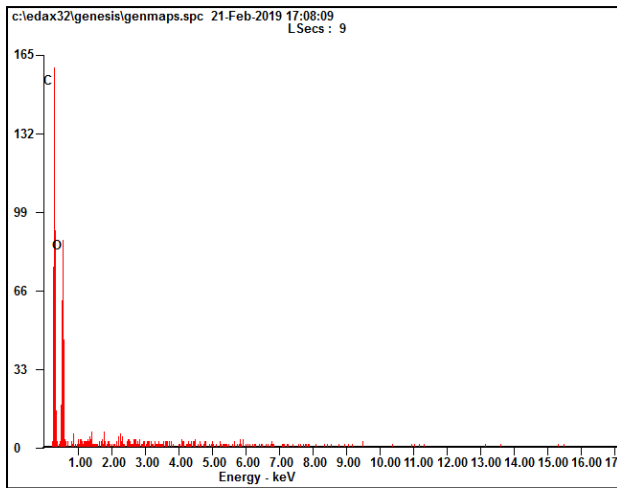| Element	Wt%	At%
CK	60.56	68.11
OK	36.27	30.63
SiK	01.23	00.59
KK	01.94	00.67
Matrix	Correction	ZAF

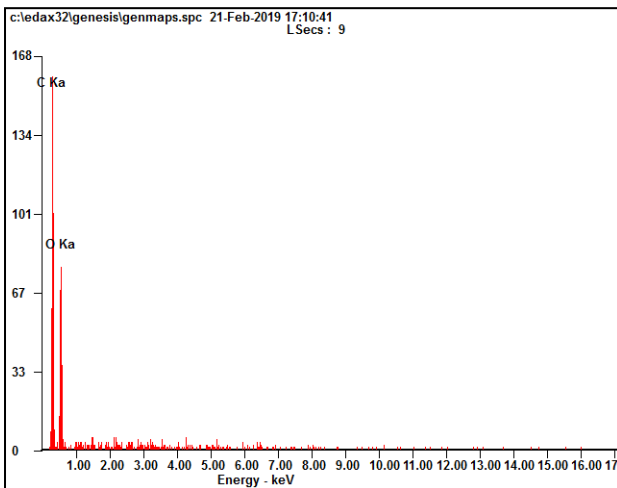| Element	Wt%	At%
CK	57.38	64.20
OK	42.62	35.80
Matrix	Correction	ZAF

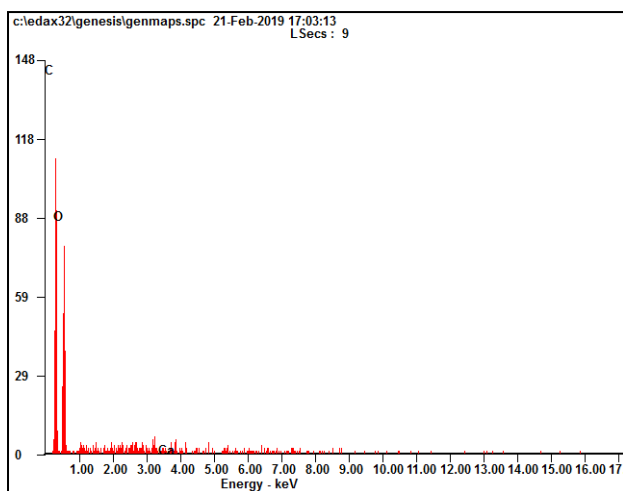Figure J- 1: EDX Analysis at Different Locations of Raw Empty Fruit Bunches

Element	Wt%	At%
CK	53.11	60.14
OK	46.89	39.86
Matrix	Correction	ZAF

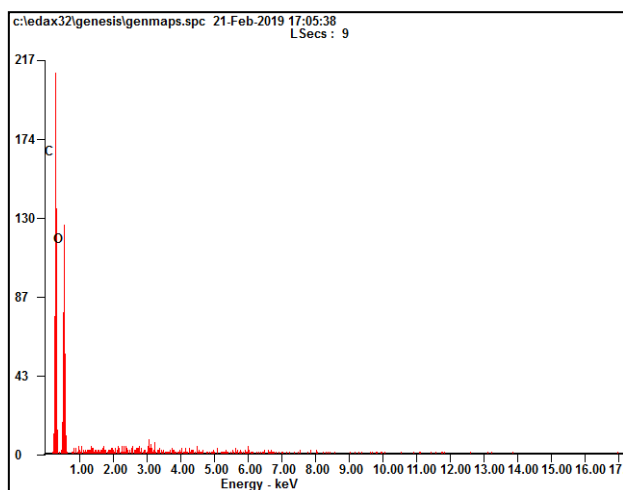| Element	Wt%	At%
CK	53.54	60.55
OK	46.46	39.45
Matrix	Correction	ZAF

Figure J- 2: EDX Analysis at Different Locations of Alkali-treated Empty Fruit Bunches
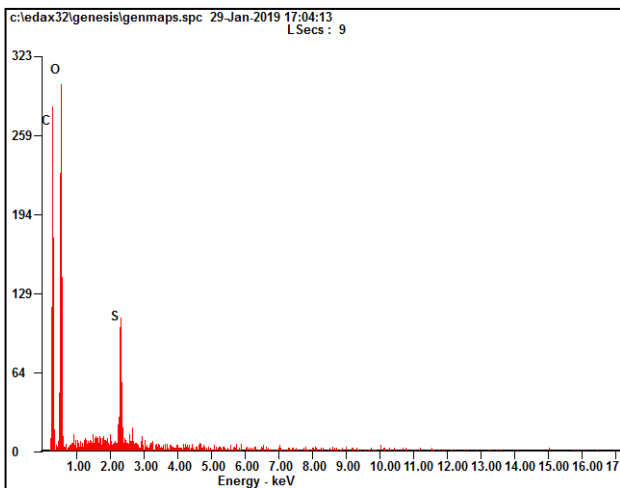
Element	Wt%	At%
CK	48.91	56.22
OK	50.50	43.58
CaK	00.59	00.20
Matrix	Correction	ZAF

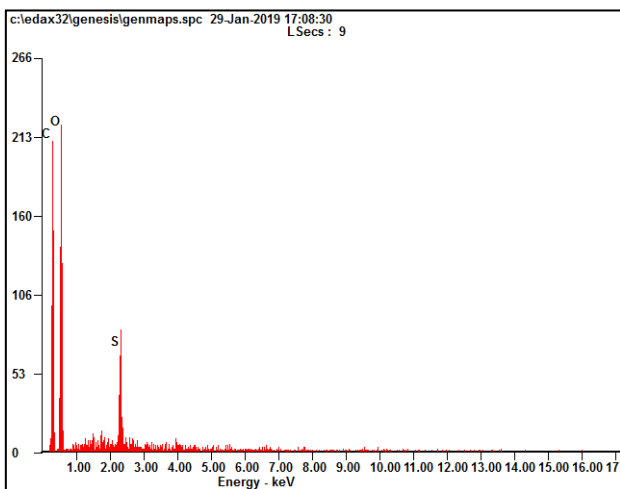| Element	Wt%	At%
CK	52.97	60.01
OK	47.03	39.99
Matrix	Correction	ZAF

Figure J- 3: EDX Analysis at Different Locations of Bleached Cellulose Microfibres

Element	Wt%	At%
CK	46.21	54.75
OK	47.99	42.68
SK	05.80	02.57
Matrix	Correction	ZAF

Element	Wt%	At%
CK	49.17	57.63
OK	45.48	40.02
SK	05.35	02.35
Matrix	Correction	ZAF

Figure J- 4: EDX Analysis at Different Locations of Cellulose Nanocrystals

APPENDIX K: Size Distribution Report by DLS

Size Distribution Report by Intensity
v2.2

Malvern

Sample Details

Sample Name:	CNC 1
SOP Name:	mansettings.nano
General Notes:	

File Name:	JKKP 2019 a.dts	**Dispersant Name:**	Water
Record Number:	651	**Dispersant RI:**	1.330
Material RI:	1.40	**Viscosity (cP):**	0.8872
Material Absorbtion:	0.010	**Measurement Date and Time:**	Thursday, March 21, 2019 10:...

System

Temperature (°C):	24.9	**Duration Used (s):**	70
Count Rate (kcps):	224.7	**Measurement Position (mm):**	5.50
Cell Description:	Clear disposable zeta cell	**Attenuator:**	8

Results

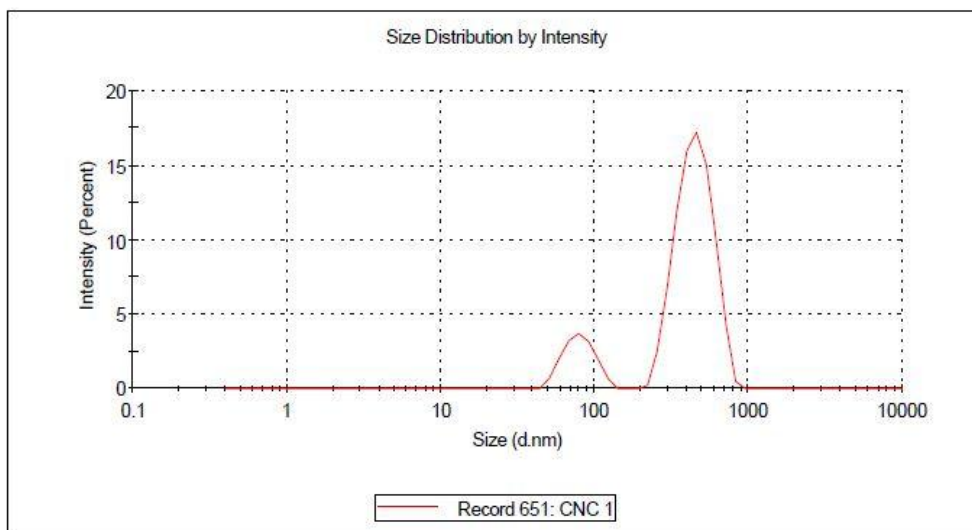|			Size (d.nm):	% Intensity:	St Dev (d.n...
Z-Average (d.nm):	642.9	**Peak 1:**	456.8	84.5	118.8
PdI:	0.552	**Peak 2:**	80.59	15.5	17.80
Intercept:	0.669	**Peak 3:**	0.000	0.0	0.000
Result quality :	**Refer to quality report**				

Figure K- 1: Size Distribution Report